NEW MODELS OF SELF-ORGANIZED MULTI-ROBOT CLUSTERING

A Dissertation

by

JUNG-HWAN KIM

Submitted to the Office of Graduate and Professional Studies of
Texas A&M University
in partial fulfillment of the requirements for the degree of

DOCTOR OF PHILOSOPHY

Chair of Committee,	Dylan A. Shell
Committee Members,	Robin Murphy
	Dezhen Song
	Suhasini Subba Rao
Head of Department,	Dilma Da Silva

December 2015

Major Subject: Computer Science

ABSTRACT

For self-organized multi-robot systems, one of the widely studied task domains is object clustering, which involves gathering randomly scattered objects into a single pile. Earlier studies have pointed out that environment boundaries influence the cluster formation process, generally causing clusters to form around the perimeter rather than centrally within the workspace. Nevertheless, prior analytical models ignore boundary effects and employ the simplifying assumption that clusters pack into rotationally symmetric forms. In this study, we attempt to solve the problem of the boundary interference in object clustering. We propose new behaviors, twisting and digging, which exploit the geometry of the object to detach objects from the boundaries and cover different regions within the workplace. Also, we derive a set of conditions that is required to prevent boundaries causing perimeter clusters, developing a mathematical model to explain how multiple clusters evolve into a single cluster. Through analysis of the model, we show that the time-averaged spatial densities of the robots play a significant role in producing conditions which ensure that a single central cluster emerges and validate it with experiments. We further seek to understand the clustering process more broadly by investigating the problem of clustering in settings involving different object geometries. We initiate a study of this important area by considering a variety of rectangular objects that produce diverse shapes according to different packing arrangements. In addition, on the basis of the observation that cluster shape reflects object geometry, we develop cluster models that describe clustering dynamics across different object geometries. Also, we attempt to address the question of how to maximize the system perfor-

mance by computing a policy for altering the robot division of labor as a function of time. We consider a sequencing strategy based on the hypothesis that since the clustering performance is influenced by the division of labor, it can be improved by sequencing different divisions of labor. We develop a stochastic model to predict clustering behavior and propose a method that uses the model's predictions to select a sequential change in labor distribution. We validate our proposed method that increases clustering performance on physical robot experiments.

DEDICATION

I dedicate this dissertation first and foremost to my Lord. I would also like to dedicate this dissertation to my family and my fiancé.

" Do not fear, for I am with you; do not be dismayed, for I am your God. I will strengthen you and help you; I will uphold you with my righteous right hand."
– Isaiah 41:10 –

ACKNOWLEDGEMENTS

I would like to express my heartfelt thanks to my advisor Dr. Dylan A. Shell for the continuous support of my Ph.D study and related research, for his patience, motivation, and immense knowledge. His guidance helped me in all the time of research and writing of this dissertation. I could not have imagined having a better advisor and mentor for my Ph.D study.

Besides my advisor, I would like to thank the rest of my dissertation committee: Dr. Robin Murphy, Dr. Dezhen Song, and Dr. Suhasini Subba Rao, for their insightful comments and encouragement, but also for the hard question which incented me to widen my research from various perspectives.

I thank my fellow labmates in for the stimulating discussions, for the sleepless nights we were working together before deadlines, and for all the fun we have had in the last six years. Many friends in my church have helped me through these difficult years. I am also grateful for everything they do for me.

Last but not the least, I would like to thank my family and my fiancé for supporting me spiritually.

TABLE OF CONTENTS

Page

LIST OF FIGURES

FIGURE Page

LIST OF TABLES

TABLE Page

1. INTRODUCTION

Studies of self-organized multi-robot systems aim at understanding how to coordinate systems consisting of large numbers of simple robots. Each robot typically has limited capabilities such as imperfect sensing, manipulation, communication, and computational powers. Despite modest capabilities of individuals, self-organized multi-robot systems have been shown to exhibit complex collective behaviors including performing manipulation tasks such as object clustering and sorting (Beckers *et al.*, 1994; Holland and Melhuish, 1999; Gauci *et al.*, 2014), and collective transport of objects (Kube and Bonabeau, 2000; Decugniére *et al.*, 2008a). Unlike the more common deliberative distributed robot teams, the group's functionality emerges through positive and negative feedback mediated by the environment and is the product of action rather than representation or calculated reasoning (Parker, 2008). For self-organized multi-robot systems, the essential research challenge is to manage emergence and harness it for engineering ends. A crucial ingredient in this is the development of models to describe rich self-organization process.

Object clustering is a widely studied problem domain for self-organized multi-robot systems that involves collecting spatially scattered objects into a single pile within the restricted workplace by the boundary. Clustering has practical applications as an initial manipulation step in a pipeline to speed subsequent processing, such as raking leaves into a pile in a yard, farming (Anil *et al.*, 2015), or preparing sites for the construction (Parker *et al.*, 2003).

Within the existing clustering work, the robots typically execute a simple control policy such as the following: each robot performs a random walk within the workplace, turning a random direction once an obstacle is encountered, and resuming their

random walk thereafter. Considering the simplicity of this collective strategy, it is surprising that the robots form clusters reliably and repeatedly. Several researchers have given explanations of how clusters emerge through this process (Beckers *et al.*, 1994; Martinoli *et al.*, 1999a). Ultimately, all these explanations boil down to a geometric argument that the size of clusters is an important determinant of whether the cluster will grow or shrink.

The classic works in multi-robot clustering either have focused on empirical demonstrations or have developed a simple model in which environmental effects or the cluster's characteristics are not considered. We can summarize shortcomings of the conventional explanations and overlooked issues as follows:

- Most previous work has pointed out that environmental boundaries affect the cluster formation process, which the boundaries can cause cluster growth itself (Maris and Boeckhorst, 1996; Holland and Melhuish, 1999). However, notwithstanding the significant influence of the boundary on the clustering process, many authors ignored environmental effects that are caused by the boundary in their models.

- Almost all previous work has not dealt with the importance of positions of forming clusters in the workspace. Environmental boundaries effects that cause not only cluster growth itself, but also an imbalanced amount of time spent by robots on the boundary. It is still remain questions of how the development and position of clusters changes the structure of the configuration for both central clusters and boundary clusters and how this feedback affects where robots can move, and the clustering dynamics.

- Many classic works focused on clustering cylindrical objects (*e.g.*, pucks, frisbees, and the like). Using square objects makes the task rather challenging

because flat edges exacerbate adhesion to the boundary. Once against the boundary, it is difficult for a cylindrical robot to move a box into the center of the environment. Clustering non-cylindrical objects brings to the challenge that remains: to describe and understand how the clustering behaviors work in different geometries of objects.

- Most still considered a simplified clustering model under the (strong) assumption that the geometry of a cluster of items is rotationally symmetric and well-packed. Moving beyond cylindrical objects, the shortcomings of this simplification become acute. There can be a vast number of variables in the stability of different arrangements of objects, and even the most stable configuration is not a smooth function of size n.

- Since the robots in self-organized multi-robot systems have limited sensing and manipulation capabilities, it can be difficult to improve the speed of collective performance. It is already known that merely increasing the number of robots will not improve the speed of the system above a certain threshold because of the interference between team members. Principled methods for maximizing system performance (in terms of speed and/or quality) remains challenging and still overlooked for self-organized multi-robot systems.

1.1 Research Objectives and Contributions

This study aims at developing new models for understanding self-organized multi-robot clustering via modeling, with a view toward improving the system performance. Particularly, by considering environmental effects and geometric characteristics (like the effect of the boundary, geometries of clusters and objects), ignored in the existing works, we examine models to analyze and describe accurately the dynamics of a

multi-robot clustering system. The original contributions of this dissertation are the following:

- Design of a novel approach for object clustering: Our practical approach involves the implementation of a clustering system in which local densities of robots are managed to prevent boundary cluster growth. We propose two complementary behaviors, twisting and digging, having different manipulation capabilities and cover regions. With a mix of robots executing the two complementary behaviors, we demonstrated that the robots successfully generated a single central cluster and overcame the problem of boundary cluster formation. Our approach exploits the mechanics of the object geometry: the boundary objects are pried loose from the wall by striking the corner of the object. We describe an effective solution which uses structured motion to take advantage of the physical packing of the items rather than relying on sensing information. Because this does not depend on the robot disambiguating particular circumstances (i.e., the robot is unaware the distinction between a boundary or any other obstacle), but rather it is the context within which the actions are executed that produces the desired outcome, this resolution is particularly satisfying from a self-organization perspective. ((Kim *et al.*, 2011; Song *et al.*, 2012) and Section 4).

- Extension of existing models of the clustering system: In order to explain how sets of clusters evolve into a single cluster without any boundary cluster being formed, we enrich prior models by treating spatially the densities of robots, specifically with respect to a difference between boundaries and the center of the workspace. Many studies have ignored or simplified the influence of the boundary when building a model by neglecting where the clusters are formed.

This is fallacious because the boundaries themselves buttress clusters, making them behave as if they are part of a much larger cluster. Thus, the boundary effect is an important factor that should be considered in the clustering model ((Kim and Shell, 2015) and Section 4).

- Derivation of a condition to avoid the boundary interference: Through analysis of our proposed model, we show that local spatial densities of the robots have a key role in the evolution of clusters. Using this model, we derive a condition that the boundary interference in the clustering system will be eliminated entirely. Since the condition prescribe circumstances to help achieve the engineering goal, we can then design the robot behaviors whose real dynamics satisfies the desired dynamics for evolution of the largest central cluster. We verify it through our proposed clustering system ((Kim and Shell, 2015) and Section 4).

- Investigation of the impact of the cluster's shape on the clustering dynamics: A common simplifying assumption underlies existing clustering models. It is that a cluster containing n objects is well-packed and rotationally symmetric. But, direct observation shows that clusters can often form into diverse shapes in practice. Previously published work has also overlooked an important factor that there can be a significant difference between two clusters of the same size according to the cluster shape. In this work, we tackle the problem of clustering objects which produce widely different packings. We examine closely how the geometry of the cluster has an influence on the cluster evolution by treating the cluster's shape as a variable in a clustering model. We first introduce a concise descriptor, a measure of compactness, to quantify the shape of clusters, showing that it captures useful information and can result in improved models.

Using the measure of the compactness, we propose probabilistic models (like the geometric probability of cluster modification) to predict the geometry of clusters that arise during the clustering process (Section 5).

- Extended analysis of clustering systems across different object shapes: We extend the analysis of the clustering system by considering various rectangular objects beyond the regular polygonal objects. We build the geometric probability models that reflect the cluster shapes and the object geometry. An interesting observation is that cluster shape reflects object shape. In other words, while clustering objects with high aspect ratio (the ratio of the longest to the shortest side) is more likely to produce clusters with high aspect ratios than when clustering objects of more moderate shape. Based on this observation, we develop probabilistic cluster occurrence models to describe the clustering dynamics according to the object geometry. So far as we know, it is the first in-depth study of the effects of the geometric characteristics of clusters and objects on the clustering dynamics (Section 5).

- Sequencing strategy to maximize the system performance: The self-organized multi-robot systems have two inevitable constraints. The first constraint is that the interaction between robots and environment is uncertain. Consequently, since a task progress is non-stationary, it is difficult to predict accurately the system's result. Therefore, a prediction model for such uncertain system is necessary for forecasting the system's result and improving the performance. Second, due to the limited sensing capabilities of robots, the global state of the system is usually unobservable or partially observable. Such a system can be also regarded as a potentially sensorless robotic system because the robots with limited sensing capabilities do not have a complete feedback loop to control

the system's performance. Furthermore, a control policy through individual units can be ineffective to manage the whole system's performance. Therefore, it is hard to control a self-organized system with local-level parameters. In this work, we predict the clustering progress by applying the stochastic approach using a Markov chain model which captures the geometric state during a clustering process. The stochastic model allows for optimizing a sequence of changes to the division of labor to maximize the task performance in the sensorless system. This reveals that managing global level behaviors like the division of labor can control self-organized multi-robot systems. This method will give insight and provide solutions to improve the system performance in different collective manipulation tasks performed in self-organized multi-robot systems ((Kim and Shell, 2013) and Section 6).

1.2 Outline

The remainder of this dissertation is organized as follows. In Section 2, we will review related literature on object clustering with self-organized multi-robot systems. Section 3 provides extended models of multi-robot clustering systems with a focus on the matter of the boundary and conditions to prevent boundary cluster growth. We also introduce a new method for clustering objects that could successfully cluster square objects. In Section 4, we examine closely how the geometry of the cluster affects the cluster evolution by treating the cluster's shape as a variable in a clustering model, and develop cluster occurrence models across different object shapes. In Section 5, we address the question of how to maximize the clustering performance, and propose a sequencing strategy to improve the performance. Section 6 concludes this dissertation with a general discussion and describes our future work.

2. RELATED WORK *

Studies of self-organized multi-robot systems consider multiple agents, each with limited individual capabilities, but with the capacity for synergistic interaction in order to collectively perform tasks. In general, self-organized multi-robot systems have attractive potential advantages as follows. In the aspect of system configuration, by designing the robots as a simple mechanism, hardware, and software, the complexity of system is reduced. From these, the system is able to accomplish a high level of redundancy as well as reduce the cost and the weight of the robot. In addition, the system can be scalable because the individual robot has an identical structure; robots can be interchanged flexibly with other robots without reorganization (Sharkey, 2007).

Self-organized multi-robot systems are often called swarm robotic systems or collective robotic systems because groups of simple robots can achieve collectively team-level task. Swarm behavior is a collective behavior that is exhibited by large numbers of insects or animals in nature such as aggregating together or moving into same direction. Through the collective behavior, a group can perform a task beyond individual's capability (Dorigo and Roosevelt, 2004). Beni (2005) described that a group in swarm is not just a simple group, but has particular characteristics, which are found in social insects such as absence of synchronization, decentralized control.

The collective behaviors of self-organized systems are ubiquitous in biological systems (Okubo, 1986; Deneubourg and Goss, 1989; Bonabeau *et al.*, 2000; Camazine, 2003; Fialkowski *et al.*, 2006; Copeland and Weibel, 2009). The collective behaviors

*Parts of this section are reprinted with permission from "Self-organized clustering of square objects by multiple robots" by Y. Song, J.-H. Kim, and D. A. Shell, *Swarm Intelligence*, 7461:308-315, Copyright[2012] by Springer.

of social insects, such as the termites' nest-building and the wasps' construction, has also been studied in biology (Garnier *et al.*, 2007). Social insects dose not possess the information about global status of their inhabited colony as well as there is no leader to manage all individual entity to achieve their goals. Nonetheless, it is remarkable that the group's functionality emerges and accomplish their goal through the collective behaviors. Franklin (1996) explained this phenomenon through stigmergy, a term coined by Grassé (1959) in studying wasp nest construction. Stigmergy is an indirect communication between individuals via their shared environment; a modified environment affects the their next motions. Through the implicit communication, the environment is changed, the change of the environment then cause again changing the insect's behavior, and finally complex, intelligent structures appear at the environment. This dynamical process is shown in the nest building of termites (Bonabeau *et al.*, 1999). Bonabeau *et al.* (1999) defined these collective behaviors emerging through this dynamical process as self-organizing behaviors and explained how social insects create complex collective behavior for accomplishing their goal. Many researchers has studied in various fields by applying the self-organizing behaviors to inanimate entities which show parallel behaviors (Whitesides and Grzybowski, 2002; Mondada *et al.*, 2004; Soh *et al.*, 2011).

Many researches based on self-organization theories have studied and published in various fields of collective robotics: aggregation (Trianni *et al.*, 2003; Bahgeçi, 2005; Garnier *et al.*, 2005; Soysal and Şahin, 2007; Dimarogonas and Kyriakopoulos, 2008), flocking (Turgut *et al.*, 2008; Çelikkanat and Şahin, 2010; Ferrante *et al.*, 2012), pattern formation (Yamaguchi and Beni, 1996; Balch and Arkin, 1998; Desai *et al.*, 1999; Flocchini *et al.*, 2008; Kaminka *et al.*, 2008), construction (Wawerla *et al.*, 2002; Werfel and Nagpal, 2006; Stewart and Russell, 2006; Yun *et al.*, 2011), exploration (Everett *et al.*, 1994; Gage, 1995; Amat *et al.*, 1997; Rekleitis *et al.*, 1997;

Damer *et al.*, 2006), and mapping (Cohen, 1996; Ichikawa and Hara, 1996; Rothermich *et al.*, 2005; Howard *et al.*, 2006). In addition, researches on task allocation to solve the complex task through the division of labor in swarm robotics have been conducted (Jones and Matarić, 2003; McLurkin and Yamins, 2005; Groß *et al.*, 2008; Ducatelle *et al.*, 2009).

For object manipulation tasks thorough collective behaviors, object transportation is a widely studied task. Through collective navigation behaviors, groups of robots can cooperatively handle an heavy object or scattered multiple objects and transfer them into a goal position. Groß and Dorigo (2009) proposed the self-organized robotic system to transport objects of different sizes and shapes through collective behaviors of robot teams. Kube and Bonabeau (2000) drew inspiration from ants' behaviors that they transport collectively preys, and demonstrated in physical robot system that a group of six robots can push an heavy object towards a goal in a distributed way. Besides those researches, many studies on collective transport of objects have conducted (Campo *et al.*, 2006; Decugniere *et al.*, 2008b; Berman *et al.*, 2011; Ferrante *et al.*, 2013).

Object clustering, this dissertation is focusing on, is a canonical task for self-organized multi-robot systems. Deneubourg *et al.* (1991) first introduced a distributed clustering algorithm inspired by ants brood sorting behavior and demonstrated how the ant's behavior could be used in a simulated multi-agent system. Clustering was achieved with a simple algorithm with only a local density sensor and without any direct communication between robots and hierarchical organization. Thereafter, inspired by earlier biological models (Franks and Sendova-Franks, 1992), Beckers *et al.* (1994) conducted a physical robot experiment and demonstrated clustering without needing a density sensor by employing a binary threshold sensor. They also explained the emergence of clusters on the basis of the geometry of the

clusters.

Holland and Melhuish (1999) extended the task of object clustering to spatial sorting, requiring the classification of objects based on their types. Most relevant to this paper, they had a detailed description of the effect of environment boundaries. They conducted several experiments in which clusters formed at the edge of their arena. Flat boundaries, after all, have all the properties of a very large cluster. We believe that their paper is the most systematic empirical study of this boundary effect and how it might be overcome to date. They proposed an algorithmic solution to the problem: since their U-bots can detect and measure the distance to the boundary, the robots opted not to deposit frisbees (the objects they cluster) if they are too close to the boundary. Since our robots are unable to distinguish objects, robots, and boundaries, their solution cannot be applied to our scenario.

Several of the preceding studies (Deneubourg *et al.*, 1991; Beckers *et al.*, 1994; Holland and Melhuish, 1999) explained clustering through stigmergy, as we already explained. It describes how an environment, modified by agents' actions previously, affects subsequent task performance by the agents. Although far from being a concrete engineering principle, the observation that this idea is applicable in several contexts is powerful. More connections between robot clustering and biological models have been published (Scholes *et al.*, 2005).

Parker and Zhang (2006) examined a site preparation task in which their approach has several elements of the original clustering algorithms: simple robots employ a threshold-based sensing system in order to push several items. The force threshold is exceeded once piles of a sufficient size have been created. That work, and research in the multi-robot construction domain using square building-blocks (*e.g.*, Jones and Matarić (2004)) suggest that if such self-organized systems are to be used, a broader class of objects should be clustered.

Almost all previously published work in robotic clustering considers cylindrical pucks. Using square objects makes the task rather challenging because flat edges exacerbate adhesion to the boundary wall. Once against the wall, it is particularly difficult for a cylindrical robot to move a box into the center of the workspace. This can be observed in the video posted by Vaughan's Autonomy Laboratory (Vaughan, 2007) in which 36 iRobot Creates successfully created clusters of square objects running only their default demonstration program. Most of the clusters form on the boundary.

Table 2.1 is a comparative summary with robots' capabilities and experimental environments in the most closely related work, most papers employ richer sensing: including sensors to detect and differentiate other robots, objects, and boundaries. Many of the robots are equipped with manipulation mechanisms of one sort or another (grippers, C-shaped scoops, shovel, etc.) that pick up or hold objects.

In this research, we consider simpler robots than prior published accounts. The robots are only equipped a front bumper and a single IR proximity sensor without any object manipulator. The robots are able to recognize the existence of an obstacle in the IR sensor, but cannot recognize its type. Interestingly, the most simple robots either produce boundary clusters or give them special treatment. For example, Maris and Boeckhorst (1996) considered objects to be lost once they were pushed against a wall.

This research describes an effective solution that uses structured motion to take advantage of the physical packing of the items rather than relying on sensing information. Because this does not depend on the robot disambiguating particular circumstances (*i.e.*, the robot is unaware the distinction between a boundary or any other obstacle), but rather it is the context within which the actions are executed that produces the desired outcome, this resolution is particularly satisfying from a

self-organization perspective. The approach is more consistent than prior work in that the clustering process is also described as depending primarily on the physics of the robot-environment interaction for its success.

In general, the robots in self-organized multi-robot systems typically do away with adaptive planning, representation, or calculated reasoning at run-time. In contrast, producing desirable behavior in such systems often focuses on design decisions, employing theory and analysis off-line. One successful approach is to model such systems mathematically as a stochastic processes, which can be a natural fit given the non-determinism often inherent to such systems. The Rate Equation (Lerman and Galstyan, 2004; Martinoli *et al.*, 2004; Lerman *et al.*, 2001; Agassounon *et al.*, 2004) has been used as a useful tool for analysis of collective dynamics of swarm robotic systems.

In a mathematical analysis of clustering dynamics, Martinoli *et al.* (1999b) introduced a probabilistic model to quantify this geometric notion under the assumption of rotationally symmetric piles. The idea is essentially that in order to draw a puck away from a cluster, a robot must move past it at a particular angle. Small clusters have more angles from which pucks will be removed than big clusters and, additionally, larger clusters are proportionately more likely to be encountered for puck deposits. Kazadi *et al.* (2002) also proposed a mathematical model of clustering dynamics with rate equations, describing cluster growth properties and arguing along similar geometric lines to Martinoli. Both studies assume that a cluster is rotationally symmetric, a fact often violated in practice especially as one explores objects with a variety of shapes.

The previous work in robotic clustering mentioned above either focused on empirical demonstrations or considered a simple model in which environmental effects (like boundaries, the characteristics of clusters and objects) play no role. In this

dissertation, we address this challenge by considering environmental effects as well as geometries of clusters and objects.

Work	Pucks/Seeds/Cubes/Boxes		Environment		Notes
	Sensing	Manipulation	Sensing	Boundary & Effects	
Beckers *et al.* (1994)	◇ Detect circular pucks with force sensor in C-shaped scoop	◇ Push circular objects ◇ Control the number of carried pucks with a microswitch	◇ Two IR sensors for obstacle avoidance	◇ A square arena ◇ Side-steps the effect of boundary by using a deformable boundary	◇ The robots can push pucks trapped on the boundary due to a deformable wall
Martinoli *et al.* (1999b)	◇ Discriminate between circular seeds and obstacles with distinct IR sensor signatures	◇ Grasp, carry and release seeds	◇ Six IR proximity sensors for detecting obstacles	◇ A square arena ◇ Effect of the boundary ignored	◇ The robots can recognize and access clusters geometrically
Holland and Melhuish (1999)	◇ Detect circular pucks by sensing backward force on gripper	◇ Grip, retain, and release circular pucks with semicircular gripper	◇ Four IR proximity sensors for sensing the boundary	◇ An octagonal shaped arena with rigid boundary ◇ Use the probability of detecting a wall	◇ Robots cannot discriminate between other robots and the boundary ◇ The strategy of varying the wall probability introduces the false positive ◇ The robots overcome the effect of boundary with sensors
Maris and Boeckhorst (1996)	◇ No sensing of the cubes	◇ Cubes pushed until obstacle detected	◇ Six IR proximity sensors for obstacle detection	◇ A square arena ◇ Consider pushed cubes against the boundary as "lost"	◇ The robots manipulate cubes by only pushing behavior for clustering task ◇ Robots pass over cubes on the boundary
Vaughan (unpublished)	◇ Detect square boxes with bumpers	◇ Push and leave a box by a bumper's threshold	◇ No sensor for detecting objects except for boxes	◇ A rectangular arena ◇ Effect of the boundary ignored	◇ Several clusters formed on the boundary
This dissertation	◇ Detect square boxes with bumpers	◇ Push and leave a box by a bumper's threshold	◇ A single IR proximity sensor for sensing the objects on the right side	◇ An octagonal shaped arena with rigid boundary ◇ Overcome the effect of boundary using motion strategies	◇ No puck manipulator ◇ Use few sensor information (1-bit IR sensor, 1-bit bumper) ◇ **The robot unknowingly overcomes the effect of boundary without the sensor for distinguishing boundary**

Table 2.1: A comparison of robot capabilities within related research.

3. SCOPE AND LIMITATIONS

In this section, we describe precisely the experimental testbed used in this research to investigate how clustering occurs, and report assumptions and limitations in our approach.

3.1 Environmental Setting

While classic works considered only cylindrical objects (e.g., pucks, frisbees), our work has been exploring the task with square and rectangular objects. For a problem where the conventional wisdom explaining the clustering process hinges on geometric arguments, it is somewhat surprising that no consideration has been given to varying the shape of the objects. Using square objects makes the task rather challenging because flat edges exacerbate adhesion to the boundary wall. Once against the wall, it is particularly difficult for a cylindrical robot to move a box into the center of the workspace. This can be observed in the video posted by Vaughan's Autonomy Lab in which 36 iRobot Creates robots successfully created clusters of square objects running only their default demo program (Vaughan, 2007). As shown in Figure 3.1, most of the clusters form on the boundary. We call the interference of boundaries with single central cluster growth "the boundary effect".

To address the problem of the boundary effect in object clustering, we studied the experimental setting as follows.

- Robot platform – we use iRobot Create platforms. Since we attempt to implement the clustering system with simple robots without any object manipulator and richer sensing information, the device is a suitable platform for our clustering system. The robot (about 32 cm in diameter) similar in size to the autonomous vacuum cleaning devices made by the same company in

Figure 3.1: Demonstration for object clustering [by Autonomy Lab at the Simon Fraser University]. Many clusters form on the workspace perimeter (See the yellow circles).

widespread use (See Figure 3.2). The robots are equipped with two wheels operated via a differential drive mechanism and a passive caster. This allows the robot platform to move forward, or backward, perform turns while moving, and also to turn in place. Two kinds of sensors are used in our object clustering experiments:

1. The robot has left and right bumpers, which are used to detect the presence of objects in front of the robot. The bumpers operate independently and are only depressed when the pushing force against them exceeds a threshold.

2. The robot has an IR sensor on its right side, which is used for sensing the distance to the wall to the right side of the robot and enables it to perform simple wall following.

This constitutes a minimalist multi-robot system: simple control algorithms, few sensors and no explicit communication nevertheless suffice to produce cooperative box pushing and cluster formation. Unlike the majority of the existing work, the robots employed do not have a specially shaped scoop, or shovel,

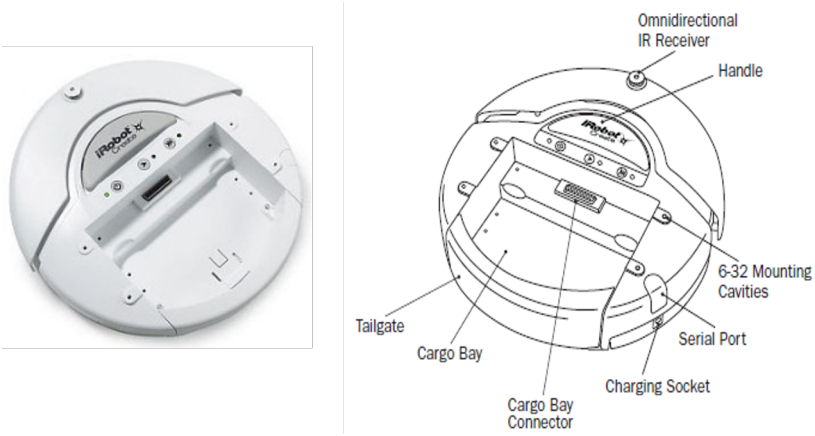

Figure 3.2: iRobot Create platform

for manipulating the objects used for clustering. Without this specifically constructed apparatus (sometimes they also include a specialized puck sensor), and given the role physics play in the collection process itself, these experiments may be considered to use fewer structured resources to execute the clustering task.

- Objects – We consider square boxes whose size is 35 cm×35 cm, similar to a robot's size, as the object for clustering. For practicable operation with our robots the boxes have the following crucial property: two boxes together have sufficient mass to depress the bumper although an individual box is inadequate to activate the sensor. Later in this work, we consider various rectangular objects by varying its aspect ratio.

- Arena – Similar to Holland and Melhuish (1999) we use an octagonal shaped arena, because a square arena would result in square boxes getting stuck in the 90° corner. Our arena has a size of 4.5 m×4.5 m. To analyze the robots' spatial distribution, we divide the octagonal arena into center and boundary

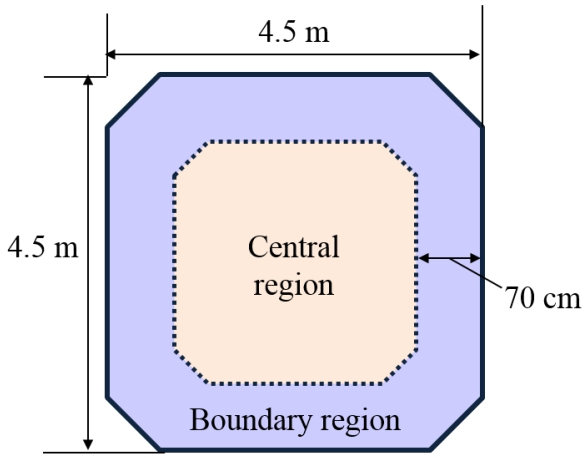

Figure 3.3: Octagonal shaped arena.

Figure 3.4: An example of object clustering scenario: 20 square objects (brown boxes) and 5 robots (white round devices).

regions. The boundary line between regions is drawn 70 cm from the boundary, which approximately the same as the width of the sum of width of a robot and a box, and ratio of center to boundary areas is 52:48. Figure 3.3 illustrates the octagonal shaped arena's size and regions.

Figure 3.4 shows the experimental set-up and the box clustering behavior.

3.2 Assumptions

We list here assumptions underlying our clustering system.

- Bounded workspace: Robots perform the clustering task within a finite workspace bounded by a non-deformable boundary.
- Homogeneous robots: All robots move at a constant speed and push only a single object because two objects together have sufficient mass to activate the bumper sensor.
- Identical objects: Clustering objects have identical frictional coefficients and mass. Thus, we assume that all objects have the same physical characteristics such as a sliding friction and static friction force.

On the basis of these assumptions, we analyze the clustering dynamics and develop clustering models. The first assumption permits treating the spatial densities of robots and modeling the clustering dynamics with respect to a difference between the central region and the boundary region of the workplace. Also, the second assumption implies that a group of more than two objects can be a seed of the cluster.

3.3 Limitations

In this study, we focus on solving the problem of the boundary interference. Accordingly, we consider square objects that exacerbate the adhesion against a wall because of their flat edge, and design the motion behavior that is applicable to the manipulation of the square objects. For clustering other types of objects such as triangular and hexagonal objects, one may have to devise different motion strategies to manipulate them.

For the analysis of the clustering dynamics, we only consider interactions between robots and objects. We assume that our clustering results will be interpretable with-

out considering any consequences of the robot-to-robot interactions in our experimental setting. The size of a group can be a critical factor in the system performance since interactions between robots increase with greater numbers of robots (Lerman and Galstyan, 2002). In order to grasp the general effects of the number of robots on the clustering performance, it is necessary to explore additional experimental conditions.

Another limitation is that our experimental setting fixes the proportion of the arena's area to the occupied area of objects. Thus, our work does not deal with the relationship between the densities of objects and the arena's scale. (Note: when we conducted the clustering experiments with the same area ratio the arena to objects (e.g. an arena twice the original size and double objects), the clustering dynamics in each case showed the same results).

4. A NEW STRATEGY AND MODELS FOR OBJECT CLUSTERING: A MATTER OF THE BOUNDARY*

Several earlier studies have pointed out that clustering along the boundary of the workplace harms central clustering performance; a wide range of solutions have been proposed for producing such central clusters despite the boundaries. For example, Holland and Melhuish (1999) conducted empirical study of this boundary effect and proposed a method that the robots opted not to deposit the objects by measuring the distance to the boundary. Since our robots are unable to recognize boundaries, their sensor-based solution cannot be applied to our scenario. Also, despite the significant influence of the boundary on the clustering process, many researchers have still ignored or simplified the effect of the boundary when building a clustering model. One standard way is to ignore consideration of where the clusters are formed, ignoring their positions. This is fallacious because the boundaries themselves buttress clusters making them behave as if they are parts of a much larger (even infinite) cluster.

In this section, we design a clustering system to generate a single central cluster. We use simpler robots than previous approaches and propose an effective solution that is able to overcome the boundary effect by managing the spatial densities of robots. we also introduce an extended analysis of the clustering system by considering the effect of the boundary and derive a condition that is required to avoid the boundary interference. To be specific, we will enrich prior models by treating

*Parts of this section are reprinted with permission from "Self-organized clustering of square objects by multiple robots" by Y. Song, J.-H. Kim, and D. A. Shell, *Swarm Intelligence*, 7461:308-315, Copyright[2012] by Springer Berlin Heidelberg and "A new model for self-organized robotic clustering: Understanding boundary induced densities and cluster compactness" by J.-H. Kim and D. A. Shell, *2015 IEEE International Conference on Robotics and Automation*, 5858-5863, Copyright[2015] by IEEE.

spatially the densities of robots, with respect to a difference between boundaries and the central region of the workspace, and seek the solution that the boundary interference in the clustering system is negligible or eliminated entirely. We then validate the derived condition for evolution of the largest central cluster through analysis of the local densities of the robots in our approach.

4.1 A Novel Approach for Object Clustering

Almost all previous works employ richer sensing: including sensors to detect and differentiate other robots, objects, and boundaries. Many of the robots are equipped with manipulation mechanisms of one sort or another (C-shaped scoops, grippers, shovel, etc.) that pick up or hold objects. In this study, by using the simple robots, iRobot Create platform (See Section 3), we attempt to implement the clustering system in which the robot unknowingly overcomes the boundary effects with only motion behavior without the sensor for distinguishing boundaries.

4.1.1 Motion Strategies

We first implemented a strategy based on examples in the literature, called the basic mode, as a Baseline for comparison. We then introduce a new approach we call the mixed strategy, so named because it involves two complementary behaviors that the robots in the group execute concurrently. These two novel behaviors twisting and digging are described below. We stress that both are simple modes of operation, and since a single square object is effectively invisible, both overcome partial sensor blindness through open-loop control strategies. These local rules depend on the geometry of the objects being clustered: manipulation and contact uses the shape and size of the items under consideration, configuration of the boxes depends on the packing, itself a function of the object geometry.

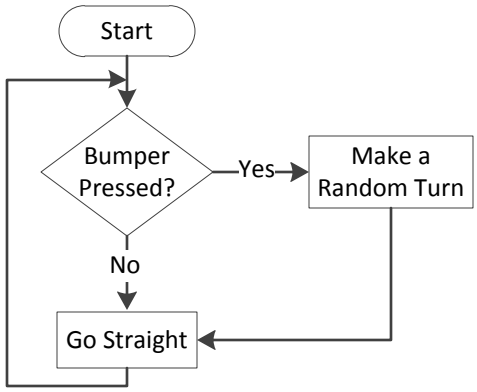

Figure 4.1: Flowchart of the basic mode.

4.1.1.1 Basic Strategy

Based on previously reported controllers, we designed a simple mechanism shown in Figure 4.1. Robots employ their bumpers in order to avoid any object that they encounter and which they cannot push. The robot's bumpers only detect box clusters and walls. Thus, in the basic mode, the robot drives straight, and if it detects either, it will make a random turn. The details are below.

```
Rule 1:
   if (Left bumper pressed or Right bumper pressed) then
      Make a random turn and go forward
Rule 2:
   Go forward
```

4.1.1.2 A Geometry Aware Strategies

In this section, we propose two new strategies in order to increase the performance of robots at the task, i.e., at forming a central cluster with square objects by overcoming the boundary effects. Our approach exploits the mechanics of square

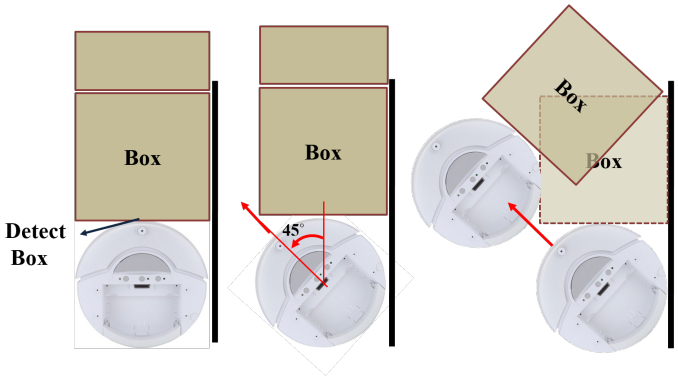

Figure 4.2: Prying motion to detach an object from the wall.

objects: as shown in Figure 4.2, striking the corner of a square object can pry it loose from a tight packing. This reduces the area in contact with the wall and makes subsequent separation more likely, especially if repetitive motions are used. Figure 4.3 shows a progress that square object is separated from the boundary by the sequence of repetitive prying motions.

Based on this concept, we introduce two new behaviors, twisting or digging. Either of them have the prying motion. The next sub-sections show details of those behaviors. Each robot employs either the twisting behavior of operation or the digging behavior of operation. But because they involve two complementary behaviors that the robots in the group execute concurrently, we call the overall approach the mixed strategy. We name a robot in the twisting behavior a twister and a robot in the digging behavior a digger. Compared to the basic strategy, only one IR proximity sensor is added to the robots.

Twisters are likely to push objects against the boundary or bring objects into the center. On the other hand, diggers further separate twisted objects from the boundary, but there is comparatively little chance that twisted objects will be brought into the center because those robots stay near the boundary. We simplify this by

Figure 4.3: Square object detaching progress by repetitive prying motions.

assuming that diggers only interact with boundary objects by performing the prying action, whereas twisters interact with all objects by randomly moving in the entire workplace. Data in Figure 4.4 provides the evidence that supports this idea by showing a spatial distribution of a twister and a digger.

4.1.1.2.1 Twisting Behavior The algorithm of a twister is detailed below.

```
Rule 1 :
   if ( Left bumper pressed  or  Right bumper pressed ) then
      if ( Timer is on ) then
         Rotate and push the object
         Disable timer
      else
         Make a random turn and go forward

Rule 2 :
```

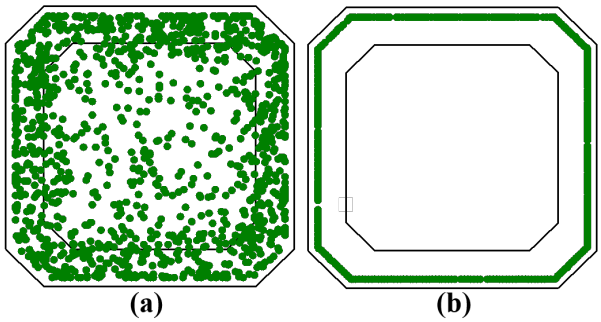

Figure 4.4: Spatial distribution of (a) a twister and (b) a digger. 1200 positions of a single twister and a single digger are plotted in the workplace, without any object, every second. In the ideal case without any interactions with other objects, the twister covers most areas of the workplace, while the digger moves around the perimeter of the boundary.

```
   if ( Wall is detected and Timer is off ) then
      Enable timer
      Follow the wall

Rule 3:
   if ( Timer is on ) then
      Follow the wall
      Reduce timer
   if ( Timer has timed out ) then
      Rotate and push the object
```

The essential idea is that a single robot's twisting motion is to strike the box at 45 degree (which it does for 3 seconds). The box is shifted through this twisting motion. Other robots that contact the box subsequently push the twisted box, and, through consecutive contacts, will robot completely detach the box from the wall, as shown in Figure 4.5. At best, two trials will affect this operation, which itself is

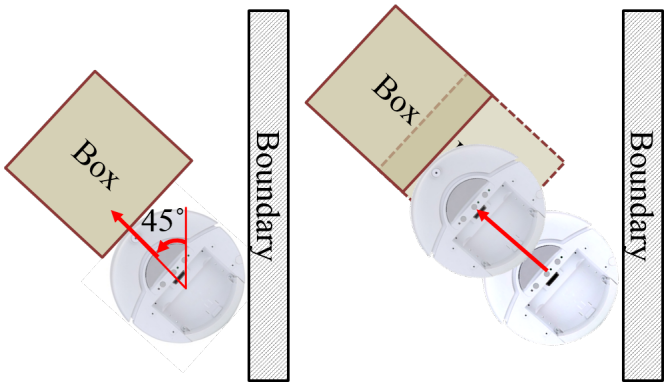

Figure 4.5: Twisting behavior on the boundary.

sufficient to increase the likelihood of central clusters. Since the bumper will not be pressed if there is a single box at the boundary, the robot will simply keep pushing the box. In this case the box is pushed into the corner of the arena. Also, since it can be counter-productive to continue wall following, the robot uses a timer to follows the wall for a maximum of 5 seconds. The twister then performs a prying motion and moves in the interior of the arena. Figure 4.6 shows the flowchart of the twister's detailed algorithm.

4.1.1.2.2 Digging Behavior Although the twisting behavior alone is able to detach the boundary objects from the wall, the majority of the boxes remained close to the boundary. Thus, we developed a digging behavior to improve separation of the boxes from the wall. The main purpose of this behavior is to clear up twisted boxes from the walls; it does this by having the robot steadily follow the wall. This method increases the probability that a robot will contact a box and separate the box from the wall. The robot finds a wall by moving in a curved path. The details are below.

```
Rule 1 :
   if ( Left Bumper pressed  or  Right Bumper pressed ) then
```

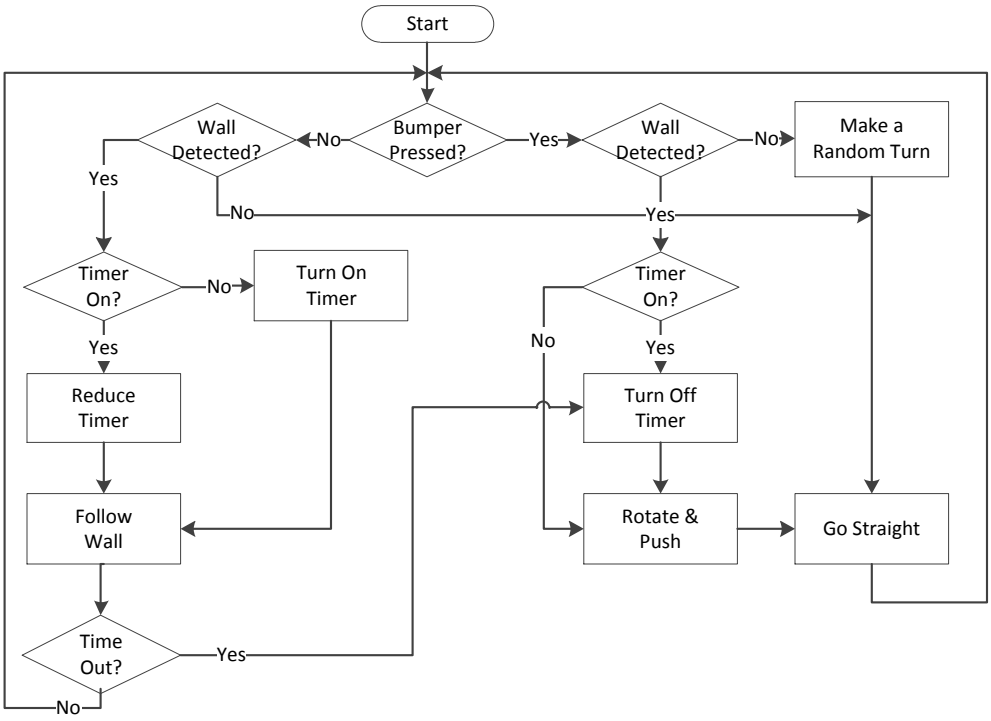

Figure 4.6: Flowchart of the twisting behavior.

```
      if ( timer is on ) then
         Rotate and push the object
         Disable timer
      else
         Make a random turn and go forward

Rule 2 :
   if ( Wall is detected  and  Timer is off ) then
      Enable timer
      Follow the wall
```

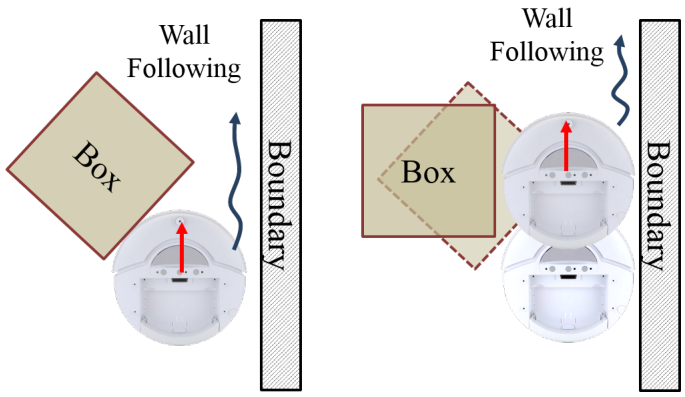

Figure 4.7: Digging behavior on the boundary.

```
Rule 3:
   if ( Timer is on ) then
      Follow the wall
   else
      Move along curved arc
```

Figure 4.7 shows the concept of separating the box by digging behavior. Since no timer is employed during wall following, the probability that the robot contacts with the box on the wall is increased. If there is an object in front of the robot, the diggers perform the same as the prying motion as twisters. The flowchart detailing the digging behavior is in Figure 4.8.

Figure 4.9 depicts scenarios possible with the robot behaviors during a clustering process.

4.1.2 Resulting Cluster Dynamics

In order to analyze the cluster dynamics by motion strategies, three trials, each lasting 90 minutes, were conducted for each experimental condition. Experiments used 5 robots and 20 objects. All experiments were recorded on a video camcorder

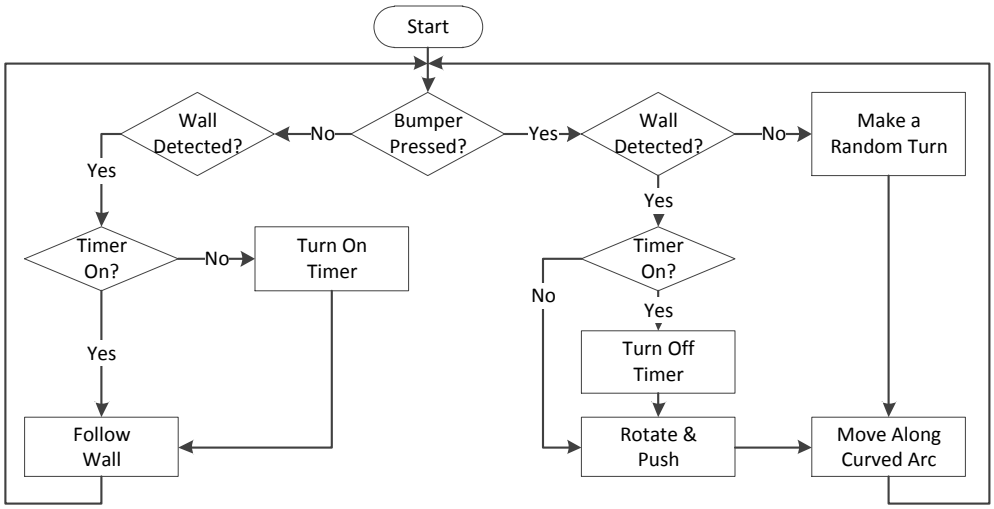

Figure 4.8: Flowchart of the digging behavior.

and annotated by observing frames at intervals of 5 seconds. We employed the following criteria for analyzing cluster dynamics. The size of a cluster was defined as a group of more than three boxes. Additionally, we distinguish between boundary clusters and central clusters.

4.1.2.1 Resulting Cluster Dynamics in the Basic Strategy

Figure 4.10 (b) shows the final configuration of the first execution of the basic strategy. In all three trials, the robots produced clusters of square objects, but most clusters formed on the boundary. Figure 4.11 (a), (c), and (e) show the development and changes in the number of objects in each cluster in the basic strategy. Notice, however, that several central clusters were formed initially. Continuous collisions with robots resulted in them being broken down within 15 minutes. By the end of the allotted time, no central cluster had formed, while several boundary clusters had emerged. The results underscore the earlier statement: the boundary has a critical effect on the cluster formation since a wall has all the properties of a large cluster.

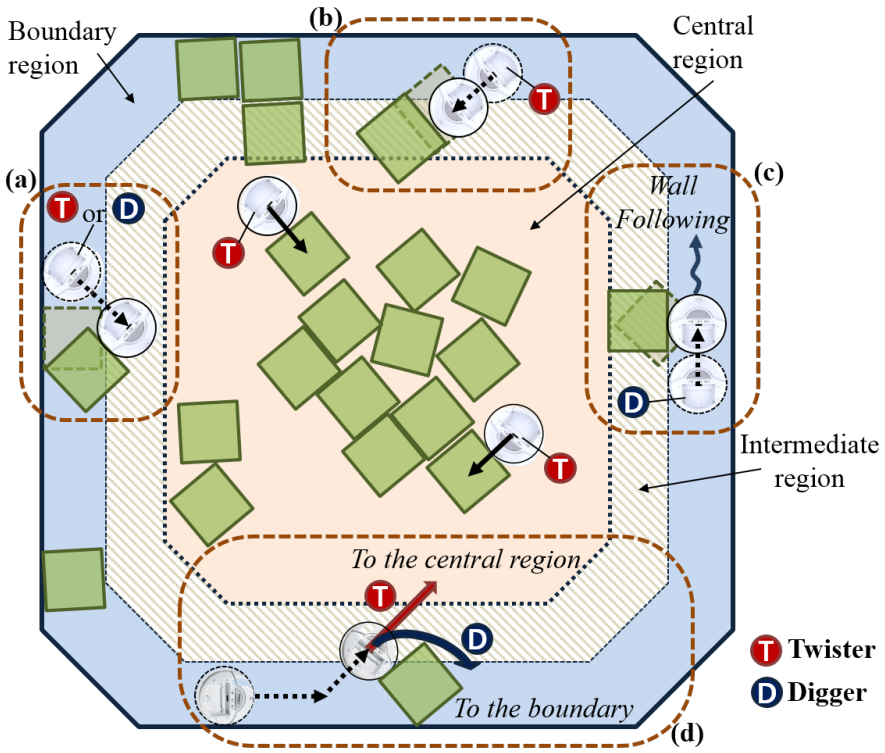

Figure 4.9: Pictorial representation of the clustering process. (a) Prying objects away from the boundary. Both the twister and the digger can pry an object loose from the boundary by hitting the corner of the square. (b) Twisting behavior on the boundary. A twister pushes the box shifted through the prying motion and brings it into the central region. (c) Digging behavior on the boundary. A digger forms gaps between boxes and boundaries and assist the prevention of boundary cluster growth. (d) Trajectories of the twister and the digger after the prying motion. Twisters move into the center, while diggers proceed along curved path to detect the boundary.

(a) (b) (c)

Figure 4.10: Physical experiments. (a) Initial configuration. (b) Final configuration using the basic strategy. (c) Final configuration using the mixed strategy (2 twisters and 3 diggers).

The workspace walls buttress the partial structures, and the box's flat edge means that the motion required to dislodge such boxes occurs only infrequently. Once a box is attached on the boundary, it is unlikely to move into the central region.

4.1.2.2 Resulting Cluster Dynamics in the Mixed Strategy

We also carried out three experimental trials under the conditions identical to the basic strategy case in order to verify the clustering performance of the mixed strategy. Five robots were used in our trials for the mixed strategy, two employed the twisting behavior and three the digging behavior. Although the twisting and the digging operations are complementary, the division of labor affects the overall performance. We present the details of the performances and clustering dynamics under different divisions of labor in next section. Figure 4.10 (c) shows the final configuration of the first trial in the mixed strategy. Unlike to the basic strategy, a single large cluster emerged in the middle of the arena in all three trials, as shown in Figure 4.11 (a), (c), and (e). The robots successfully detached the boxes in the boundary clusters and conveyed them to the central region. Figure 4.12 shows the average size of the biggest central clusters and their standard deviations through the time for the basic and mixed strategies. Although several clusters were formed

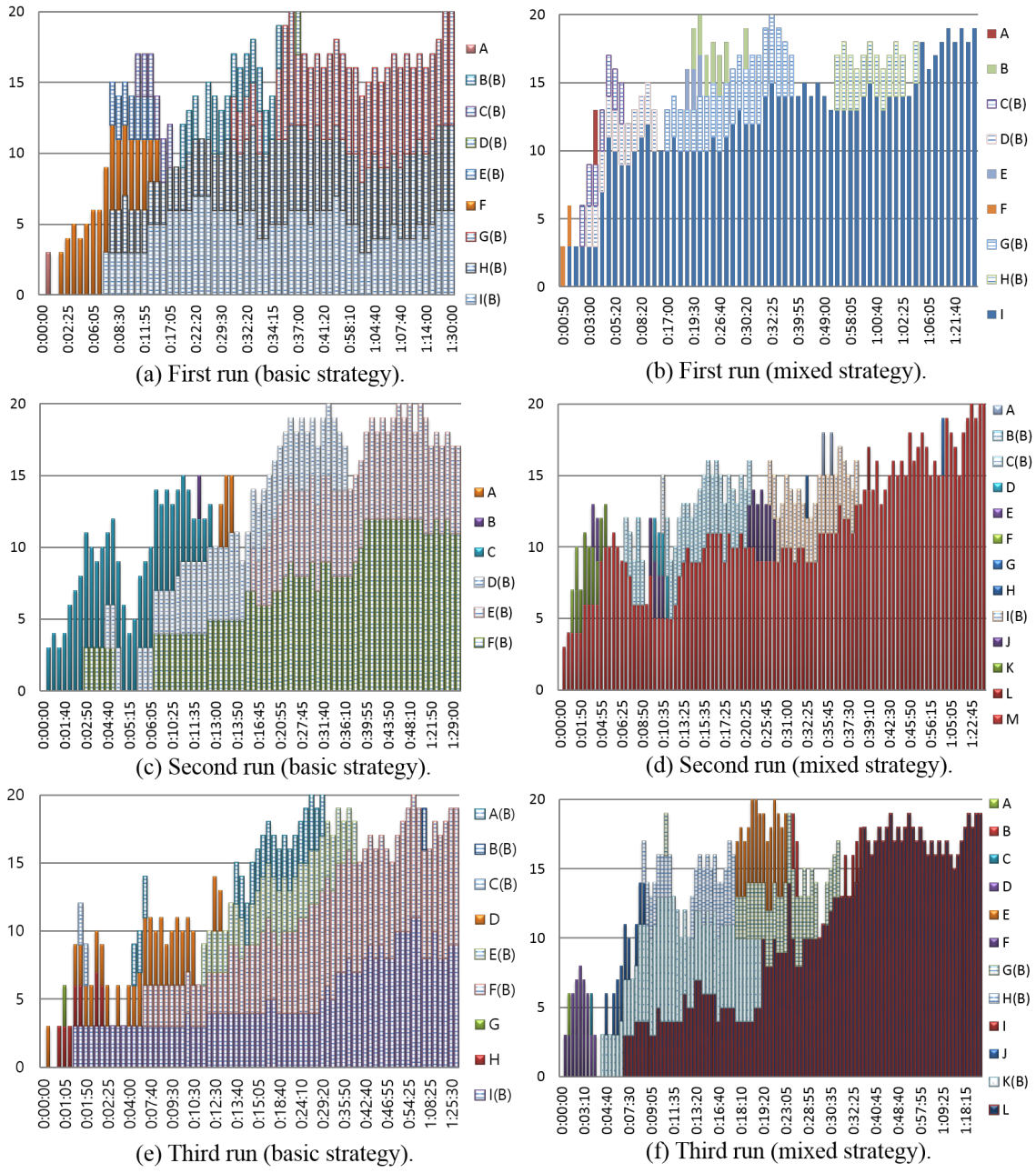

Figure 4.11: Cluster dynamics in basic and mixed strategy (2 twisters and 3 diggers).

initially in the central region, frequent collisions with the robots, in the basic strategy, provoked the collapse of central clusters within 20 minutes in any of the trials. At the end, no central cluster had been constructed, while several boundary clusters emerged in the workspace. In contrast, the average size of the remaining clusters with the mixed strategy after 90 minutes was 19.33 while no boundary cluster had formed.

In addition, the lifetimes of all boundary and central clusters were recorded in seconds throughout the experiments. Compared to basic mode, boundary clusters had much shorter lifetimes in mixed mode, and central clusters had much longer lifetimes in mixed mode (Table 4.1). There are multiple aspects which contribute to this: robots spent more time on the boundary due to the wall following behavior; they were not only taking out boxes from the boundary either in twisting or digging mode, also blocking out-going boxes. Also, the longer lifetime of central cluster in mixed mode means a dominant cluster remains in the center of the arena for a long time. The average lifetimes of all boundary clusters were 2298.13 and 719.00 seconds, and standard deviations were 2083.71 and 403.01 seconds for basic and mixed strategies. The results verify that our proposed motion strategy can overcome successfully the boundary effect and collect spatially distributed objects into only one pile at the designated position.

4.1.3 Analysis of Division of Labor

The successful results of the mixed strategy caused us to broaden our scope to consider the problem of improving the overall efficiency by tuning the division of labor. Therefore, we extended the experiments to various cases with the different ratios of twisters to diggers, and then analyzed experimental results in each case. The most significant difference between twisting and digging behaviors is the spatial

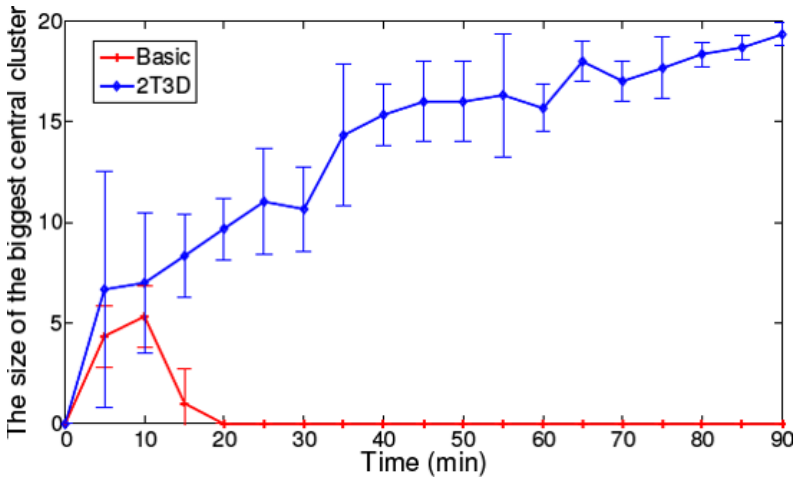

Figure 4.12: A comparison of clustering performance between basic and mixed strategies. Vertical axis is the size of the largest central cluster (essentially the same performance metric employed by Beckers *et al.* (1994).) The horizontal axis is time measured in minutes.

Table 4.1: Lifetime of clusters in basic and mixed strategies.

		Central cluster		Boundary cluster	
		Max	Mean	Max	Mean
Basic (h:m:s)	1st	0:15:00	0:07:50	1:22:25	0:35:51
	2nd	0:11:35	0:04:07	1:22:20	0:43:45
	3rd	0:12:40	0:04:48	1:28:35	0:38:26
Mixed (h:m:s)	1st	1:28:50	0:20:44	0:21:50	0:12:26
	2nd	1:29:15	0:11:01	0:15:20	0:08:28
	3rd	1:23:15	0:11:28	0:20:10	0:14:53

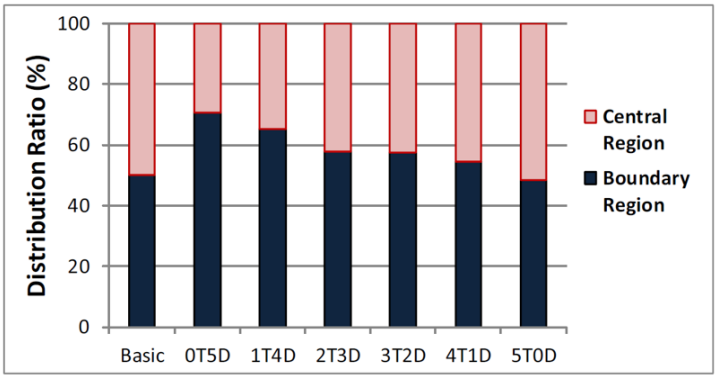

Figure 4.13: Averaged spatial distributions of the robots for particular divisions of labor (Central regions vs. boundary regions).

distribution of the robots. Due to the low probability of detecting a wall for the twister, twisters end up going around the workspace, while diggers spend comparatively more time near walls. Figure 4.13 shows the averaged spatial distributions of the robots for particular divisions of labor (these data were collected without any boxes as a baseline.) Note: we assume that the robots in basic strategy are uniformly distributed due to their random turn. The numbers of robots for each case are normalized by the number of robots in the basic case. As the ratio of diggers increases, a box on the boundary is more likely to be separated from the wall. However, it does not guarantee that the separated object will be brought into a central cluster since a digger will remain along the wall after the prying operation. From those analyses, we next consider how these differences in spatial distribution might affect clustering task progress.

4.1.3.1 Clustering Performances of Differing Divisions of Labor

We conducted three trials for all possible combinations of the twister (T) and the digger (D), from no twisters and five diggers (0T5D) to five twisters and no diggers (5T0D), under identical conditions as the previous experiments. Figure 4.14

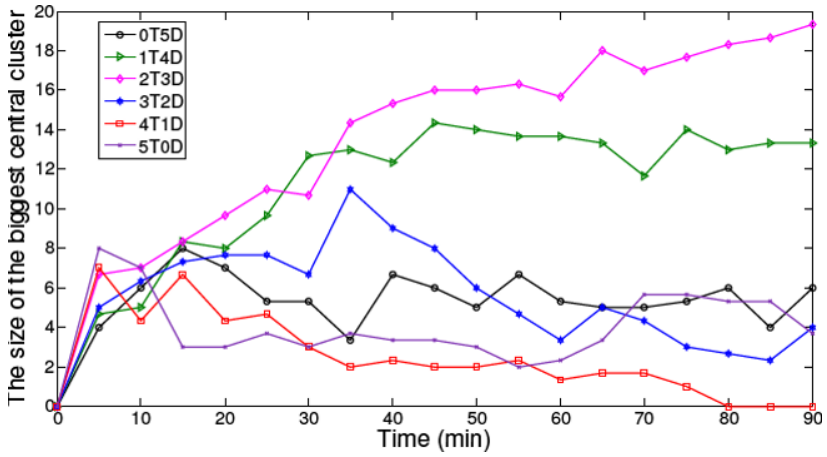

Figure 4.14: A comparison of averaged clustering performance between divisions of labor.

shows the averaged size of the largest central clusters for each case. Contrary to our expectation that all cases could achieve a satisfactory clustering performance, only three trials succeeded in forming a single central cluster having all 20 objects within 90 minutes except for 2T3D case. The successful cases were the first and second trials in 1T4D, and the third trial in 0T5D. Because Figure 4.14 is a comparative summary of many experiments and shows the means of the three trials for each division of labor, it hides a few interesting facts. For example, the 1T4D case appears to perform poorly compared to 2T3D. In fact, it was a very capable division of labor and once form a complete central cluster in the shortest observed time of 25 minutes. However, 1T4D also failed in one of its three trials. This illustrates that while 2T3D is to be preferred for reliable clustering, 1T4D may be preferred for efficient clustering.

This suggests that, given a preference between reliability and efficiency, an appropriate mix could be determined. Based on this observation, we will also address the question of how to improve the system performance by sequencing different divisions of labor in Section 6.

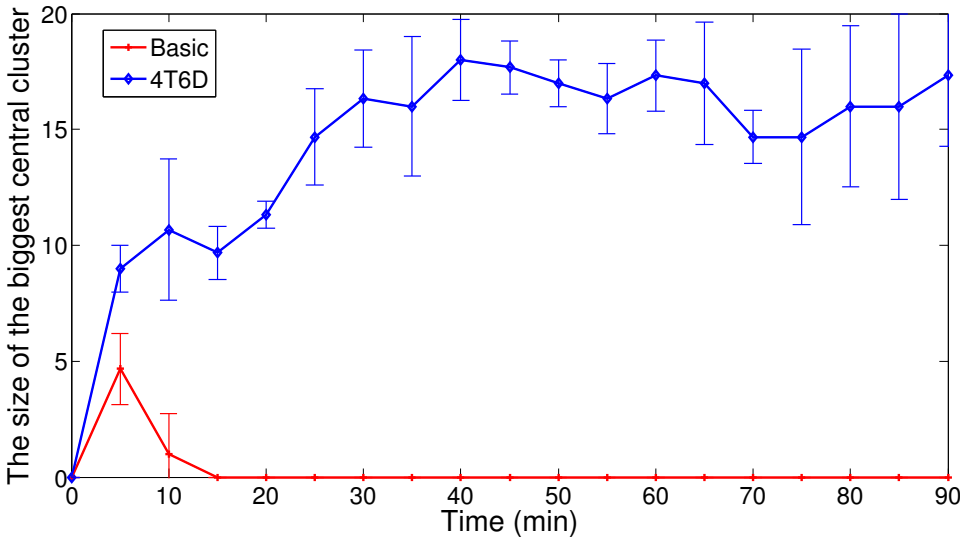

Figure 4.15: A comparison of clustering performance between the basic and mixed strategies (20 boxes and 10 robots).

4.1.4 The Effect of the Number of Robots

We also explored the effect of additional robots on the characteristics of the clustering task performance. Maris and Boeckhorst (1996) showed that the size of a robot group is a critical factor in system performance since robot-to-robot interactions increase with greater numbers of robots. They presented data showing that the mean time to achieve a single central cluster first decreases with additional robots, but then increases after the certain point. Although interactions can improve the overall performance, it can also be harmful, potentially breaking down existing clusters. In order to understand the effect of the number of robots, we carried out experiments with 10 robots, maintaining proportions consistent with the previous case for 2T3D. In other words, we used four twisters and six diggers. The basic strategy was also evaluated.

Figure 4.15 shows a clustering performance of the basic strategy and the mixed strategy (4T6D). Compared to the 5 robot cases (see Figure 4.12), the task perfor-

mances of both the basic and mixed strategies had qualitatively similar tendencies. In the basic strategy, few small central clusters were formed initially, but no central cluster emerged. In contrast, in the mixed strategy, the clustering performance increased gradually with time and formed the cluster having 19 boxes in the end in two of the three runs; the third run produced two central clusters, but no boundary clusters. However, some interesting differences between 5 and 10 robots experiments should be noted: the progress of clustering task was faster. With 10 robots, central clusters, in basic strategy, were easily broken down compared to the 5 robots case, taking an average time of 17 minutes (compared to 10 minutes) until all central clusters were disappeared. On the other hand, in the mixed strategy, less time was required to reach a single central cluster having 16 boxes (80%) as the number of robots changes from 5 to 10: the average time decreases from 48 minutes to 33 minutes. Although the greater numbers of robots reduce the required time, it appeared to cause the performance to fluctuate more.

4.2 New Models of Robotic Clustering Systems

In this section, we introduce new models that describes the clustering dynamics. Our models treat the spatial densities of robots by dividing the workplace into the boundary region and the central region.

First of all, we need to investigate clustering models that were developed in earlier studies. Figure 4.16 illustrates an abstract state diagram of the clustering system in the conventional model. The existing clustering model explains the clustering process without distinction of the formed locations of clusters in the workplace. But since this model ignored the interactions between the boundary objects and robots (the part shown within a dotted line), which occur in practice, it cannot address the problem of boundary effects in clustering systems. In order to analyze the clustering

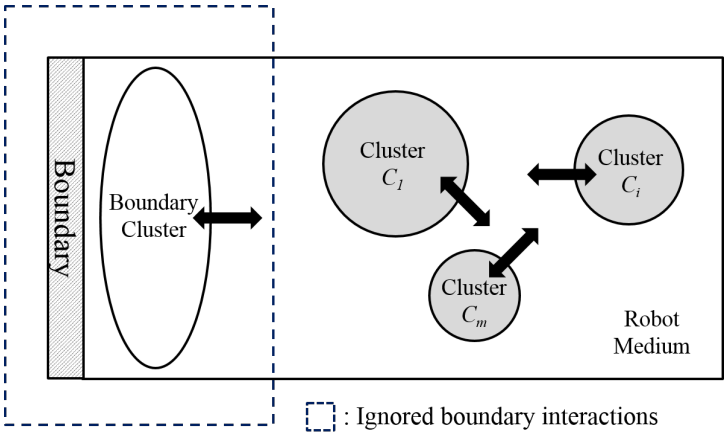

Figure 4.16: An abstract state diagram of the clustering system shown in the conventional model.

system with consideration of the boundary interference, we divide the workplace into a central region and a boundary region. In practice, multiple clusters emerge in the central region or the boundary through interactions between robots and objects in the workplace. We now extend the clustering model to consider the effect of the boundary.

4.2.1 A Model for the Boundary Region

If we assume that the robots possess a special treatment to release stuck boxes from the boundary, we can model a transition back toward the center region. (If not, this flux will work out to be zero, as expected).

Figure 4.17 shows the abstract state diagram of our clustering scenario. The robots are capable of pushing an object, and depositing or removing an object from any cluster. This means that robots can be thought of as a medium in which the clusters occur. Here, we consider one form of robot media for the boundary and another for the central region. We also assume that the objects in the workplace belong to one of four possible states: the object on the boundary (O_b), an object

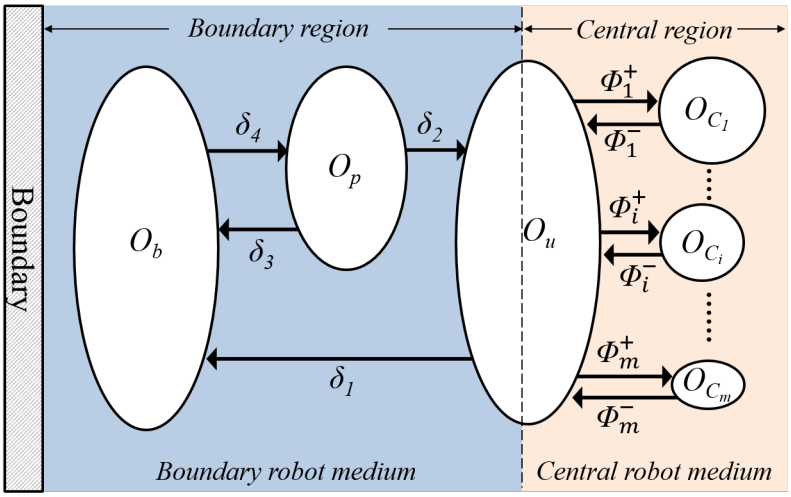

Figure 4.17: An abstract state diagram of the proposed clustering system.

pried away from boundary (O_p), the unclustered object in the central region (O_u), and the object belonging to any central cluster (O_{Ci}).

Let us first examine the robot medium and objects in the boundary region (we will investigate the central region in the following section). While clustering work proceeds from the efforts of multiple robots, the unclustered objects in the central region O_u can be transferred to the boundary O_b through the boundary robot medium. On the other hand, objects belonging to O_b may still stick on the boundary of the workplace or be detached from the boundary region by robots special treatment. We define O_p as an intermediate transition state (transition from O_b to O_u), which represents objects pried away from the boundary by a special operation of robots. The objects in O_p, which are transferred from O_b, can be transferred to O_u or revert to the boundary O_b by interactions with robots moving into the boundary.

Lerman *et al.* (2001) assumed that the robots complete the state transitions on a short enough time scale in order to construct a model of collaboration in a multi-robot system. Under this assumption, they described how the dynamic variables change

in time as a series of differential rate equations. We here use the same assumption, proposed by Lerman et al. Let δ be the number of objects transferred between states during a single time interval. According to the diagram in Figure 4.17, the rates of change of the objects in the boundary region will be

$$\frac{dO_u}{dt} = \delta_2 - \delta_1, \tag{4.1}$$

$$\frac{dO_p}{dt} = \delta_4 - \delta_3 - \delta_2, \tag{4.2}$$

$$\frac{dO_b}{dt} = \delta_1 + \delta_3 - \delta_4. \tag{4.3}$$

In general, self-organized clustering progress is non-stationary because the robots in the medium randomly interact with objects within the workplace. On the basis of this characteristic, we assume that the rate of change of objects in each state depends on the averaged frequency of interactions between individual robots and objects in the same region. That is, the more frequent contacts between scattered objects and the robots available to manipulate them, the greater the number of the state transitions of objects. Then δ can be expressed in terms of the local densities of robots available to remove an object and the likelihood of object removal. Let $\rho^{\circ}(\cdot)$ be the time averaged local densities of robots capable of removing objects in a certain state (or a condition causing a state transition). Also, let $L^{-}(\cdot)$ denote the likelihood of object removal in a certain state by robots. With this notation, each δ

can be written as

$$\delta_1 = \rho^{\circ}(O_u \to O_b) \cdot L^{-}(O_u), \tag{4.4}$$

$$\delta_2 = \rho^{\circ}(O_p \to O_u) \cdot L^{-}(O_p), \tag{4.5}$$

$$\delta_3 = \rho^{\circ}(O_p \to O_b) \cdot L^{-}(O_p), \tag{4.6}$$

$$\delta_4 = \rho^{\circ}(O_b \to O_p) \cdot L^{-}(O_b). \tag{4.7}$$

4.2.2 The Synthesis of an Entire Model

We developed an extended model that reflects the dynamics of boundary objects. With this extension, we can explain how clustering systems operate, including the effect of the boundary.

Now suppose the entire workplace is partitioned into a central region and a boundary region. The clustering process in the central region can be treated with models such as those by Martinoli *et al.* (1999b) or Kazadi *et al.* (2002). As shown in Figure 4.17, multiple central clusters interact with each cluster and unclustered objects in the central robot medium. By picking subscripts, without loss of generally, we assume that the sizes of central clusters are $C_1 > \cdots > C_i > \cdots > C_m$. That is, C_1 is the largest central cluster and C_m is the smallest one. The rate of change of the i^{th} central cluster will be

$$\frac{dO_{C_i}}{dt} = \Phi_i^{+} - \Phi_i^{-}, \tag{4.8}$$

where Φ_i^{+} is the number of unclustered objects that are deposited into the i^{th} central cluster and Φ_i^{-} is the number of objects that are removed from the i^{th} central cluster. According to a probabilistic analysis based on geometric characteristics of clusters, larger clusters will be more likely to obtain objects and less likely to lose objects

than smaller clusters.[†] That means

$$\frac{dO_{C_i}}{dt} = \Phi_i^+ - \Phi_i^- > 0, \tag{4.9}$$

$$\frac{dO_{C_m}}{dt} = \Phi_m^+ - \Phi_m^- < 0. \tag{4.10}$$

Under a recurrence of this clustering process, the large clusters grow bigger, while the smallest cluster becomes smaller and will eventually disappear. The model for central clusters will also be extended by the notion of the compactness of the clusters in the next section.

By considering clustering dynamics not only in the central region but also in boundary clusters, we can understand the evolution of the largest central cluster more precisely, and also the decay of boundary clusters.

4.2.3 Conditions to Prevent the Problem of Boundaries

So far, we have developed rate equations to describe the extended clustering system. We now turn to examine a condition to prevent boundary clusters from growing.

A net flow of objects between the boundary region and the central region is determined by interactions between the boundary robot medium and O_u. That is, if $\frac{dO_u}{dt} = \delta_2 - \delta_1 > 0$ in the boundary region, the number of objects in O_b will decrease and the quantity of O_u will increase, as time progresses. If we assume that the number of objects in O_p is stationary, existing in an intermediate state, we obtain $\frac{dO_p}{dt} = \delta_4 - \delta_3 - \delta_2 = 0$. Rearranging $\delta_2 - \delta_1 > 0$ and $\delta_4 - \delta_3 - \delta_2 = 0$, we can find that $\delta_2 > \delta_1$ and $\delta_2 = \delta_4 - \delta_3$.

Thus, a condition required for O_u to grow and for O_b to shrink may be written

[†]The basic argument is that it is easier to strike a smaller cluster at an oblique angle that draws away an object than a large one. A very large cluster has only tangents to the cluster perimeter.

as

$$\delta_4 - \delta_3 - \delta_1 > 0 \tag{4.11}$$

and so

$$\delta_1 + \delta_3 < \delta_4. \tag{4.12}$$

Equation (4.12) is ultimately the same as $\frac{dO_b}{dt} < 0$.

From Equations (4.4), (4.6), (4.7), and (4.12) we obtain

$$\rho^{\circ}(O_p \to O_b) \cdot L^{-}(O_p) + \rho^{\circ}(O_u \to O_b) \cdot L^{-}(O_u) < \rho^{\circ}(O_b \to O_p) \cdot L^{-}(O_b). \tag{4.13}$$

If the majority of robots, possessing a special treatment for boundary objects, that encounter objects on the boundary successfully pry them away from the wall, we can assume that $L^{-}(O_b) \simeq 1$. Furthermore, if robots can always push a single object, such as an unclustered or a pried object without loss, we assume that $L^{-}(O_p) \simeq 1$ and $L^{-}(O_u) \simeq 1$. Under these assumptions, in order for boundary objects to be removed from the boundary region,

$$\rho^{\circ}(O_p \to O_b) + \rho^{\circ}(O_u \to O_b) < \rho^{\circ}(O_b \to O_p). \tag{4.14}$$

We hypothesize that if the time averaged local densities of employing robots satisfy (4.14), the boundary interference in the clustering system will be negligible or eliminated entirely.

4.3 Robot Spatial Distribution with Respect to Division of Labor

In the previous section, we showed that the spatial density of robots can be an important factor that should be considered in clustering tasks. Structures in an

environment involve the mechanics of subsequent cluster formation and the distribution of robots. The position of robots in basic mode is less sensitive to a change of environments, but robots in mixed mode actually reflect environmental changes (more objects in the central region, fewer robots in the central region). This latter aspect may contribute to the successful movement of all the objects to the workspace center.

Through theoretical models, we also derived the condition to be able to prevent boundary cluster growth by managing the time averaged local densities of robots. In this section, we investigate our clustering systems meet the requirements for evolution of the largest central cluster in order to verify our hypothesis that if the time averaged local densities of robots satisfy the condition (4.14), the boundary interference in the clustering system will be negligible or eliminated entirely.

In order to examine how the local densities of the robots influence the formation and destruction of boundary objects, we implemented a simulator to measure the spatial densities of robots by divisions of labor. The simulator is implemented with Box2D, which is a widely used physics simulator engine[‡]. The simulation environment is designed to the scale of our real environment, which we conducted in the previous section. We performed simulations for all mixes of the Twister (T) and the Digger (D) with 5 robots: 1T4D, 2T3D, 3T2D, and 4T1D. We also used 20 objects, and 20 runs, each lasting 20 minutes, for each experimental condition (simulation speed is six times faster than the physical experiment). Figure 4.18 shows our simulator that conducts clustering 20 square objects with 5 robots (2T3D).

In the previous section, for our clustering system composed of twisters and diggers, we explained that diggers only interact with boundary objects O_b, whereas

[‡]Box 2D is a 2D physics engine for games and an open source C++ engine for simulating rigid bodies in 2D (Catto, 2009).

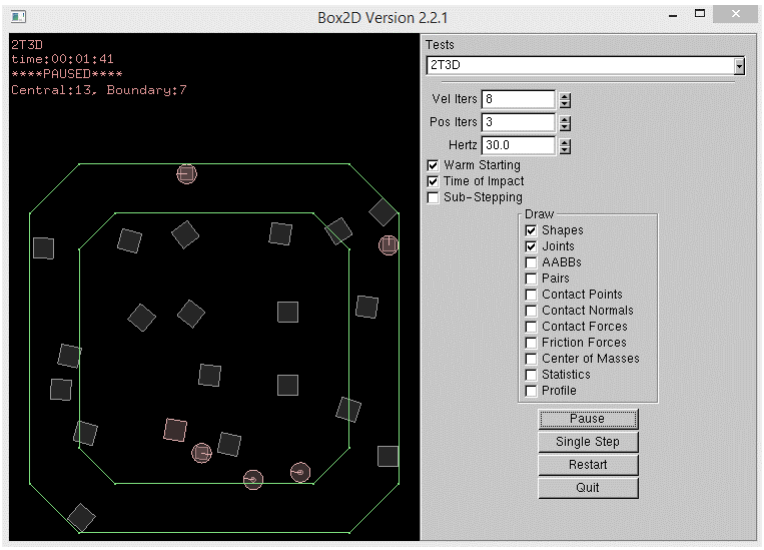

Figure 4.18: Simulator for multi-robot clustering systems with Box2D (Circles are robots, and squares are objects.)

twisters interact with all objects in the entire workplace. Thus, $\rho^{\circ}_{(O_p \to O_b)} = \rho^{\circ}_{T(O_p \to O_b)}$, $\rho^{\circ}_{(O_p \to O_u)} = \rho^{\circ}_{T(O_p \to O_u)}$, $\rho^{\circ}_{(O_u \to O_b)} = \rho^{\circ}_{T(O_u \to O_b)}$. Since prying motions by diggers more frequently occur than twisters, we can assume that $\rho^{\circ}_{(O_b \to O_p)} = \rho^{\circ}_{D(O_b \to O_p)}$. Accordingly, each δ in Equations (4.4), (4.5), (4.6), and (4.7) can be written as

$$\delta_1 = \rho^{\circ}_{D(O_b \to O_p)} \cdot L^{-}_{D}(O_b), \tag{4.15}$$

$$\delta_2 = \rho^{\circ}_{T(O_p \to O_b)} \cdot L^{-}_{T}(O_p), \tag{4.16}$$

$$\delta_3 = \rho^{\circ}_{T(O_p \to O_u)} \cdot L^{-}_{T}(O_p), \tag{4.17}$$

$$\delta_4 = \rho^{\circ}_{T(O_u \to O_b)} \cdot L^{-}_{T}(O_u). \tag{4.18}$$

Since almost all diggers that encounter objects on the boundary successfully detach them from the boundary, we assume that $L^{-}_{D}(O_b) \simeq 1$. Furthermore, since twisters can always push a single object and deposit it into a cluster, such as an unclustered or a pried object without any loss, we also assume that $L^{-}_{T}(O_p) \simeq 1$

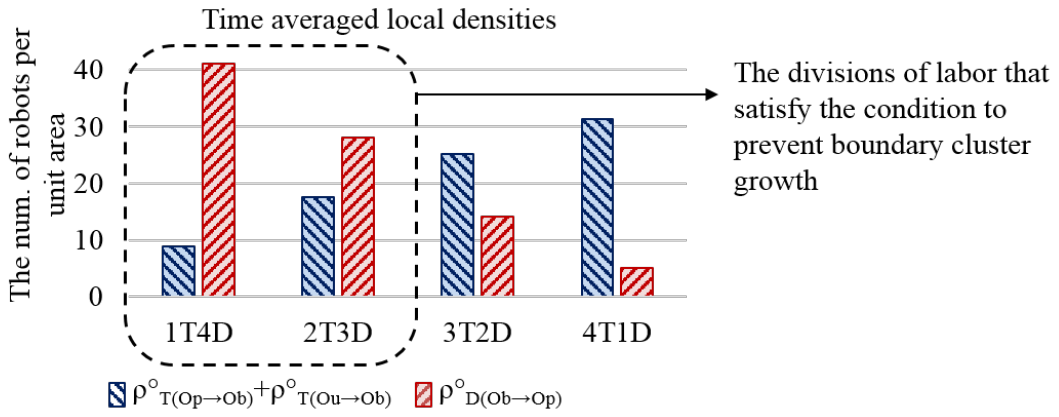

Figure 4.19: The time averaged local densities with respect to the ratio of twisters to diggers.

and $L_T^-(O_u) \simeq 1$. Hence, the condition to prevent boundary cluster growth in our clustering system will be

$$\rho^\circ_{T(O_p \to O_b)} + \rho^\circ_{T(O_u \to O_b)} < \rho^\circ_{D(O_b \to O_p)}. \tag{4.19}$$

Here we obtain the local densities of available robots capable of manipulating objects, $\rho^\circ_{T(O_p \to O_b)}$, $\rho^\circ_{T(O_u \to O_b)}$, and $\rho^\circ_{D(O_b \to O_p)}$, which only affect the condition (4.19). To measure the sum of $\rho^\circ_{T(O_p \to O_b)}$ and $\rho^\circ_{T(O_u \to O_b)}$, we observe the frequency of the twisters moving from the central region to the boundary region through the intermediate region during all trials of each mixed strategy. Then, we can obtain the sum of $\rho^\circ_{T(O_p \to O_b)}$ and $\rho^\circ_{T(O_u \to O_b)}$ by dividing the frequency by the perimeter of the central region. And $\rho^\circ_{D(O_b \to O_p)}$ is computed by counting the number of diggers passing on one point in the boundary region during the same period of time.

Figure 4.19 shows the time averaged local densities for the particular ratio of twisters to diggers in the simulation. According to our hypothesis, 1T4D and 2T3D

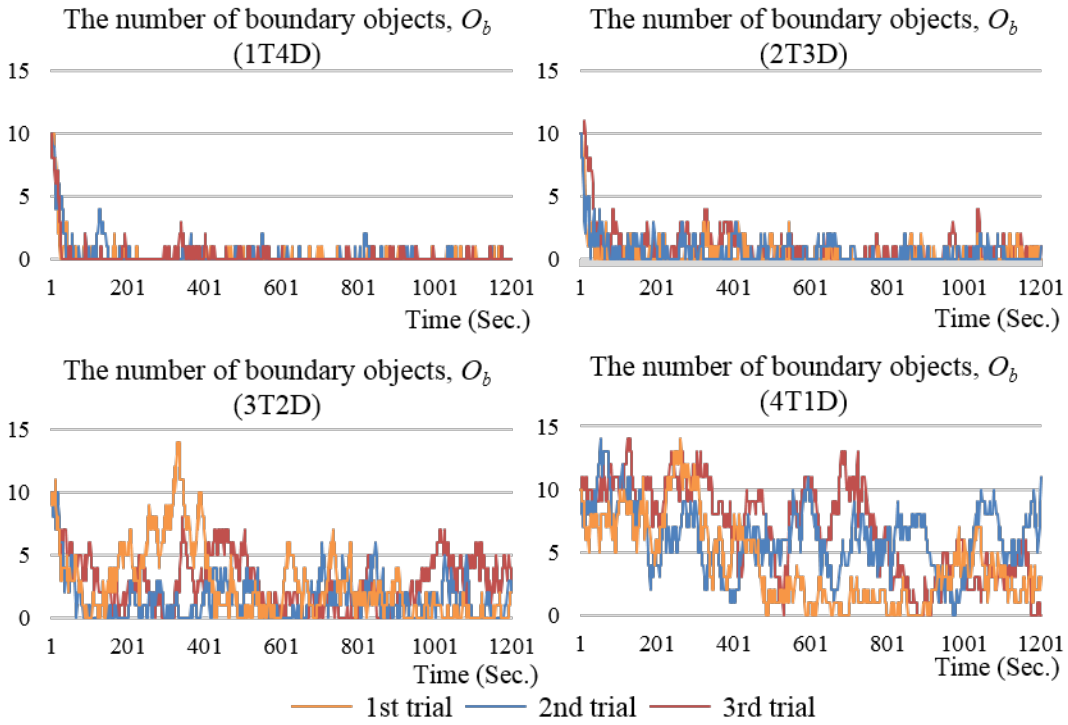

Figure 4.20: A number of objects located on the boundary region over time during the clustering process. Observed data of three of 20 trials for each labor mix are plotted.

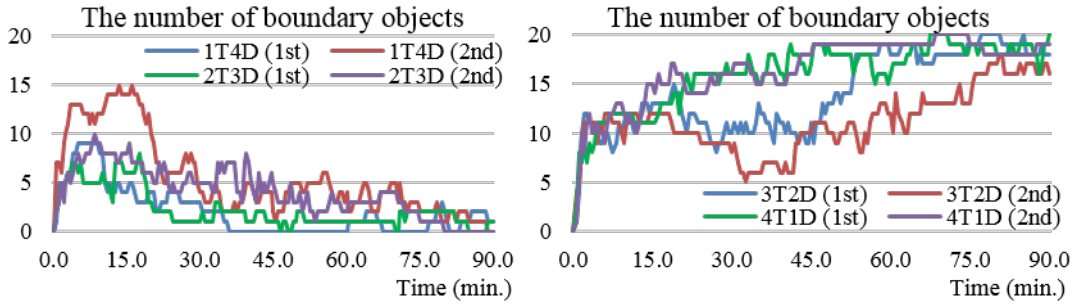

Figure 4.21: Boundary objects observed over time in physical experiments

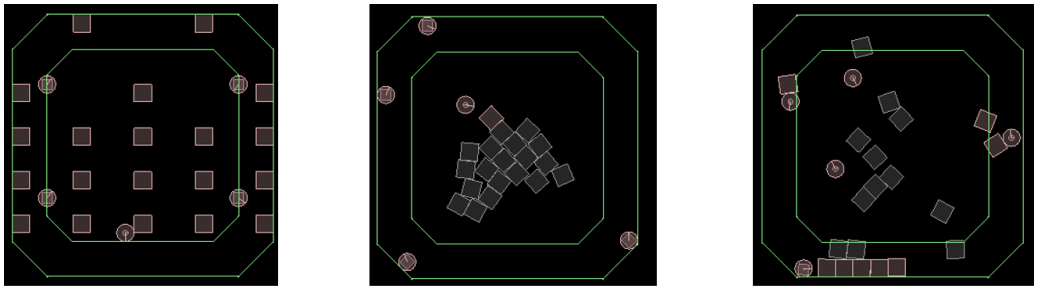

(a) (b) (c)

Figure 4.22: Simulation experiments. (a) Initial configuration (10 unclustered objects and 10 boundary objects). (b) Configuration using 1T4D (at 16 min). (c) Final configuration using 4T1D (at 20 min).

(a) (b) (c)

Figure 4.23: Physical experiments. (a) Initial configuration. (b) Final configuration (1T4D). (c) Final configuration (4T1D). Each trial lasted 90 minutes, with 5 robots and 20 objects.

Table 4.2: Averaged object distribution (The average of 20 trials in each mixed strategy).

	The number of objects		
	O_u	O_p	O_b
1T4D	18.345	1.3708	0.3006
2T3D	17.712	1.6706	0.6344
3T2D	15.431	2.2206	2.3647
4T1D	11.995	2.3119	5.7097

are strategies that satisfy the condition (4.14) to stop boundary cluster growth. In order to validate our hypothesis, we analyzed the frequency of boundary objects over time. Figure 4.20 presents the number of boundary objects with respect to the robot division of labor during the clustering process in the simulation. As hypothesized, all trials for 1T4D and 2T3D successfully detached objects from the boundary. In contrast, the robots of 3T2D and 4T1D failed to eliminate the boundary objects and even made the boundary clusters grow. Table 4.2 shows the averaged object distribution of 20 trials in each mixed strategy. We can observe that since the average size of O_b in 1T4D and 2T3D is below 1, those strategies can prevent forming boundary clusters. However, 3T2D and 4T1D struggled to eliminate the boundary objects. The results support our hypothesis, and are also reflected in simulation experiments.

In physical experiments, the results are similar to simulation results. As shown in Figure 4.21, all trials of 1T4D and 2T3D successfully prevented forming boundary clusters. However, 3T2D and 4T1D failed to remove objects from the boundary and eventually formed only boundary clusters. Figure 4.22 and Figure 4.23 show the results of each mixed strategy in the simulation and the physical experiments. We observe in both environment that 1T4D successfully forms a single central cluster, but 4T1D failed throughout.

In short, if we can control the local densities of each robot having a different purpose (here, twisting and digging behaviors), we can prevent the boundary interference in the clustering system which harms central clustering performance. We are not aware of other work which has influenced the density of robots in order to influence cluster formation, let alone in some systematic way.

4.4 Summary and Contributions

In this section, we proposed two complementary behaviors, twisting and digging, for clustering square objects. Through physical robot experiments, we also demonstrated that the mix of two behaviors permits the robots to overcome the boundary effect and successfully form only a single central cluster. Our approach focused on managing spatially the densities of robots, executing only motion behavior without any special manipulator.

We also developed a mathematical model to describe the dynamics of a multi-robot clustering system. We contribute a model which considers heterogeneity in different behavior as a function of location. Through this model, we can capture a notion of local spatial density, and enable us to analyze the clustering system with consideration of the boundary interference. Also, using this model, we can find out the solution that the problem of the boundary in the clustering system is negligible by the appropriate local densities of robots.

Additionally, we investigated how different proportions of the diggers and the twisters affect the clustering progress and verified that selection of the appropriate ratio is important for the cluster evolution. This shows a new task domain for division of labor problems. In this regard, it is a departure from the focus within the literature, which assumes a uniform distribution of robots. It suggests that one way to direct such self-organized systems might be to influence where they spend their time in the environment. This simple idea can be a new approach to implicitly coordinate self-organized multi-robot robot systems.

5. THE IMPACT OF CLUSTER SHAPE AND OBJECT GEOMETRY ON THE CLUSTERING DYNAMICS *

Thus far, we extended prior models by dealing with the spatial densities of robots and cluster's position. Many studies pointed out that the cluster's geometry is an important determinant of whether the cluster will grow or shrink. A common simplifying assumption underlies existing clustering models, including the classic work (see Section 2) and our previous work. It is that a cluster containing n objects is well-packed and rotationally symmetric. Yet there are no *a priori* limits on the specific arrangement of objects and direct observation shows that clusters can often form a diverse set shapes in practice. Few would dispute that the clustering process depends on the geometric characteristics of clusters, but perhaps the conventional explanation falls short: the explanation for the emergent phenomenon proffered hinges exactly that aspect —cluster geometry— which is also approximated in only the grossest way.

In truth, the existing research has focused on cylindrical objects such as pucks and frisbees and these are settings where the rotationally symmetric and well-packed assumption is probably most innocuous. Here we tackle the problem of clustering square and rectangular objects which produce widely different packings. This study first analyzes the clustering system of square objects to investigate the impact of the cluster's geometry on the clustering dynamics. Then we extend the analysis of the clustering system by considering various rectangular objects beyond the regular polygonal objects, developing the cluster occurrence models based on a probabilistic method.

*Parts of this section are reprinted with permission from "A new model for self-organized robotic clustering: Understanding boundary induced densities and cluster compactness" by J.-H. Kim and D. A. Shell, *2015 IEEE International Conference on Robotics and Automation*, 5858-5863, Copyright[2015] by IEEE.

Figure 5.1: An example of an asymmetric cluster in an experiment. The cluster is elliptical in shape (see red oval).

5.1 Existing Mathematical Models of Clustering Dynamics

Two influential mathematical models of clustering dynamics relate to our work for object clustering. First, Martinoli *et al.* (1999a,b, 2004) proposed a method of building probabilistic clustering models in collective robotics, applying it to an aggregation experiment. They focused on describing the clustering process with numerical models rather than by statistical analysis of clustering progress and results. In contrast, Kazadi *et al.* (2002, 2004a,b)'s mathematical model of clustering dynamics described cluster growth properties by connecting geometric characteristics of the clusters to the probability of cluster modification such as object deposit or removal in the cluster. Both studies assume in common that a cluster is rotationally symmetric and circular, a fact often violated in practice especially as one explores objects with a variety of shapes. Figure 5.1 indicates an example of an asymmetric and loosely packing cluster in a physical clustering experiment, motivating closer examination of the geometries involved in order to better understand what influences the cluster modification probability. First, let us take a look closely at mathematical clustering models in existing studies.

5.1.1 Martinoli's Probabilistic Model for the Prediction of the Clustering Performance

Martinoli (1999) proposed a method of developing probabilistic models to predict clustering dynamics. In order to understand the aggregation experiment with a group of autonomous robots, he attempted to explain the clustering process by the numerical and probabilistic models rather than by descriptions of clustering results based on statistical analysis. He pointed out that the statistical analyses in existing clustering studies can not identify the systems parameters which affect the clustering performance as well as high variability in the clustering performance by random interactions in the non-deterministic environment.

His approach is to predict the clustering performance with probabilistic simulations by modeling parameters that are influential on clustering progress. As shown in Figure 5.2, the simulation based on the probabilistic model is made up parallel processes of multiple robots, while updating the change of the environmental state in every step. This clustering model is flexible since the parallel processes or the probabilistic blocks can be easily added in the model.

In this model, a robot's behavior is also implemented to a probabilistic model based on a control policy in a robot controller and interactions between robots and the environment. The probabilities that robots encounter an object or a cluster are calculated by the ratio of their area to the area of the whole workplace; the probabilities of modifying clusters is computed by the geometric characteristics of the cluster.

In calculating the cluster modifying probabilities, he considered three modifying probabilities: 1) the probability of incrementing the cluster's size, 2) the probability of decrementing the cluster's size, and 3) the probability of leaving the cluster un-

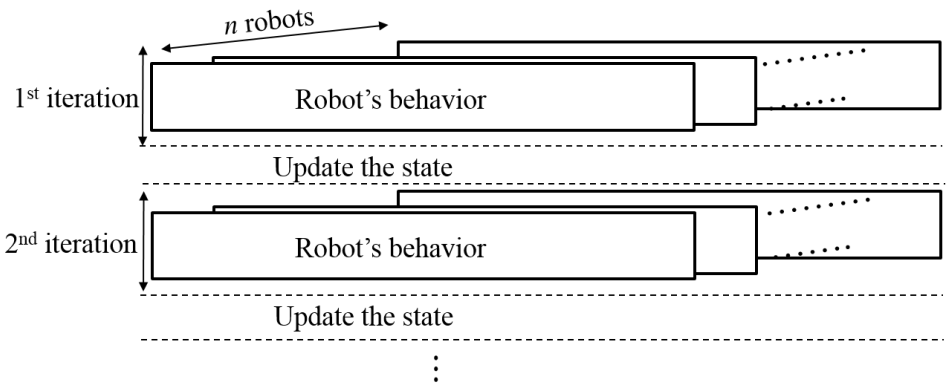

Figure 5.2: A flowchart illustrates Martinoli's simulation model by parallel processes of individual robots' behaviors.

modified. These probabilities are calculated under an assumption that the cluster's size is increased or decreased by one object through interactions with robots. The probability of incrementing the cluster can be easily obtained by considering only robot's holding state since robots carrying an object always deposit successfully it into a chosen cluster. Whereas, for computing the geometric probability of decrementing cluster's size, the approaching angle and the contact point between a robot and cluster are important factors. For example, when an empty robot strikes an edge of a cluster, the cluster can be more likely to loose an object than hitting at middle points of the cluster. Figure 5.3 illustrates the method that is used to calculate the geometric probability of decreasing a cluster, denoted $P^{-}(C)$. The main idea to compute $P^{-}(C)$ is that all possible approaching points, where robots can remove an object from the cluster, integrate. If the cluster is rotationally symmetric, $P^{-}(C)$ can obtain by integrating all possible points on one side of a cluster over 360° in polar coordinates. Then, the geometric probability of decreasing a cluster $P^{-}(C)$ can be expressed as

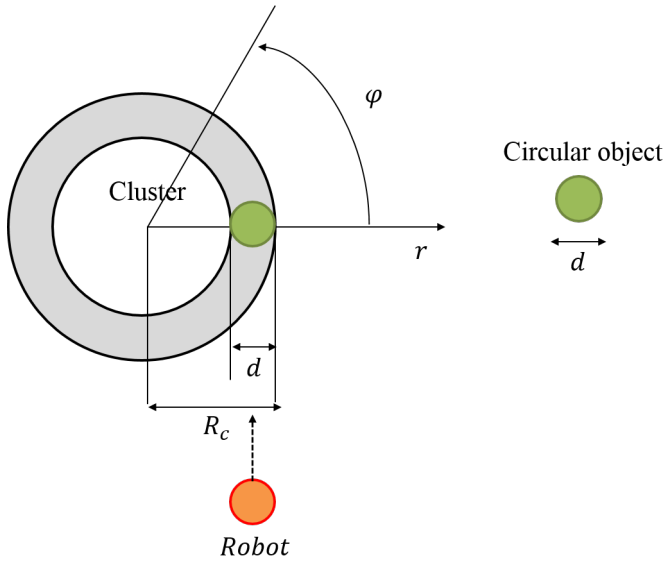

Figure 5.3: A method for calculating the geometric probability of object removal in a rotationally symmetric cluster. R_c is a cluster's radius and d is a diameter of an circular object. A shaded region shows the area that an object can be removed by a robot's pushing behavior.

$$P^{-}(C) = \int_{0}^{2\pi} \int_{R_c-d}^{R_c} p(r,\varphi)\partial r \partial \varphi, \tag{5.1}$$

where, R_c is a radius of a cluster, d is a diameter of an circular object.

Therefore, depending on the robot's holding state and robot's approaching direction into the cluster, the chosen cluster can be increased or decreased. With the logical flow by these probabilities, the clustering model predicts the clustering dynamics.

However, since this probabilistic model can analyze clustering dynamics within a limited range of the shape of the cluster (only considering symmetric forms), it has a still limited explanation on the specific arrangement of objects or a diverse shapes in practice.

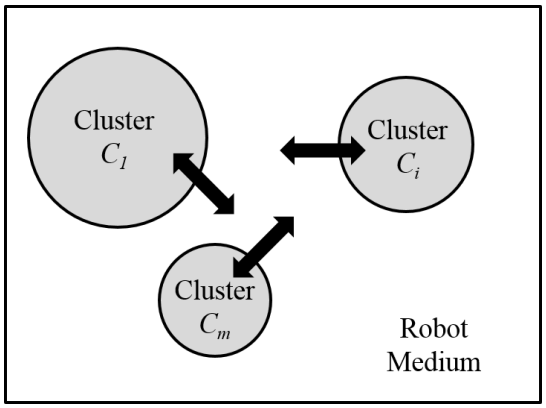

Figure 5.4: An abstract clustering systems. Each cluster is considered as effectively reservoirs of objects, and robots are considered as pathways for objects to transfer between clusters.

5.1.2 Kazadi's Mathematical Model for Clustering Dynamics

Kazadi *et al.* (2002) also proposed the mathematical model to explain clustering dynamics. They examined the clustering systems of robots and clusters in which robots are considered as a transport media which is able to randomly select clusters and interact with them (See Figure 5.4).

The interactions between robots and clusters are dictated by the state whether the robots are capable of removing an object in the selected cluster or carrying an object to be able to deposit it in the cluster. They then explained clustering dynamics by mathematically describing a iterative process whereby an individual robot interacts with a randomly selected cluster at each time step. They also pointed out that the size of the chosen cluster is also a variable that can affects the consequence for clustering dynamics through the robots' interactions. In particular, they attempted to derive conditions to generate a single cluster by approaching the question of whether a cluster will evolve or degrade or not depends on the interactions with the other clusters. To be specific, through the interaction between clusters via robot medium,

each cluster can produce unclustered objects which may be deposited into any cluster as well as absorb evaporated objects. On the basis of these assumptions, they developed the rate equations of change of objects in a system of m clusters (clusters $C_1, ..., C_i, ..., C_m$ contain $N_{C_1}, ..., N_{C_i}, ..., N_{C_m}$ objects) as follows,

$$\frac{dN_{C_1}}{dt} = N^{\bullet}_{robot} \cdot P^{+}(C_1) - N^{\circ}_{robot} \cdot P^{-}(C_1), \tag{5.2}$$

$$\frac{dN_{C_2}}{dt} = N^{\bullet}_{robot} \cdot P^{+}(C_i) - N^{\circ}_{robot} \cdot P^{-}(C_i), \tag{5.3}$$

$$\vdots$$

$$\frac{dN_{C_m}}{dt} = N^{\bullet}_{robot} \cdot P^{+}(C_m) - N^{\circ}_{robot} \cdot P^{-}(C_m), \tag{5.4}$$

where, $P^{-}(C_i)$ is the probability of object removal in the cluster C_i, $P^{+}(C_i)$ is the probability of object deposit in the cluster C_i, N°_{robot} is the number of available robots to remove an object from a cluster, and $N^{\bullet}_{robot}$ is the number of robots carrying an object.

If it is assumed that the number of transfered objects in the robot media is stationary, then

$$\frac{dN_{C_1}}{dt} + \cdots + \frac{dN_{C_i}}{dt} + \cdots + \frac{dN_{C_m}}{dt} = 0. \tag{5.5}$$

From equations (5.2), (5.3), (5.4), and (5.5), solving for N_{C_m} gives

$$\frac{dN_{C_m}}{dt} = (N^{\circ}_{robot} + N^{\bullet}_{robot}) \frac{\sum_{i \neq m} (P^{+}(C_m)P^{-}(C_i) - P^{+}(C_i)P^{-}(C_m))}{\sum_i P^{+}(C_i) + \sum_i P^{-}(C_i)}. \tag{5.6}$$

If C_m is the smallest among clusters, then the condition required for C_m to shrink given that $C_1 > \cdots > C_i > \cdots > C_m$ can be written as

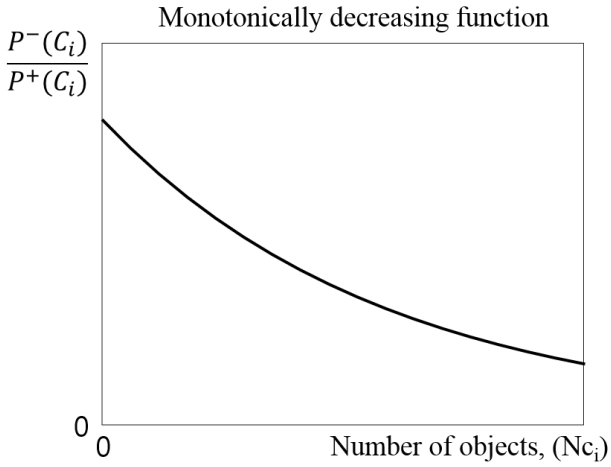

Figure 5.5: When $\frac{P^-(C_m)}{P^+(C_m)}$ is a monotonically decreasing function, it is a sufficient condition to grow for the largest cluster.

$$\frac{dN_{C_m}}{dt} < 0. \tag{5.7}$$

Therefore, from equations (5.6) and (5.7), if a system of multiple m-clusters satisfies the condition that

$$\frac{P^-(C_m)}{P^+(C_m)} > \frac{\sum_{i \neq m} P^-(C_i)}{\sum_{i \neq m} P^+(C_i)}, \tag{5.8}$$

the smallest cluster will shrink and finally be extinct as time passes. That means, by repeating the degeneration of the smallest cluster, a single cluster finally emerges in the clustering system. In addition, they claimed the cluster growth property that if $\frac{P^-(C_m)}{P^+(C_m)}$ is monotonically decreased, it is a sufficient condition for the growth for the largest cluster. Figure 5.5 is an example that the characteristics of $\frac{P^-(C_m)}{P^+(C_m)}$ satisfies the sufficient condition.

However, since Kazadi et al. developed the clustering model only with the size of

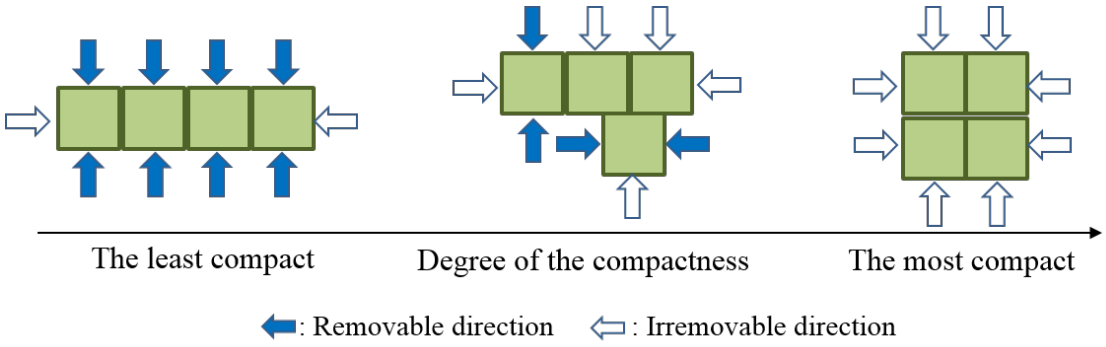

Figure 5.6: Differing degrees of compactness for clusters of the same size ($n = 4$). The more compact cluster is stable and strong because direction of contact, that the robot can remove the object, is small.

the cluster without regard to the physical geometry of the cluster in the workplace, the model has limited to explain the clustering process according to the cluster's geometry, including the physical shape of the cluster. For example, if multiple clusters exist as the same size but are formed into different shapes, the dynamics of those clusters cannot be predicted by Kazadi's clustering model.

5.2 Extended Analysis of Clustering Systems: The Shape of Clusters

As mentioned in Section 5.1, prior studies have attempted to develop theories to understand how clustering systems work and, necessarily, the theories introduced simplifying assumptions. The shape of an existent cluster affects subsequent arrangements of objects by either forming a buttress for subsequent accretive actions, or surrounding objects which are then less likely to be removed. In this section, we will examine closely how the geometry of the cluster affects the cluster evolution by treating the cluster's shape as a variable in a clustering model.

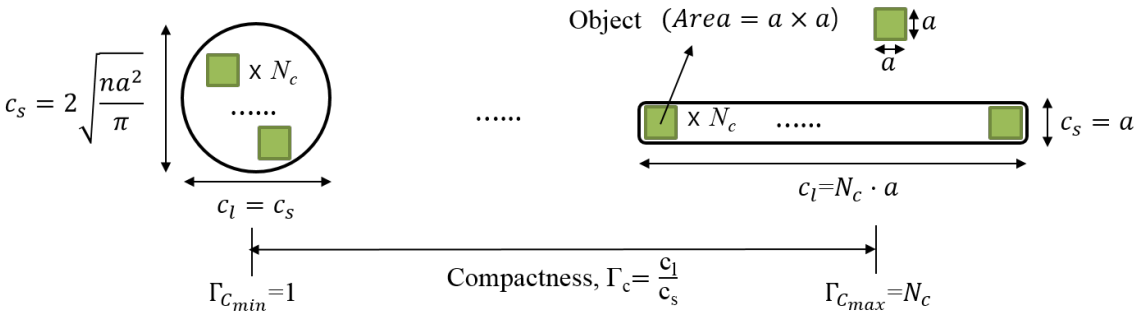

Figure 5.7: Differing shapes of the clusters of the same size N_c. N_c is the size of the cluster, c_l and c_s are the lengths of the major and minor axes of the cluster, respectively.

5.2.1 The Compactness of Clusters

First, a concise descriptor of cluster shape is needed. We begin by introducing a measure that reflects the degree of dispersion of the items packed within the cluster because, as we now argue, this is the essential information that is necessary for the clustering process.

Consider two clusters each containing n objects. Despite having the same size, the clusters may be formed into a variety of shapes depending on the particular arrangement of objects. Whatever the shape, the probability of modifying a cluster is determined by a cluster's persistence against external impulses provided by the robots. Intuitively, if objects in a cluster are distributed as closely to the cluster's centroid as possible, the cluster is more likely to persist. Conversely, clusters with objects dispersed far from the centroid are more easily broken by impulses from outside. Figure 5.6 shows the relationship between a cluster's compactness and its persistence. We clearly observe that the compactness relates to the number of ways that objects can be removed from the cluster.

To quantify the degree of compactness, we compute the ratio of the cluster's

major axis to its minor axis, measuring how much the cluster deviates from being truly circular. Then, the compactness of a cluster, denoted Γ_c, is defined as

$$\Gamma_c = \frac{c_l}{c_s}, \tag{5.9}$$

where, c_l is the length of the major axis (the longest diameter of a cluster) of the cluster of the size N_c, and c_s is the length of the minor axis (the shortest diameter) of the cluster of the size N_c. In particular, the compactness of a circular cluster is 1 because $c_l = c_s$, and the compactness of an elliptical cluster is greater than 1 since $c_l > c_s$.

As shown in Figure 5.7, a cluster of N_c objects has area equal to the sum of the area of N_c objects. If we use $a \times a$ square objects, the area of N_c objects is $N_c \cdot a^2$. For the most compact cluster, $c_l = c_s$, the area of the cluster will be approximately $\pi(\frac{c_l}{2})^2$ (or $\pi(\frac{c_s}{2})^2$), the area of a circle with a diameter of c_l (or c_s). Assuming that a cluster's area is the sum of the area of N_c objects, we have $\pi(\frac{c_l}{2})^2 = \pi(\frac{c_s}{2})^2 = n \cdot a^2$, hence c_l and c_s of the most compact cluster is approximately $2\sqrt{\frac{n \cdot a^2}{\pi}}$. For the least compact cluster, since the square objects are arranged in a line, we obtain $c_l = N_c \cdot a$ and $c_s = a$.

More generally, let $\Gamma_{c_{min}}$ and $\Gamma_{c_{max}}$ denote the minimum and maximum compactness of N_c size cluster, respectively. From Equation (5.9), the most compact cluster's compactness $\Gamma_{c_{mic}}$ is 1 because $c_l = c_s$. Whereas, $\Gamma_{c_{max}}$ of the least compact cluster of N_c square objects will be N_c because $c_s = a$ and $c_l = N_c \cdot a$. Thus, the minimum and maximum compactness of the cluster containing N_c square objects may be written

as

$$\Gamma_{c_{min}} = 1, \tag{5.10}$$

$$\Gamma_{c_{max}} = N_c. \tag{5.11}$$

All clusters of size N_c would be formed into any shapes between the least and the most compact clusters, so we quantify the degree of compactness by scaling the ratio of the cluster's axes into a value between $\Gamma_{c_{min}}$ and $\Gamma_{c_{max}}$, $[1, \frac{c_l}{c_s}]$.

5.2.2 Clustering Dynamics with Cluster Compactness

5.2.2.1 Modifying a Single Cluster

While prior probabilistic models use $P(C(N_c))$ to explain the dynamics of clusters formed symmetrically, we can now supplement this with the compactness descriptor. Let the probability of object removal and object addition to a cluster with N_c and Γ_c be written as $P^-(C(N_c, \Gamma_c))$ and $P^+(C(N_c, \Gamma_c))$, respectively. Next, we argue for reasonable values for these two probability functions.

When a robot carrying an object encounters a cluster in the workplace, it always successfully deposits the objects into the cluster. Under this observation, we can assume that

$$P^+(C(N_c, \Gamma_c)) = 1. \tag{5.12}$$

On the other hand, if a robot without any object strikes a cluster, the robot may draw away an object from the cluster, but this depends on the striking direction relative to the cluster's perimeter (in Figure 5.6, we already captured this notion with external forces around the perimeter of the cluster). As illustrated graphically in Figure 5.8, since the area of the removable region depends on the cluster's compactness, the probability of object removal is also determined by the compactness of

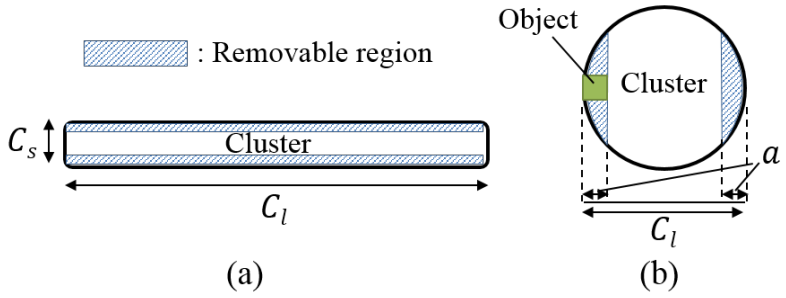

Figure 5.8: Removable regions of (a) the least cluster and (b) the most compact cluster. The compactness relates to the removable region that items can be eliminated from the cluster.

the cluster.

For the least compact cluster illustrated in Figure 5.8 (a), the objects are readily removed since the robots only make contact by approaches from any point on the long side of the cluster. Thus, the probability of object removal of the least compact cluster can be expressed as $\frac{c_l}{c_l+c_s}$. Whereas for the most compact cluster shown in Figure 5.8 (b), the robots must strike the edge of the cluster to remove the object, because if the robot hits the middle region of the cluster, the cluster is likely to withstand the pushing force of the robots. Since the shape of the most compact cluster is circular and symmetric, we can estimate the probability by considering one side of the cluster; the probability of object removal of the most compact cluster of size will be $\frac{2a}{c_l}$.

Let $P^-_{min}(C(N_c, \Gamma_c = \Gamma_{c_{min}}))$ and $P^-_{max}(C(N_c, \Gamma_c = \Gamma_{c_{max}}))$ be the probability of object removal of the most and the least compact cluster of size N_c, respectively. In Figure 5.7, we estimated c_l and c_s of the most and the least compact cluster. With these estimates, the minimum and maximum probabilities of object removal may be written as

$$P^{-}_{min}(C(N_c, \Gamma_c = \Gamma_{c_{min}})) = \frac{2a}{c_l} = \frac{a}{\sqrt{\frac{N_c \cdot a^2}{\pi}}} = \sqrt{\frac{\pi}{N_c}}, \tag{5.13}$$

$$P^{-}_{max}(C(N_c, \Gamma_c = \Gamma_{c_{max}})) = \frac{c_l}{c_l + c_s} = \frac{N_c \cdot a}{N_c \cdot a + a} = \frac{N_c}{N_c + 1}. \tag{5.14}$$

To estimate the probability of object removal a cluster, $P^{-}(C(N_c, \Gamma_c))$, we compute its eccentricity, a measure of how much a conic section† deviates from being circular (Ayoub, 2003). The eccentricity of an elliptical cluster ϵ_c is defined as

$$\epsilon_c = \sqrt{1 - \frac{c_s^2}{c_l^2}}, \tag{5.15}$$

hence,

$$\epsilon_c = \sqrt{1 - (\frac{1}{\Gamma_c})^2}. \tag{5.16}$$

A circle (i.e. $c_l = c_s$) has an eccentricity of zero and an ellipse with a high ratio of a major axis to a minor axis (i.e. $c_l \gg c_s$) has an eccentricity of approximately one,

$$\epsilon_{c_{min}} = 0 \leq \epsilon_c < \epsilon_{c_{max}} = 1. \tag{5.17}$$

To estimate $P^{-}(C(N_c, \Gamma_c))$ of any cluster, we measure ϵ_c—a value in the range $[0, 1]$, we then scale it to a value between $P^{-}_{min}(\cdot)$ and $P^{-}_{max}(\cdot)$:

$$\begin{aligned} &\frac{P^{-}(C(N_c, \Gamma_c))) - P^{-}_{min}(C(N_c, \Gamma_c = \Gamma_{c_{min}}))}{P^{-}_{max}(C(N_c, \Gamma_c = \Gamma_{c_{max}})) - P^{-}_{min}(C(N_c, \Gamma_c = \Gamma_{c_{min}}))} \\ &\quad = \frac{\epsilon_c - \epsilon_{c_{min}}}{\epsilon_{c_{max}} - \epsilon_{c_{min}}}. \end{aligned} \tag{5.18}$$

†A conic section is a taken slice through a cone. We here consider the ellipse and the circle that is a special case of the ellipse.

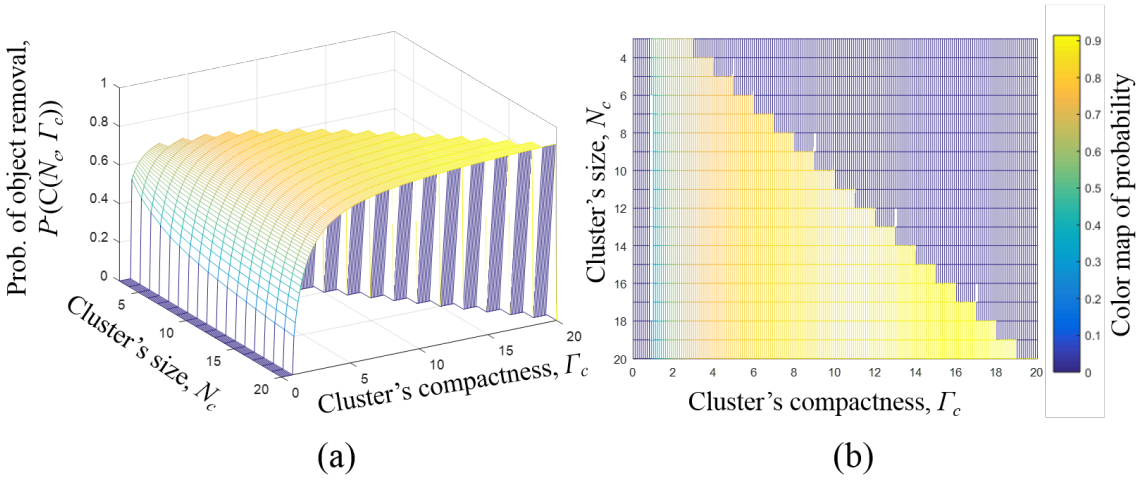

Figure 5.9: (a) The probability distribution of object removal according to the cluster's size and compactness. (b) A top view of the 3-dimensional graph (a). The color map represents the probability values.

From Equations (5.13), (5.14), (5.16), (5.17), and (5.18), we obtain

$$P^-(C(N_c, \Gamma_c))) = \sqrt{1 - (\frac{1}{\Gamma_c})^2}(\frac{N_c}{N_c + 1} - \sqrt{\frac{\pi}{N_c}}) + \sqrt{\frac{\pi}{N_c}}. \tag{5.19}$$

Figure 5.9 presents a plot of this function over a range of cluster size and compactness. As the cluster is more compact (approaching 1) and its size increases, the probability of object removal is decreased monotonically. Thus, the largest and the most compact cluster among multiple clusters evolves into the dominant cluster with high probability. Figure 5.9 (b) shows how clusters of a variety shapes occur as cluster size increases (see, specifically, the yellow region). We can also observe that our extended geometric probability in the various shapes of clusters can represent numerically.

5.2.2.2 Clustering Dynamics with Multiple Clusters

The previous section used geometric arguments to estimate the probability of a modification being made to a given cluster. By comparing these probabilities for the various clusters forming in the workplace, a prediction of the stochastic dynamics of the system can be produced. Although it does not capture the individual accretion and attrition actions that occur between clusters as mediated by the robots, it describes the broader collective behavior of the cluster system as a whole.

To analyze the dynamics of the multiple clusters, we extend the probabilistic model proposed by Martinoli (1999) to include richer characteristics of the cluster's geometry, modeling the evolution of the system as characterized by two coordinates N_c and Γ_c. Like Martinoli's model conduct the Monte Carlo trials based on the parallel probabilistic processes. Figure 5.10 shows an abstract flowchart of robotic clustering with this probabilistic model, and Figure 5.11 provides the flowchart for an individual robot's behavior as used for the probabilistic processes. The probability that a robot encounters a cluster is calculated from the ratio of the area of the selected cluster to the area of all clusters.

We conducted simulations of clustering systems composed of multiple clusters, which are formed into various shapes and sizes. We used 20 objects and three robots with a simple behavior (the robots move straight, when they encounter obstacles they turn to a random direction, and then return to moving straight). We formed six different geometries of clusters shown in Figure 5.12 as initial conditions, and compared the clustering dynamics of four combinations of the multiple clusters, conducting 15 trials in each case. A summary of the results appears in Table. 5.1, which contrasts predictions of the existing model (based on cluster size alone) with the proposed model. The plots in Figure 5.13 show that one cluster grows to become the

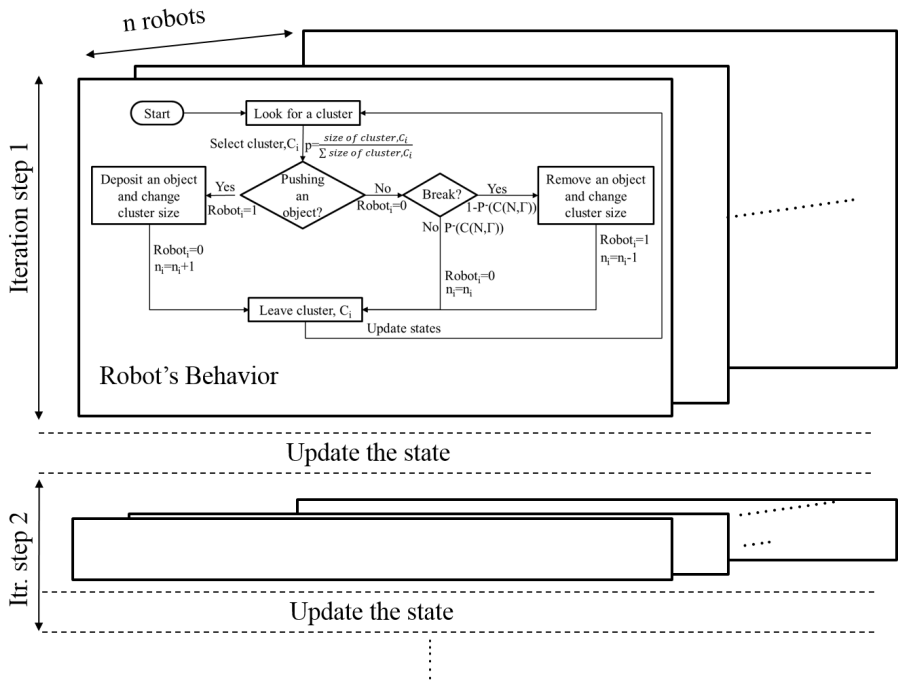

Figure 5.10: An abstract flowchart of robotic clustering. The simulation consists of multiple iterations of parallel processes for each of the multiple robots, following the methodology of Martinoli (1999). States are updated every iteration.

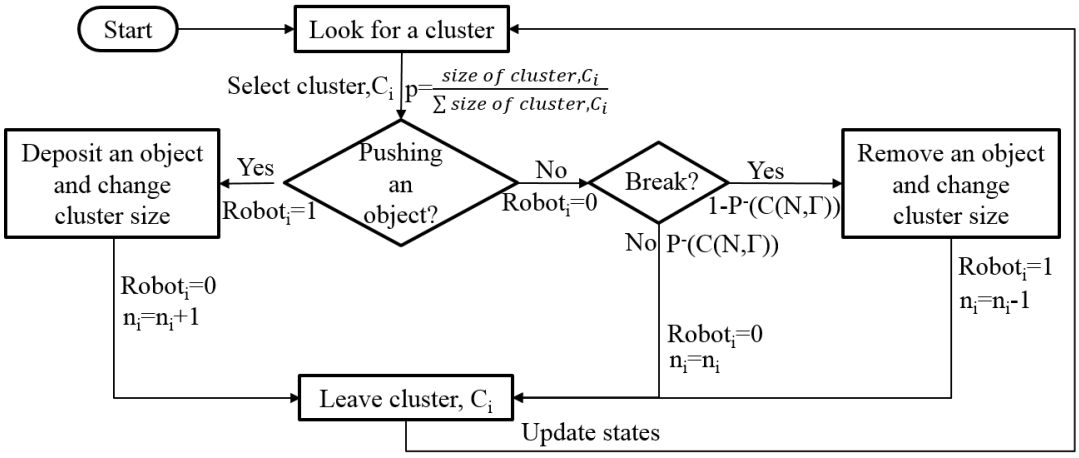

Figure 5.11: A flowchart of an individual robot's behavior.

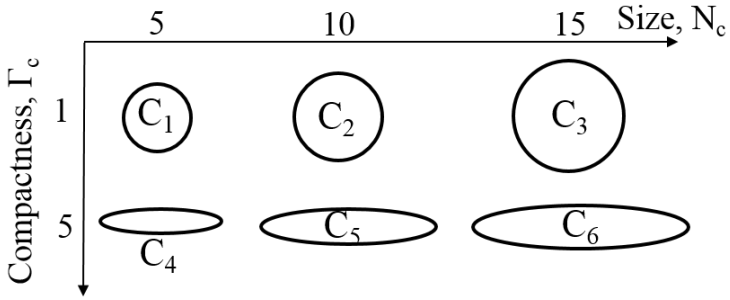

Figure 5.12: A variety of cluster geometries, $C_i(N_c, \Gamma_c)$. (Six different geometries of clusters) $C_1(5,1)$: a compact, small-sized cluster, $C_2(10,1)$: a compact, medium-sized cluster, $C_3(15,1)$: a compact, large-sized cluster, $C_4(5,5)$: a less compact, small-sized cluster, $C_5(10,5)$: a less compact, medium-sized cluster, and $C_6(15,5)$: a less compact, large-sized cluster.

Table 5.1: Comparison of cluster model predictions.

Cases	Experimental result	Existing model	Proposed model
Case 1: C_1, C_3	C_1 : 0%, C_3 : 100%	C_1 : 6.7%, C_3 : 93.3%	C_1 : 3.3%, C_3 : 96.7%
Case 2: C_1, C_6	C_1 : 93.3%, C_6 : 6.7%	C_1 : 6.7%, C_6 : 93.3%	C_1 : 93.3%, C_6 : 6.7%
Case 3: C_2, C_5	C_2 : 6.7%, C_5 : 93.3%	C_2 : 53.3%, C_5 : 46.7%	C_2 : 3.3%, C_5 : 96.7%
Case 4: C_1, C_4, C_6	C_1 : 96.7%, C_4 : 0%, C_6 : 3.3%	C_1 : 3.3%, C_4 : 3.3%, C_6 : 93.4%	C_1 : 93.4%, C_4 : 3.3%, C_6 : 3.3%

dominant cluster and the final result is a single cluster. Examining the dynamics, it is observed that the cluster with the lowest relative $P^-(C(N_c, \Gamma_c))$ finally becomes the single dominant cluster.

5.3 The Effect of Object Geometry

Thus far, we have examined the clustering dynamics of square objects only. From the perspective of model extension, an important question is: how robustly can the

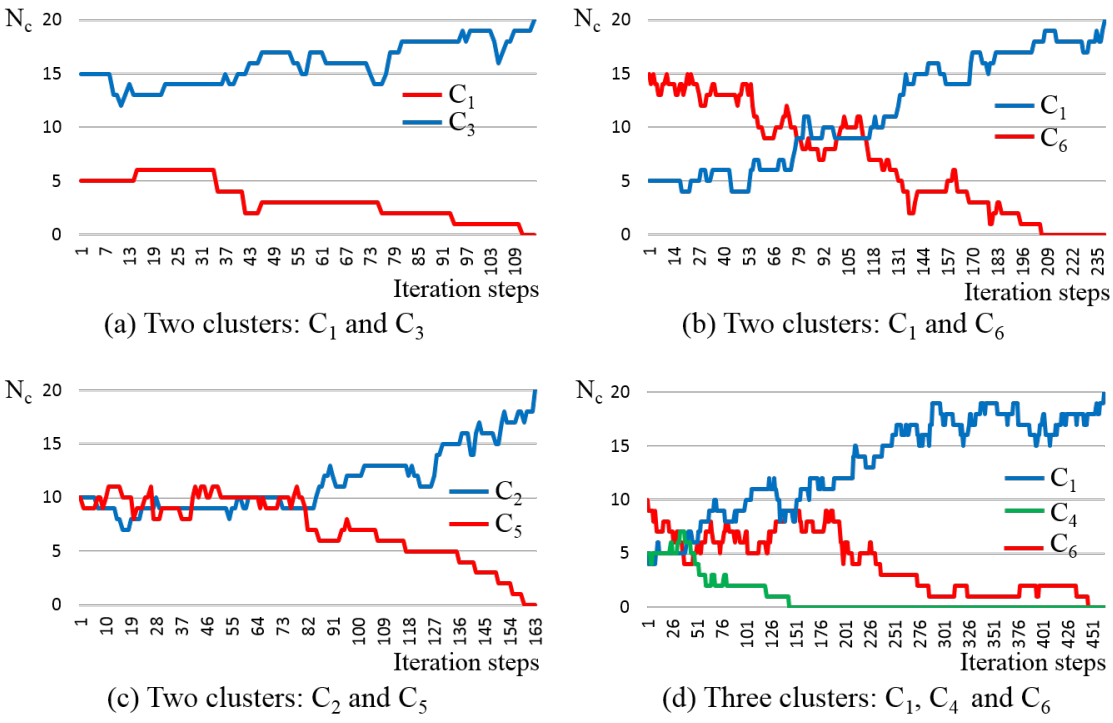

(a) Two clusters: C_1 and C_3

(b) Two clusters: C_1 and C_6

(c) Two clusters: C_2 and C_5

(d) Three clusters: C_1, C_4 and C_6

Figure 5.13: The clustering dynamics of the combinations of multiple clusters. Each result is obtained from simulations through our extended probabilistic clustering model by considering the cluster's shape.

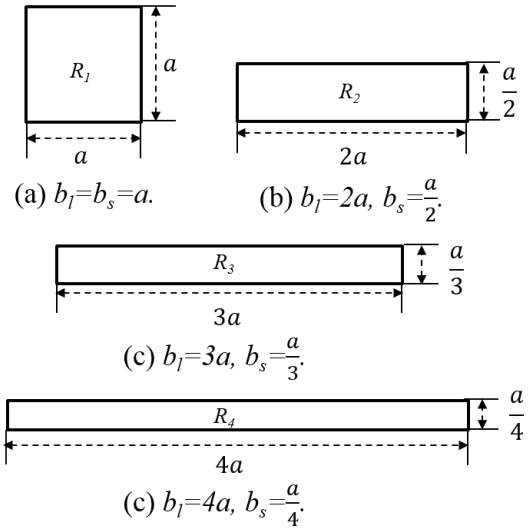

Figure 5.14: The different ratios of rectangles, $b_l : b_s = k : \frac{1}{k}$, where b_l is the length of the object's long side and b_s is the length of the object's short side. R_1 is a square. R_2,R_3 and R_4 are rectangles having the different ratios, $2 : \frac{1}{2}$, $3 : \frac{1}{3}$, and $4 : \frac{1}{4}$, respectively. All rectangles have the same area, a^2.

preceding geometric arguments be carried over to predict the behavior of clustering systems if the shape of the objects is altered? In this section, we vary the aspect ratio of the rectangles being clustered, extending the preceding analysis to account for rectangular objects with different sides length ratios.

5.3.1 The Effect of the Object's Geometry on Cluster Shape

We explore these possibilities with four rectangles (depicted in Figure 5.14) with equal area but different side ratios: $1 : 1$, $2 : \frac{1}{2}$, $3 : \frac{1}{3}$, and $4 : \frac{1}{4}$ (which we label R_1, R_2, R_3 and R_4).

Figure 5.15 through Figure 5.18 show (simulated) clustering performance over time with the four different objects (the vertical axis of the plots tracks cluster size as a function of time, there are multiple data series because there frequently multiple clusters in the workspace). As shown in Figure 5.15, square objects form a single

cluster. In contrast, rectangles produces the different results according to object shape. Figure 5.16, Figure 5.17, and Figure 5.18, show patterns of repeated cluster creation and destruction. Although thinner rectangles do sometimes have fairly large clusters, those clusters fail to become the stable, dominant cluster. Also, this lack of robustness appears to be worse with more extreme aspect ratios.

Following the ideas from the previous section, properties related to object packing density appear worthy of closer consideration. The distance d between two objects' centroids in a cluster certainly depends how the objects marry with one another and with other neighboring objects, itself depending on object geometry. Consider two rectangular objects whose sides are ka and $\frac{a}{k}$. When the two objects are adjacent to each other on the long side, d_{min} will be $\frac{a}{k}$. But d_{max} will be ka in a case of contact on the shorter side. Figure 5.19 illustrates that the minimum contact distance d_{min} and the maximum contact distance d_{max} between objects belonging to a same cluster relates to their geometry. This range of the contact distance varies in pairwise arrangement of packing objects and, taken collectively, affects the cluster's compactness too. As aspect ratio increases, the possible variability in the contact distance will also increase. This link is suggestive so next we follow through on this line of thinking, by relating the aspect ratio to the clustering properties via cluster compactness.

The range of possible values for cluster compactness is altered by changes in object geometry. Continuing our geometric reasoning, Figure 5.20 shows how both the least and the most compact clusters are influenced by the ratio of the rectangles' sides. For example, the longer the long side length of rectangle, the longer the least compact cluster as well: the c_l for square objects is na, whereas c_l for thin rectangular objects is $n \cdot ka$ (See Figure 5.20 (b) and (d)). Likewise, the shorter b_s of objects, the shorter c_s. Using Equation (5.9), we might predict that weaker clusters can be

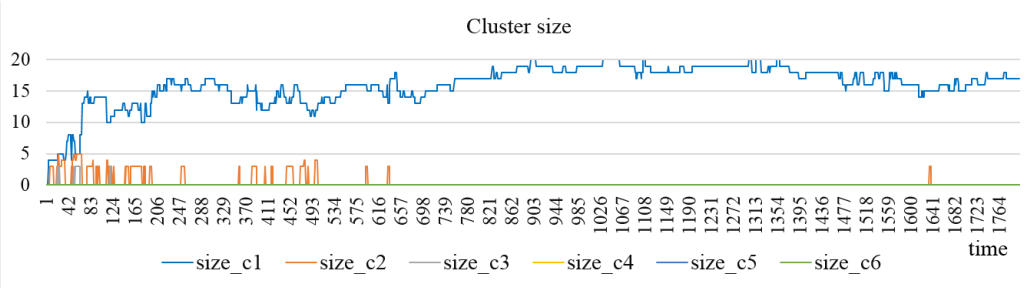

(a) 1st trial

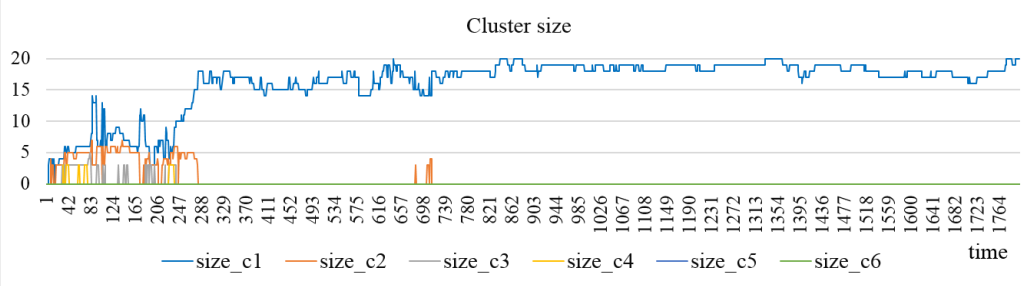

(b) 2nd trial

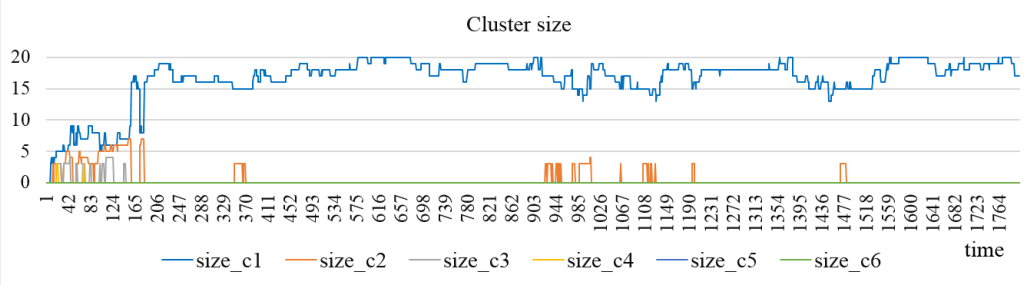

(c) 3rd trial

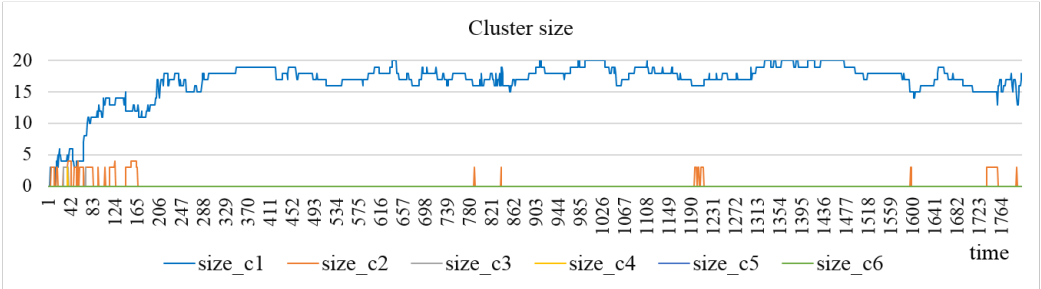

(d) 4th trial

Figure 5.15: Clustering experiments with square objects, R_1.

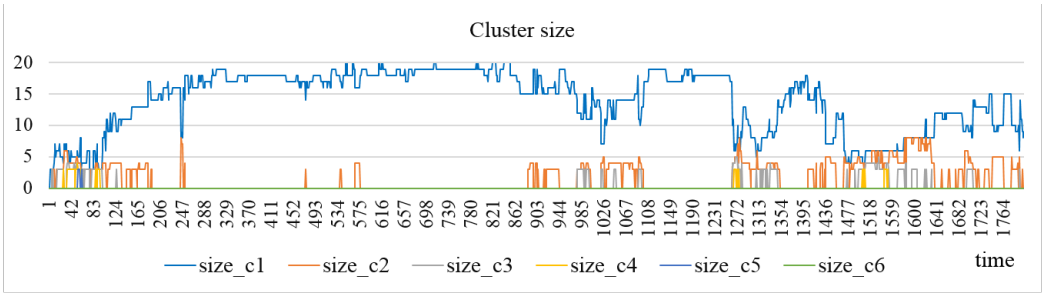

(a) 1st trial

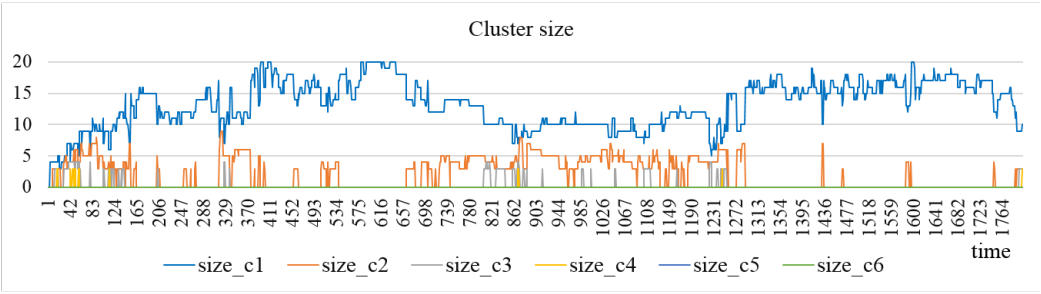

(b) 2nd trial

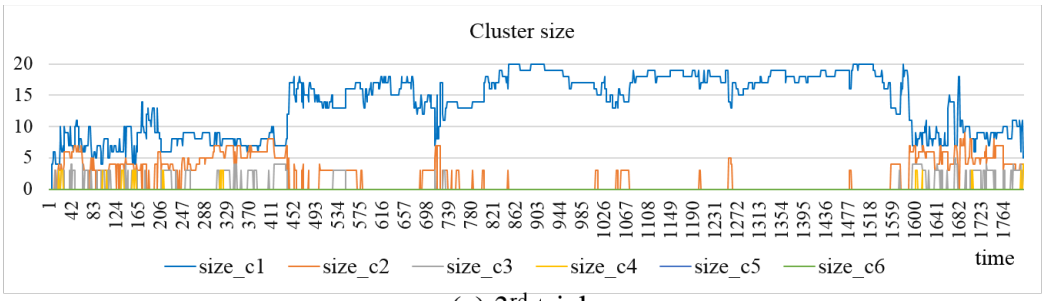

(c) 3rd trial

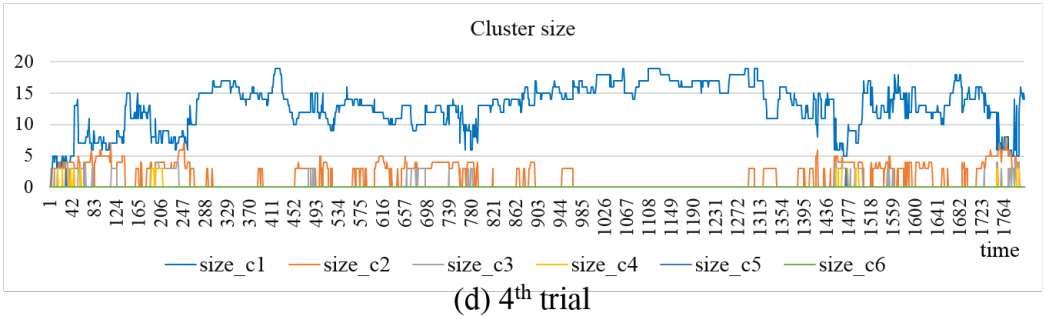

(d) 4th trial

Figure 5.16: Clustering experiments with rectangular objects, R_2.

(a) 1st trial

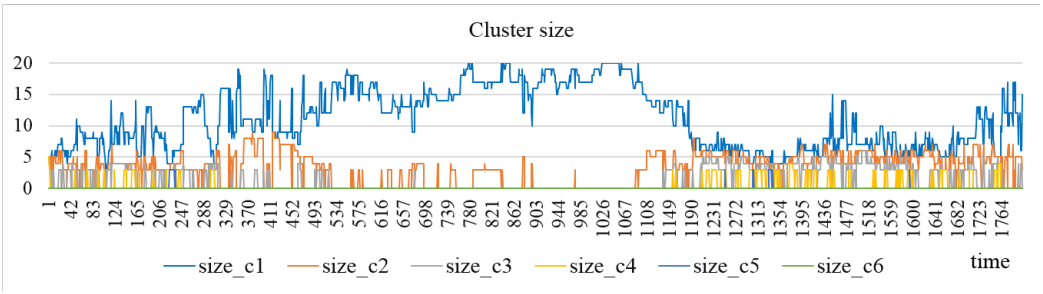

(b) 2nd trial

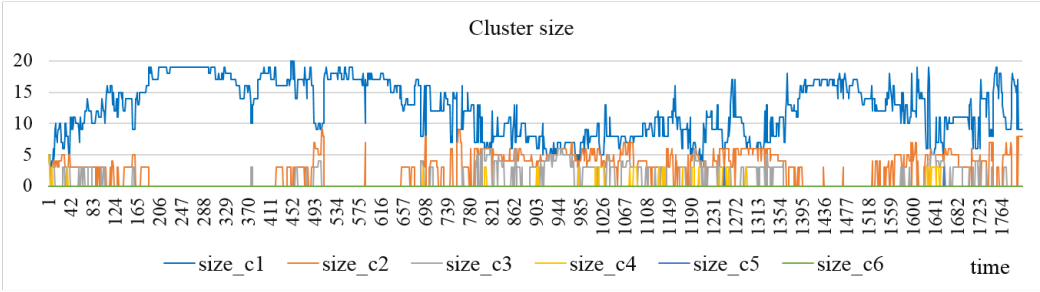

(c) 3rd trial

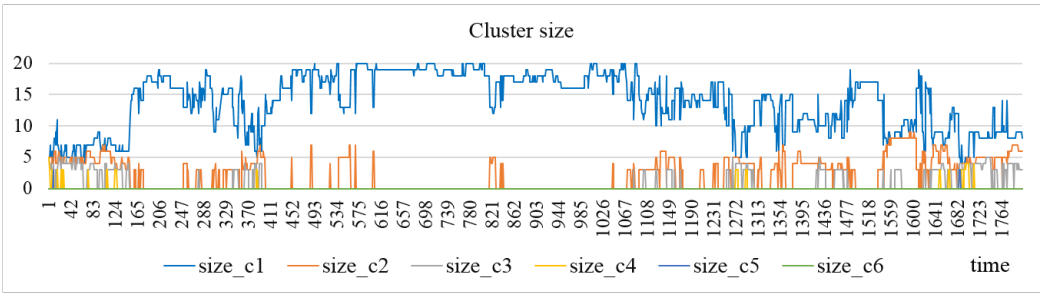

(d) 4th trial

Figure 5.17: Clustering experiments with rectangular objects, R_3.

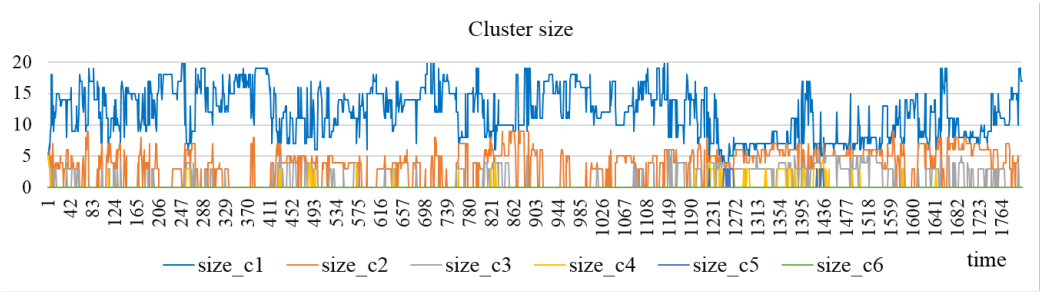

(a) 1st trial

(b) 2nd trial

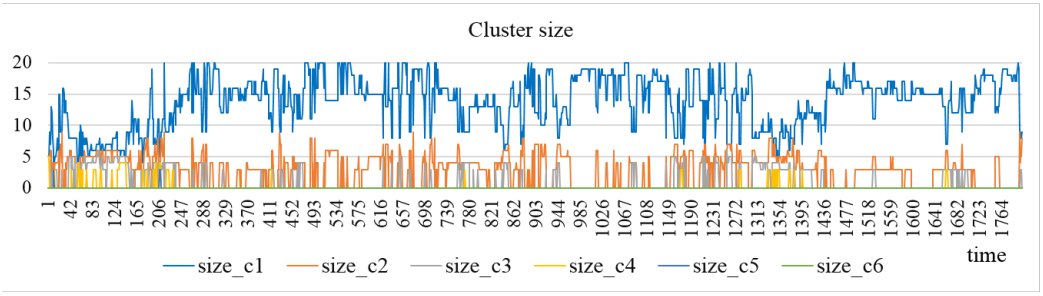

(c) 3rd trial

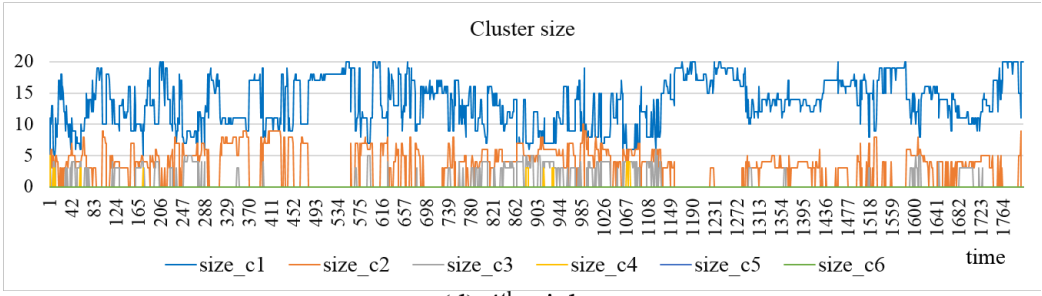

(d) 4th trial

Figure 5.18: Clustering experiments with rectangular objects, R_4.

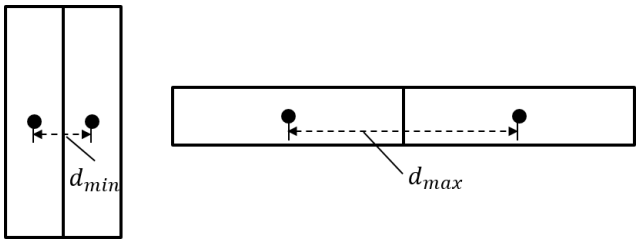

Figure 5.19: The contact distance between neighboring objects in a cluster. The contact distance is varied by the arrangement of two objects.

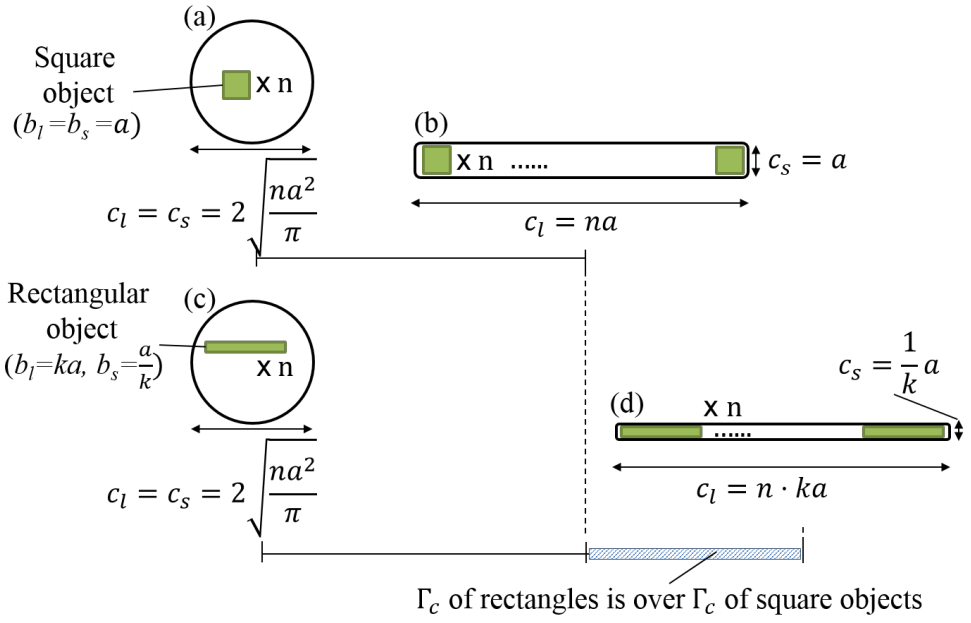

Figure 5.20: Differing the ranges of the cluster's compactness according to the object geometry. (a) The most compact cluster of n square objects. (b) The least compact cluster of n square objects. (c) The most compact cluster of n rectangular objects. (d) The least compact cluster of n rectangular objects.

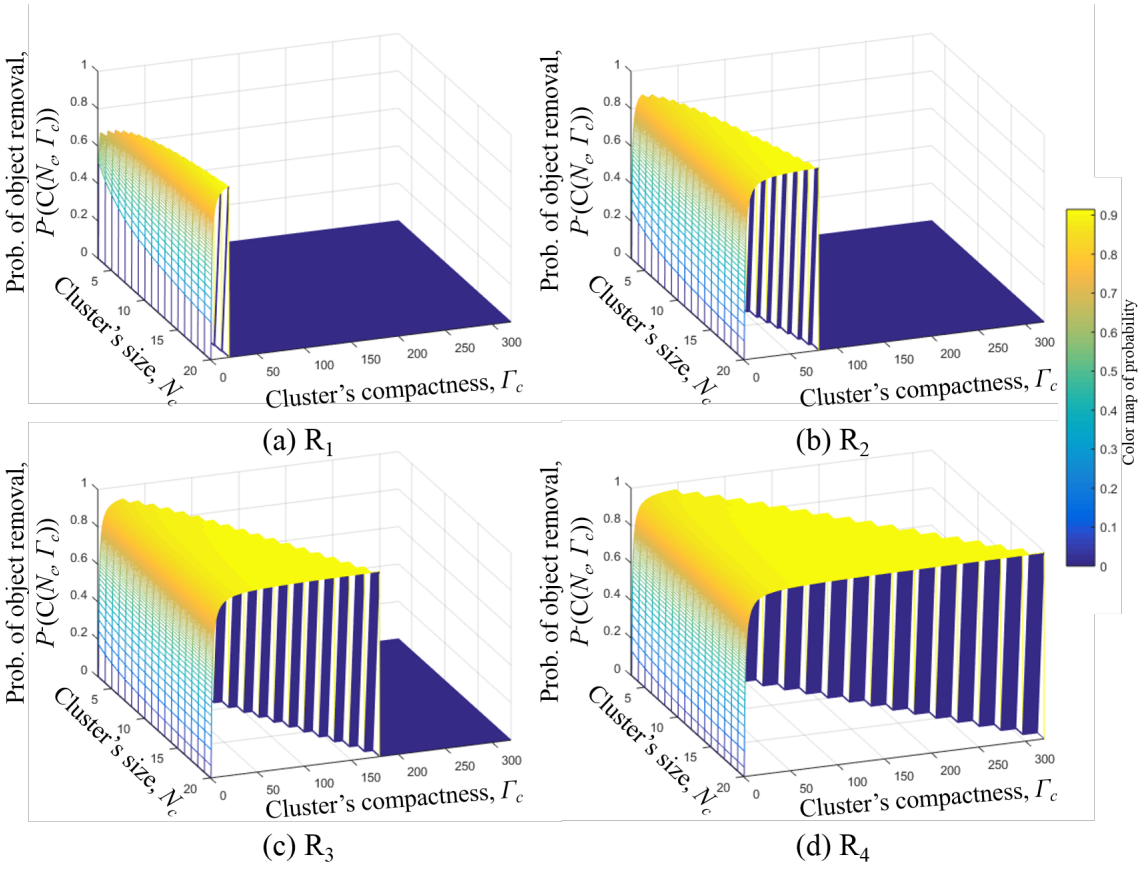

Figure 5.21: The probabilities of object removal by (a) R_1, (b) R_2, (c) R_3, and (d) R_4. The most thin rectangle R4 can be formed into the longest line-shaped cluster whose long side l_{max} can be up to 160 (In Figure 5.20, we estimated l_{max}. Here, we used that n=20, k=4 and a=2).

formed by rectangles than squares. A shaded region in Figure 5.20 represents that the extent of the range of Γ_c for rectangular objects is a superset of those Γ_c for square objects, *i.e.,* clusters of rectangular objects can form in greater variety than clusters of squares.

However, from Equation (5.19) the probability of object removal $P^-(C(N_c, \Gamma_c))$ includes cluster length as a variable. Thus, the probability values will change to scale to the range of the cluster's long side length, which is itself related to the object's geometry. Figure 5.21 shows the probability of the object removal $P^-(C(N_c, \Gamma_c))$ across different rectangular geometries. We can observe that as the rectangular object grows in length, the range of possible compactness values of the cluster increases too.

5.3.2 Cluster Occurrence Model

Generally, the largest and the most compact cluster in a certain state evolves by absorbing unclustered objects through the destruction of small clusters. On the basis of this observation, one can predict that the strongest cluster among existing clusters at any point in time has the highest likelihood of evolving into a larger and more compact cluster. The implication is that the distributions of shapes of clusters are spread (with some variance) around the shape of the most compact cluster. This section develops a model describing the frequency of occurrence of clusters' shapes. We model the joint probability distribution for clusters' size N_c and compactness Γ_c, namely $P(N_c, \Gamma c)$. We express the joint probability with lower-dimensional probability models, $P(\Gamma_c)$ and $P(N_c|\Gamma_c)$, via the product $P(N_c, \Gamma c) = P(N_c|\Gamma_c) \cdot P(\Gamma_c)$.

5.3.2.1 Probability Models for the Cluster's Compactness

Cluster size and shape certainly varies with aspect ratio, as can be seen in Figure 5.20. We hypothesize that cluster shape reflects object geometry. In other words,

while clustering objects with high aspect ratio (e.g., thin rectangles, R_4) one is more likely to produce clusters with high aspect ratios than when clustering objects of more moderate shape (e.g. R_1, R_2, or R_3).

We model the distribution of the cluster's compactness at any size as a gamma-distributed random variable with a shape parameter k and a scale parameter θ, denoted by $\Gamma_c \sim Gamma(k;\theta)$. The properties of the Gamma distribution imply $\mu_{\Gamma_c} = k\theta$ and $\sigma_{\Gamma_c} = \sqrt{k}\theta$ (Schmetterer, 2012). We suppose that μ_{Γ_c} at fixed cluster size is the same as the ratio of the clustered object's long side length to its short side length, $\frac{b_l}{b_s}$, and its standard deviation varies in the range of the difference between the object's long side and short side. Under these assumptions, we develop models for μ_{Γ_c} and σ_{Γ_c} as follows,

$$\mu_{\Gamma_c} = \frac{b_l}{b_s}, \tag{5.20}$$

$$\sigma_{\Gamma_c} \begin{cases} \approx 0, \;\; if \; b_l = b_s, \\ = (b_l - b_s), \;\; if \; b_l \neq b_s, \end{cases} \tag{5.21}$$

where, b_l and b_s are the object's long side and short side length, respectively. Equations (5.20) and (5.21) mean that the larger the aspect ratio of the rectangular object, the larger the mean of compactness of the most compact cluster as well as the larger its standard deviation. We will examine and compare results of four kinds of the rectangular objects: 2×2 square objects, 4×1, $6 \times \frac{2}{3}$, and $8 \times \frac{1}{2}$ rectangular objects. We can estimate μ_{Γ_c} and σ_{Γ_c}, and build the compactness model with those parameters.

To validate this model, we conducted clustering experiments with four kinds of rectangles R_1, R_2,R_3, and R_4 as shown in Figure 5.14 and measured the occurrence frequencies of clusters in experiments. We counted the number of times clusters of

Table 5.2: Comparison of obtained μ_{Γ_c} and σ_{Γ_c} from the probability model and the experimental data vs. object geometry.

Objects	Probability model		Experimental data	
	μ_{Γ_c}	σ_{Γ_c}	μ_{Γ_c}	σ_{Γ_c}
R_1	1	≈0	1.28	0.25
R_2	4	3	4.21	2.74
R_3	9	5.33	8.91	5.11
R_4	16	7.5	15.82	7.82

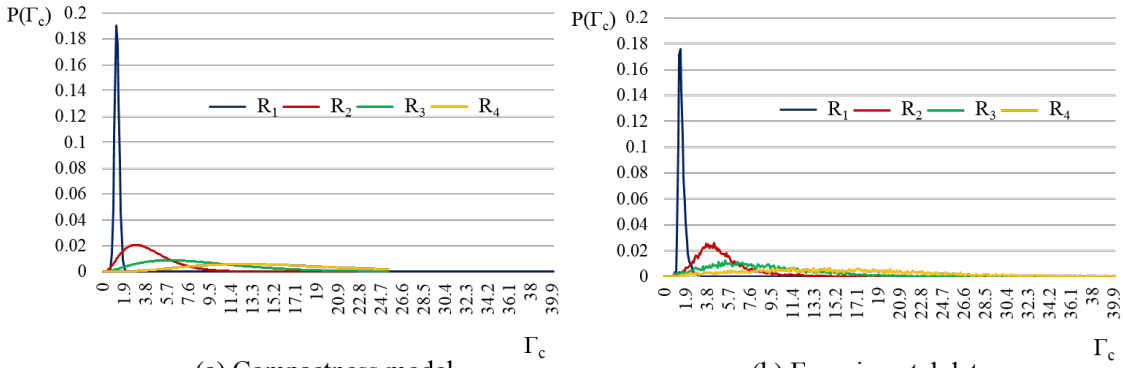

Figure 5.22: The estimated compactness modeled via the Gamma distribution juxtaposed against the experimental data.

each compactness value occurred, averaging over fifteen trials each of which lasted 30 min.

Table 5.2 shows that the measured μ_{Γ_c} and σ_{Γ_c} from the experiments are close to the value estimated using our hypotheses. Figure 5.22 also shows the distributions of $P(\Gamma_c)$ vs. rectangle shape, obtained from the model and from the experimental data. Although the apparent similarity in the distributions is promising, it is important to look more closely at the probability distributions.

5.3.2.2 Conditional Probability Model for the Cluster's Size

To build a model for the conditional probability $P(N_c|\Gamma_c)$, we hypothesize that if highly compact clusters can form shapes with low compactness, then large clusters will have much longer lifetimes as they are much more robust to external perturbations than smaller ones, and so will be most persistent. Thus, for a given compactness Γ_c, clusters of larger size occur more frequently because they persist so they feature in counts again and again. Whereas for less compact clusters all clusters, regardless of size, are feeble when pitted against the robot's pushing behavior and hence frequencies are evenly spread across all sizes.

Assuming that the peak of the distribution is located at 90% of total objects, we propose a conditional probability model for $P(N_c|\Gamma_c)$ with a Gamma distribution that is symmetric with respect to the vertical axis at center point on the horizontal axis. Let us consider the first sliced probability distribution of $P(N_c|\Gamma_c = 1)$ for the most compact cluster. Since we have 20 objects, we model a gamma distribution having $N_c = 18$ as a mode. By the characterization of parameters k and θ in the Gamma distribution, the mode of the distribution is $(k-1)\cdot\theta$ for $k \geq 1$. If a shape parameter $k = 2$, a scale parameter $\theta = 2$ because when the mode of the probability distribution is 18 at the symmetric Gamma distribution, the mode is 2 in the original Gamma distribution. In order to obtain $P(N_c|\Gamma_c = \gamma)$ for $\Gamma_{c_{min}} \leq \gamma \leq \Gamma_{c_{max}}$, if we assume that a scale parameter θ is inversely decreased as much as the increment of compactness, we obtain the distribution of the conditional probability $P(N_c|\Gamma_c)$ shown in Figure 5.23.

5.3.2.3 Joint Probability Model for the Cluster's Size and Compactness

After building models for the marginal probability $P(\Gamma_c)$ and the conditional probability $P(N_c|\Gamma_c)$, finally, we obtain the joint probability $P(N_c, \Gamma_c)$ for the cluster

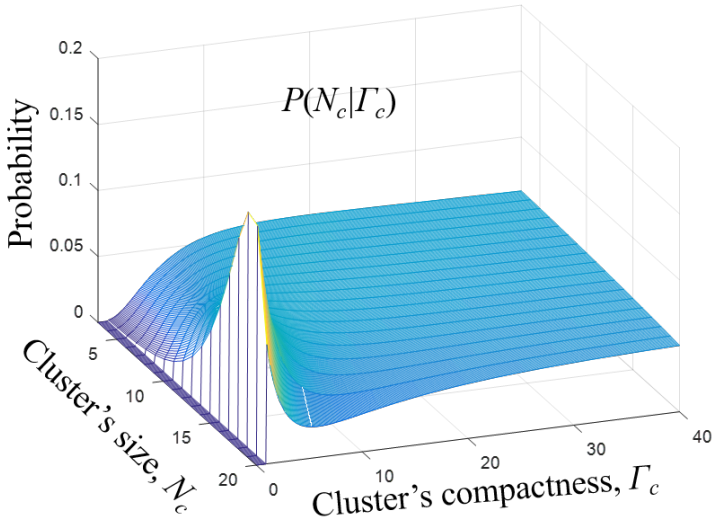

Figure 5.23: Conditional probability model for $P(N_c|\Gamma_c)$.

occurrence model. Figure 5.24 and Figure 5.25 show the joint probabilities as the object geometry changes, being remarkably close to the measured values from the experiments.

These cluster occurrence distributions give a different view of the processes that helps explain why the clustering dynamics in Figure 5.15 through Figure 5.18 vary with rectangle shape in the way they do. For the clustering of R_4 rectangles, since the clusters in any size do not pack compactly enough, the pattern of the creation and the destruction is repeated (the joint probability distribution is flat). But when the object's geometry is closer to square, the clustering dynamics are more stable since the peak of the joint probability is located in the region of the large, compact cluster. The next section provides a further account of the dynamics in Figure 5.15 through Figure 5.18.

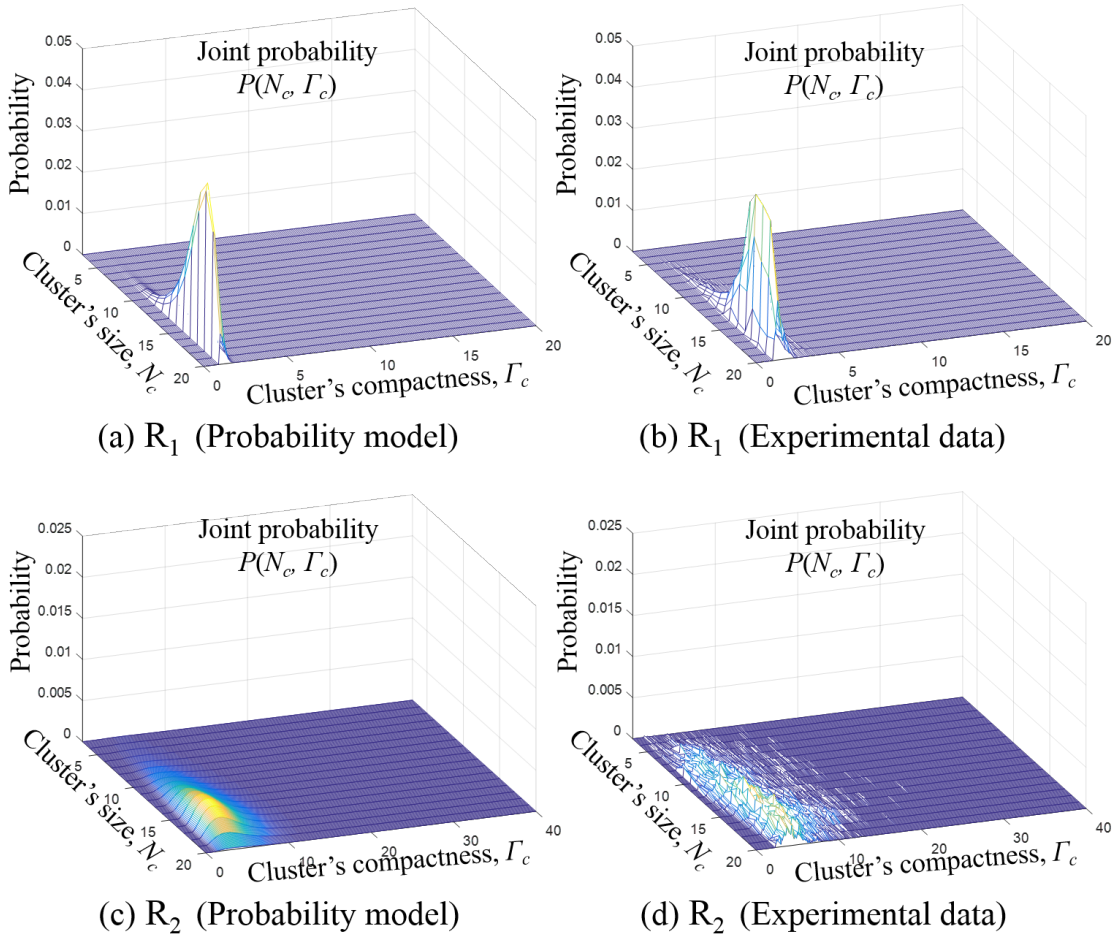

Figure 5.24: Comparison of the joint probabilities $P(N_c, \Gamma_c)$ by the object's geometry. (a) and (c) is the estimated joint probabilities from probability model for R_1 and R_2. (b) and (d) is the measured joint probabilities from experiments.

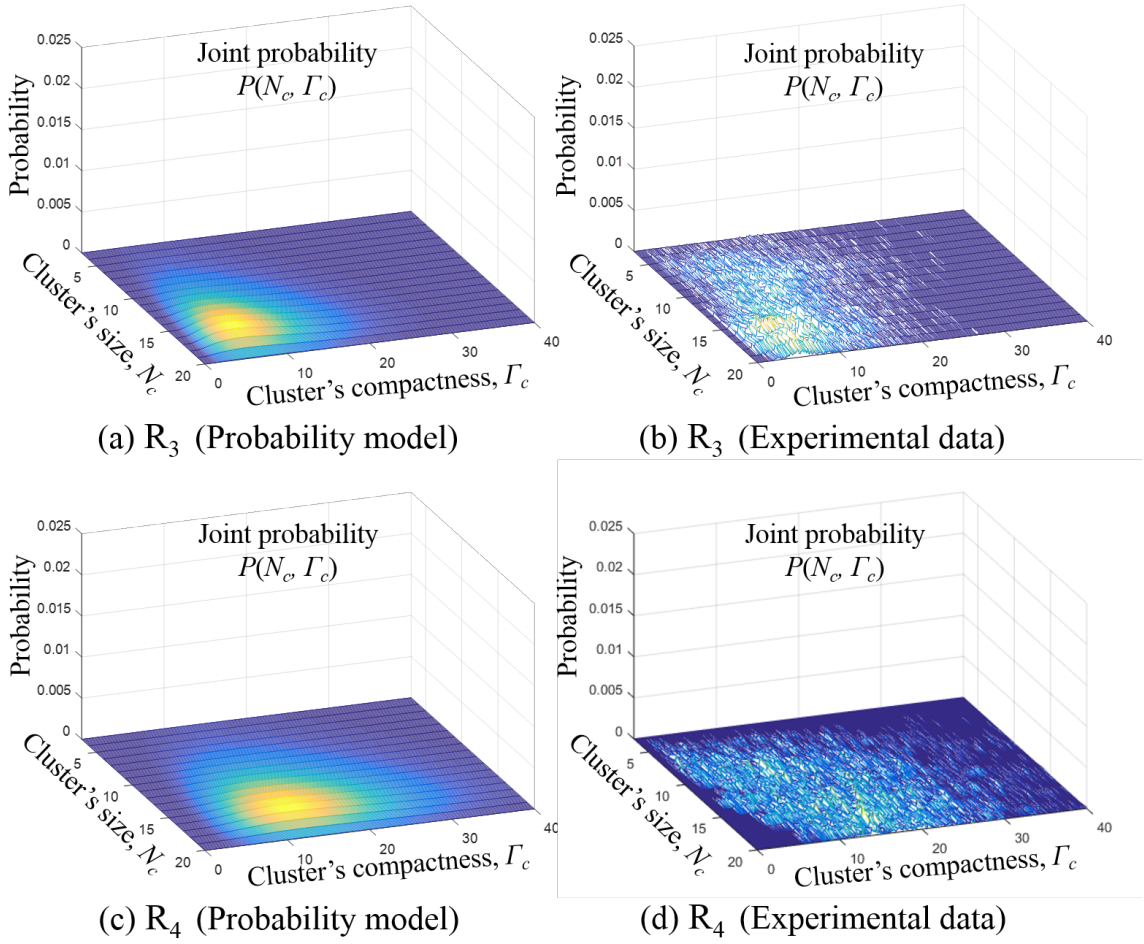

Figure 5.25: Comparison of the joint probabilities $P(N_c, \Gamma_c)$ by the object's geometry (continue). (a) and (c) is the estimated joint probabilities from probability model for R_3 and R_4. (b) and (d) is the measured joint probabilities from experiments.

5.3.3 Predicting Clustering Dynamics given an Object Geometry

In the previous section, we described development of a cluster occurrence model as a function of object geometry. Prior to that, we proposed a probabilistic model that characterizes cluster modification. In this section, we use both to describe the expected clustering dynamics for a given object geometry. The main idea is that if we can predict the probability distribution that describes how shapes of clusters occur and we can estimate the likelihood of an object being removed for each cluster shape, we can obtain the expected probability of cluster modification $E[P^-(C(N_c))]$ as follows.

$$E[P^-(C(N_c))] = \sum_{\Gamma_c=\Gamma_{c_{min}}}^{\Gamma_{c_{max}}} P^-(C(N_c, \Gamma_c)) \cdot P(N_c, \Gamma_c). \tag{5.22}$$

The averaging here allows for $P^-(\cdot)$ to account for the effects of object geometry indirectly. The form of this expectation permits direct comparison with existing models in the literature, since they characterize the dynamics in terms of cluster size N_c alone.

Figure 5.26 (a) shows the expected probabilities of object removal for each rectangular object on the basis of geometrical considerations, and Figure 5.26 (b) shows estimates from averages of experiments. We can observe that the contributions of the compactness considerations are favorable, especially by comparison to Martinoli's model.

The derivatives of the curves in Figure 5.26 also provide important information. Kazadi *et al.* (2002) proposed that a necessary condition for clusters to emerge is that the probability of object removal be a monotonically decreasing function of cluster size. Generalizing that statement slightly, one might expect that the degree to which clustering is reliably observed is proportional to the rate of decrease of that same

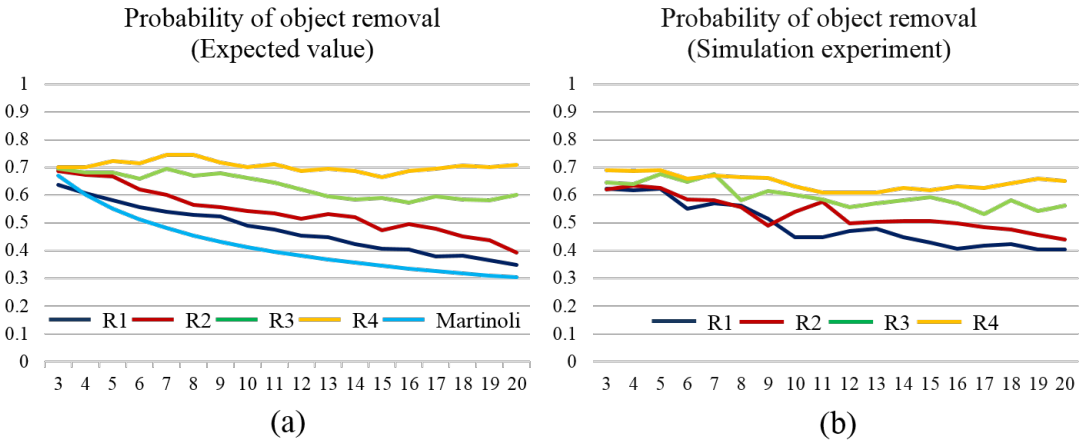

Figure 5.26: Comparison between the geometric probabilities of object removal. (a) Probability of object removal (Expected value). (b) Probability of object removal obtained (Simulation experiment).

function. We see in Figure 5.15 and Figure 5.18 that R_1 is more reliable than R_4, the latter nearly failing to show a decreasing at all in Figure 5.26 (a). When aspect ratios are exaggerated, churn seems to cause clusters to be destroyed before they can be packed more compactly.

5.4 Summary and Contributions

In this section, we described the clustering process more broadly by investigating various shapes of the cluster according to the object geometries. So far as we know, it is the first in-depth study of the effects of the geometric characteristics of clusters and objects on the clustering dynamics. This study introduced a measure of compactness to quantify the degree of dispersion of the objects packed within the cluster to represent the geometric shape of the cluster. We improved the clustering model by using the compactness as a variable. Using the measure of the compactness, we also proposed probabilistic occurrence models to predict the shapes of clusters that emerge during the clustering process. Through cluster occurrence models, we were

able to explain how the clustering dynamics are impacted by the geometry of the object. Future work could include the analysis of clustering of mixes of different objects.

6. IMPROVING THE PERFORMANCE OF SELF-ORGANZIED MULTI-ROBOT CLUSTERING*

Thus far, we focused on the clustering model to describe the clustering dynamics and implementation of a clustering system. In this section, we turn it toward improving the clustering performance by managing the group's functionality. As mentioned in Section 1, since the individual robot in self-organized multi-robot systems has limited capabilities, it can be difficult to improve the collective performance. It is already known that merely increasing the number of robots will not improve the speed of the system above a certain threshold because of the interference between members in a group (Lerman and Galstyan, 2002; Hayes, 2002; Lein and Vaughan, 2008).

Self-organized multi-robot systems have two inevitable constraints. The first constraint is that the dynamics between robots and the task environment is not deterministic. Consequently, since a task progress is non-stationary, it is difficult to predict accurately the system's performance. Second, because of the limited sensing capabilities of the robots, the global state of the system is usually partially observable. Such a system can be also regarded as a potentially sensorless robotic system because the robots with limited sensing capabilities do not have a complete feedback loop to control the system's performance. Furthermore, since a control policy through individual units can be inappropriate to manage the whole system's performance, it is hard to control a minimalist system with local-level parameters. Thus, an important question in minimalist multi-robot systems is how to accomplish system-

*Parts of this section are reprinted with permission from "Improving the performance of self-organized robotic clustering: Modeling and planning sequential changes to the division of labor" by J.-H. Kim and D. A. Shell, *2013 IEEE/RSJ International Conference on Intelligent Robots and Systems*, 4314-4319, Copyright[2013] by IEEE.

level coordination with robots that have limited capabilities and improve the system's performance.

Therefore, principled methods for managing the overall task progress and maximizing system performance (in terms of speed, quality, and/or reliability) still remains challenging for self-organized multi-robot systems.

In our previous work (Song *et al.*, 2012), we introduced a novel approach for object clustering, one of the most widely studied task domains for self-organized multi-robot systems. In Section **??**, we described the approach, we demonstrated, consisted of two complementary behaviors: *twisting* and *digging* (Figure 6.1 illustrates both). Each robot was assigned with one of these behaviors for the duration of a clustering experiments. With a mix of robots executing the two complementary behaviors, the robots separated the objects from the boundary and successfully generated a single central cluster as shown in Figure 6.2. Certain mixes of the behaviors outperformed other mixes and in different respects. For example, the mix of 2T3D (2 Twisters and 3 Diggers) had reliable performance compared to other cases while mix 1T4D (1 Twister and 4 Diggers) formed a cluster efficiently in the shortest observed time although it failed in one of its trials. This suggests that, given a preference between reliability and efficiency, an appropriate mix (or distribution of labor) could be determined. In this section, we attempt to address the question of how to maximize the system's performance by computing a policy for altering the robot division of labor as a function of time.

This research considers a sequencing strategy based on the hypothesis that since clustering performance is influenced by the division of labor, it can be improved by sequencing different divisions of labor. We construct a model in order to predict clustering behavior (in terms of likelihood of success and speed) and propose a method that uses the model's predictions to select a sequential change in labor distribution.

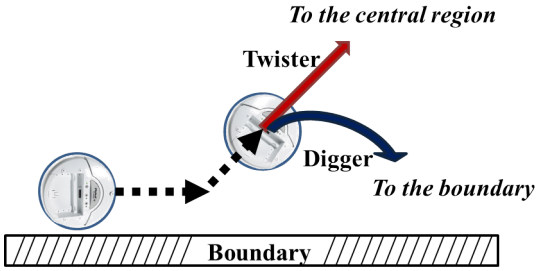

Figure 6.1: Trajectories of Twisters and Diggers on the boundary region. Basically the trajectories differ by the way they move away from the boundary wall.

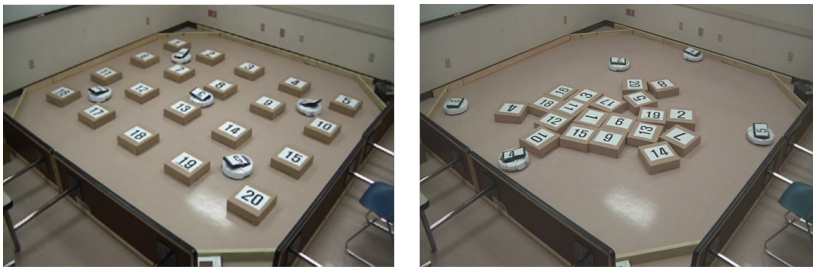

(a) (b)

Figure 6.2: The clustering process with robots executing our proposed novel behaviors. (a) initial configuration and (b) final configuration.

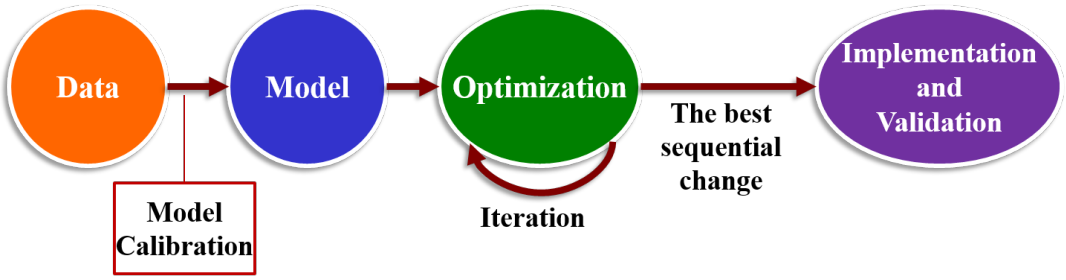

Figure 6.3: A sequencing strategy for improving the clustering performance.

Both of these aspects are performed off-line at *design time*. The model is calibrated with values from experiments in which robots maintain a constant distribution of labor. Then the analysis step is conducted in order to produce a labor policy for the robots. This is then executed on-line at *run time*. The system under this study involves robots that are unable to observe the global state like the environment's current state; fortunately, although there is a deal of stochasticity, task performance does have a degree of predictability. We constructed a Markov chain model which abstracts away many of the details of the robots but which captures the important geometric state for the clustering task. The model is used to predict task progress as a function of time, which allows for planning and evaluation of different sequences of workload division.

In this section, we will develop a practical model that we calibrate with actual data from initial experiments, and then use in order to make predictions about behavior in order to produce a division of labor policy to improve the overall clustering performance.

6.1 Approach: From a Stochastic Model to Planned Sequences

In our object clustering system, objects can be successfully clustered using a mix of robots, each employing one of the two complementary behaviors. We first

compare the clustering performance between the divisions of labor by analyzing the clustering dynamics with a low dimensional characterization. Figure 6.4 depicts a low dimensional characterization through a ternary plot describing the cluster dynamics. The system begins at an initial state in the lower left (a yellow sector), with no clusters formed. The goal is for the system to form a single central cluster of 20 objects, which is the state represented on the lower right corner (a blue sector). The top corner (a red sector) represents a trap state that objects are located on the boundary. Since any intermediate states during a clustering process can be marked as a point on the two dimensional ternary plot, this will facilitate the spatio-temporal analysis of clustering dynamics.

Figure 6.5 shows the object cluster dynamics for each of the three 90 minute runs of five physical robots for mixes 1T4D and 2T3D on a ternary plot. The axes of the ternary plot reflects the fact that groups of objects behave in qualitatively different ways depending on whether they are part of a cluster on the boundary, or are part of a cluster in the center, or are not part of any cluster.

The spread in each trial reflects changes in the clustering configuration and gives an indication of how goal-directed the cluster formation dynamics are. The plot also illustrates how fluctuations and randomness in the system become manifested as stochasticity in the evolution of the task-performance measure. This view suggested that a discrete-time Markov chain model may allow one to predict the configuration of clustering based on the current transition probabilities.

We observed that certain labor mixes outperformed others. As shown in Figure 6.5, the blue trial for 1T4D was extremely efficient, while the magenta trial ended with some objects on the boundary. The reliability (but comparatively longer time, visible in the meandering trajectory) is visible in the 2T3D case as all the paths converge to the lower right corner, the goal state. These observations suggest that an

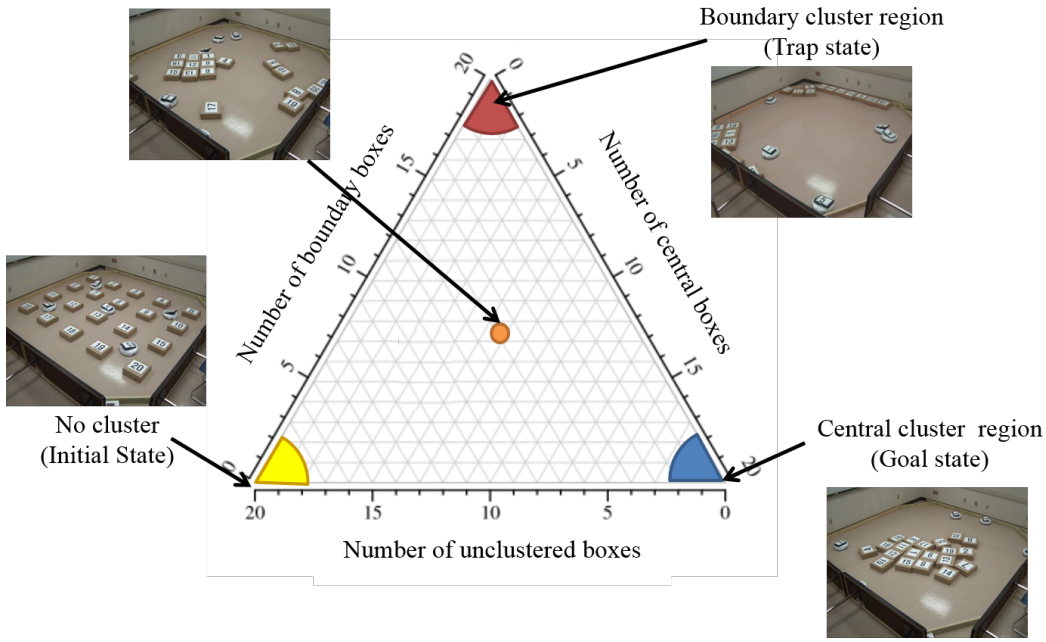

Figure 6.4: Low dimensional characterization through a ternary plot describing the cluster dynamics.

appropriate sequence of the different labor divisions might improve clustering performance. That is, by planning the sequence of labor mixes, the system can produce reliable quality and fast object clustering performance too. Table 6.1 summarize the clustering results by the division of labor.

Therefore, our sequencing strategy for improving the clustering performance is developed by following hypotheses.

- Hypothesis 1: Changing the division of labor as a function of time affects clustering performance.

- Hypothesis 2: Clustering performance can be improved by sequencing different divisions of labor.

In the remainder of this section, a state transition matrix is first computed from

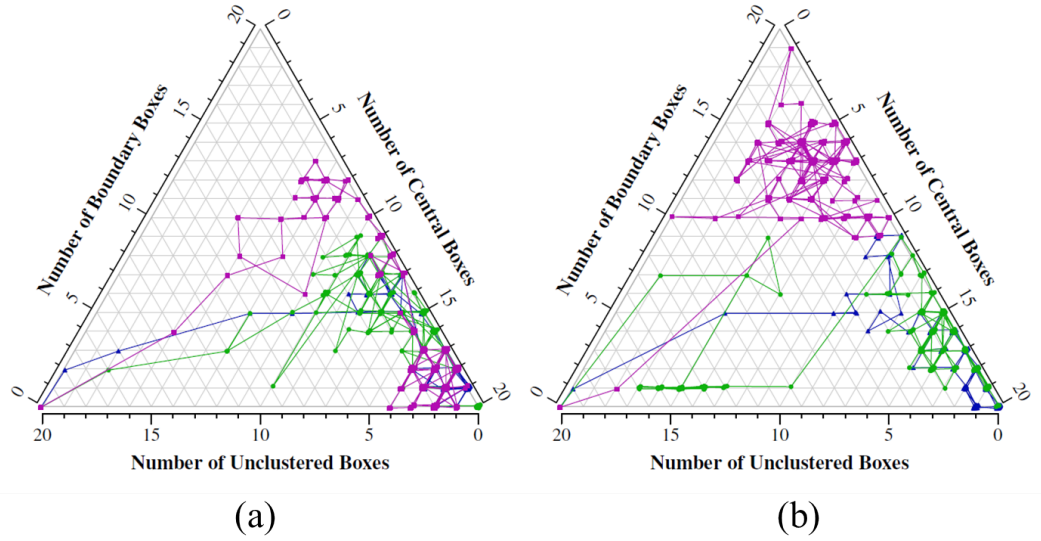

Figure 6.5: Ternary plots detailing the cluster dynamics for each trial for two divisions of labor: (a) 1T4D and (b) 2T3D.

Table 6.1: Comparison the clustering results between two divisions of labor.

	Clustering results	Reliability	Efficiency
2T3D	Success rate: 100%, Average time: 85 minutes	∨	
1T4D	Success rate: 66%, Average time: 49 minutes		∨

empirical data obtained from calibrated experiments. Then, given an initial state condition, the state after n time-steps can be predicted by using the model. Based on a Markov chain model of single strategies, we can further find a better strategy composed of the sequence of different strategies.

6.1.1 The Transition Matrix

In our problem, the system state is describes the progress of the clustering task. During the clustering process, each object in the workplace may be part of a central cluster, a boundary cluster, or neither (unclustered objects). We define the state in the Markov chain model as the number of objects in central cluster(s) and the number of objects in boundary cluster(s) $S_t = \{N_c(t), N_b(t)\}$, where $N_c(t)$ and $N_b(t)$ are the number of objects in central clusters and boundary clusters respectively at time t. Then, $N_c(t) + N_b(t) = N_0 - N_u(t)$ where N_0 is the total number of objects and $N_u(t)$ is the number of objects that do not belong to any of the clusters. The number total states is $d = \frac{N_0(N_0+1)}{2}$, and the matrix describing transitions between states has dimension $d \times d$.

As a simplification, we assume that the environment may stay in the same state or change to another state by one-state increments or decrements. Then a state transition can only occur in five directions such as $(i, j) \to (i, j)$, $(i, j) \to (i + 1, j)$, $(i, j) \to (i - 1, j)$, $(i, j) \to (i, j - 1)$, and $(i, j) \to (i, j + 1)$. The transitions between states is illustrated as a right-angled triangle in Figure 6.7.

For each edge, a transition probability is computed by the frequency counts of the objects moving between states in each time interval. In order to measure the frequency of each state transition, we define an alternative formula which assigns a certain weight in the transited state. The total weight of 1 is assigned when one transition occurred in a time interval. If the transition of the state is varies with a

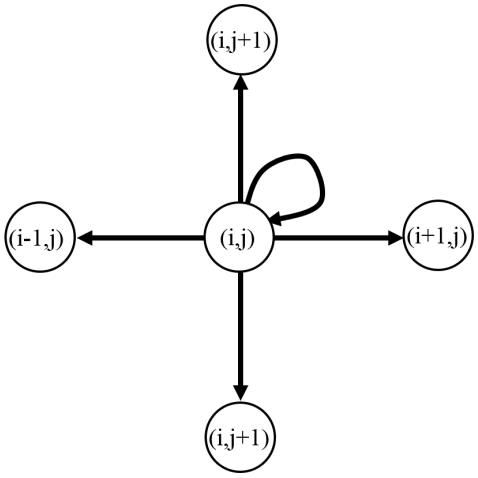

Figure 6.6: Five directions occurring state transitions at a state $S(i, j)$. The state is varied by only one-state increment or decrements.

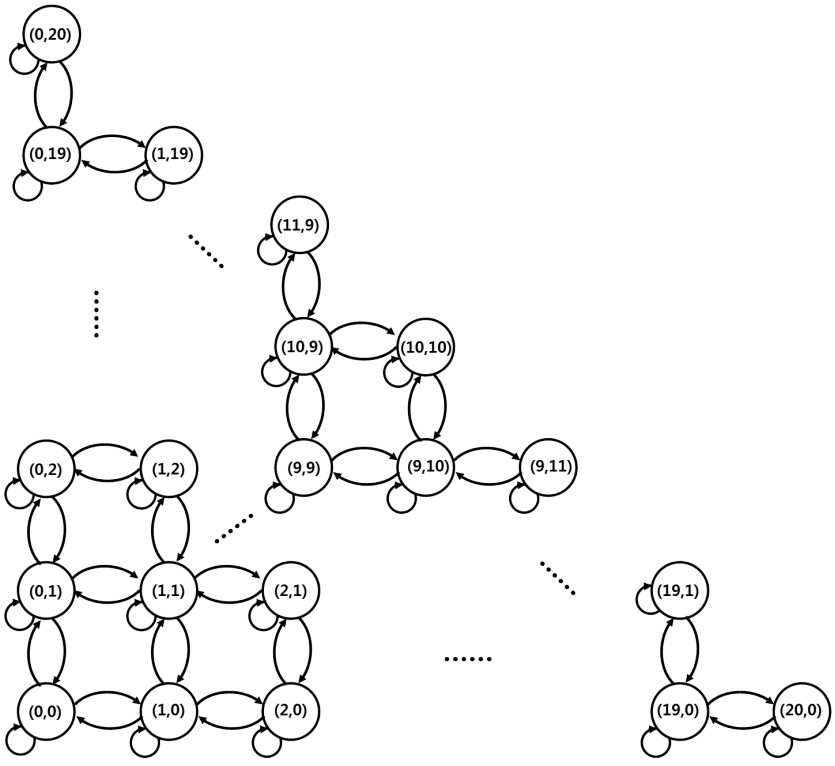

Figure 6.7: State diagram for a clustering task. Since we used 20 objects, total states are 231 states.

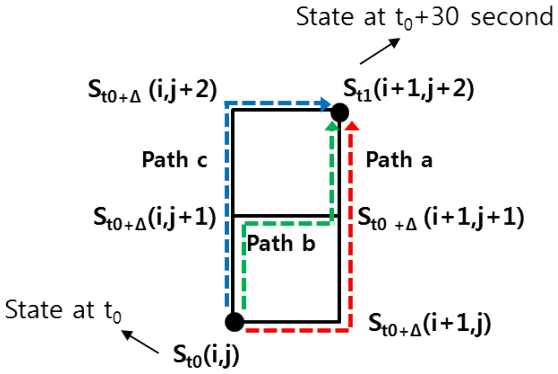

Figure 6.8: All paths from S_{t_0} to S_{t_1}. ($t_1 - t_0 = 30$ seconds).

Table 6.2: The weight of the state transition.

Edges	Weight	Note
$S(i,j) \rightarrow S(i,j+1)$	2/9	Edges included in two paths
$S(i+1,j+1) \rightarrow S(i+1,j+2)$	2/9	
$S(i,j+1) \rightarrow S(i+1,j+1)$	1/9	Edges included in one path
$S(i,j+1) \rightarrow S(i,j+2)$	1/9	
$S(i+1,j) \rightarrow S(i+1,j+1)$	1/9	
$S(i,j) \rightarrow S(i+1,j)$	1/9	
$S(i,j) \rightarrow S(i+1,j+2)$	1/9	
Total	1	Assigned in one transition

single increment, decrement, or stayed in the same, the total weight of 1 is allotted to the transition.

Let S_{t_0} be the starting state (i_0, j_0) at time t_0, and S_{t_n} be the state (i_n, j_n) after n time intervals from t_0. If we assume that the state transition occurs along edges in the state diagram, the number of steps to approach from S_{t_0} to S_{t_n} is computed by the difference of absolute values of the state grid, $|i_n - i_0| + |j_n - j_0|$. Let x be $|i_n - i_0|$ and y be $|j_n - j_0|$. With empirical data, it is possible that $x > 1$ or $y > 2$ in

a single time interval. In this case, the weight is divided equally all possible paths. That is, by considering all paths that reach from the current state to the next state via transitions, we assign a proportional weight to the number of possible routes connecting the states.

Figure 6.8 illustrates all paths that approach S_{t_1} from S_{t_0} after one time interval. The number of the shortest paths in an $x \times y$ grid type is $(x+y)!/x!y!$. All edges of each path have the weight divided by the number of edges in the shortest path, $x+y$. In other words, the weight of the edge in a selected path is as follows,

$$W_{edge} = \frac{x!y!}{(x+y)!} \times \frac{1}{x+y}. \tag{6.1}$$

In addition, since the edges can be selected multiple times as a path, the final weight of the edges will be

$$W_{total} = \frac{x!y!}{(x+y)!} \times \frac{1}{x+y} \times N_s, \tag{6.2}$$

where N_s is the number of times selected as a path.

The weight of all edges of the state transition in Figure 6.8 is shown in Table 6.2. With the rule above assigning weights, a transition matrix is generated by integrating the weighted frequencies of all state transitions that occur over the duration of the calibration experiments. The weighted frequencies are then normalized to calculate the transition probability. That is, if a transition from one state to another state occurs frequently, the probability of the transition is large. In our scenario, the matrix has 231 states, where each state has transition probabilities for 5 directions. We order the 231 states along the rows and columns of the transition matrix as $(0,0),(0,1),\cdots,(0,20),(1,0),\cdots,(1,19),\cdots,(19,0),(19,1),(20,0)$ (See Figure 6.9).

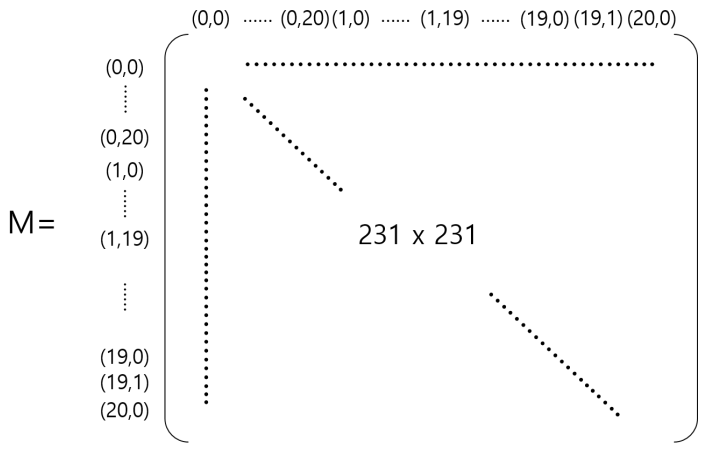

Figure 6.9: 231× 231 transition matrix in our scenario.

We constructed a model for all combinations of twisters and diggers, producing transition probability matrices for six divisions of labor from calibrated experiments with 0T5D, 1T4D, 2T3D, 3T2D, 4T1D and 5T0D.

6.1.2 Prediction of State Transition

After the transition matrix is obtained, S_{t_n} can be predicted by a discrete-time Markov chain (Ross, 2003). Let M be the state transition matrix of our system. The ij-th entry m_{ij} of M provides the probability of going from state i to state j in one time-step. Figure 6.10 illustrates an example of moving one state into other state after a time interval by the Markov chain process. Then the n-step transition matrix can be determined by $M^{(n)} = (m_{ij})^n$. Thus, we can predict the state distribution of S_{t_n} by

$$P\left\{S_{t_n} = (i_n, j_n) \,|S_{t_0} = (i_0, j_0)\right\} = S_{t_0} M^n. \tag{6.3}$$

A sequence of ternary plots in Figure 6.11 illustrates the variation of the probability distribution of states at particular time intervals, where the Markov chain

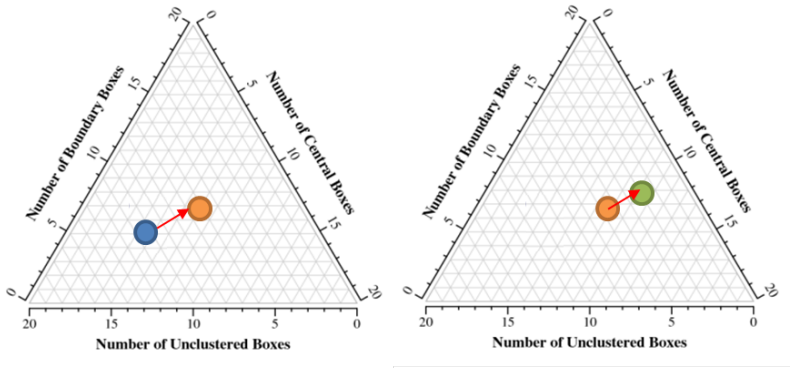

Figure 6.10: The state transition in a time interval.

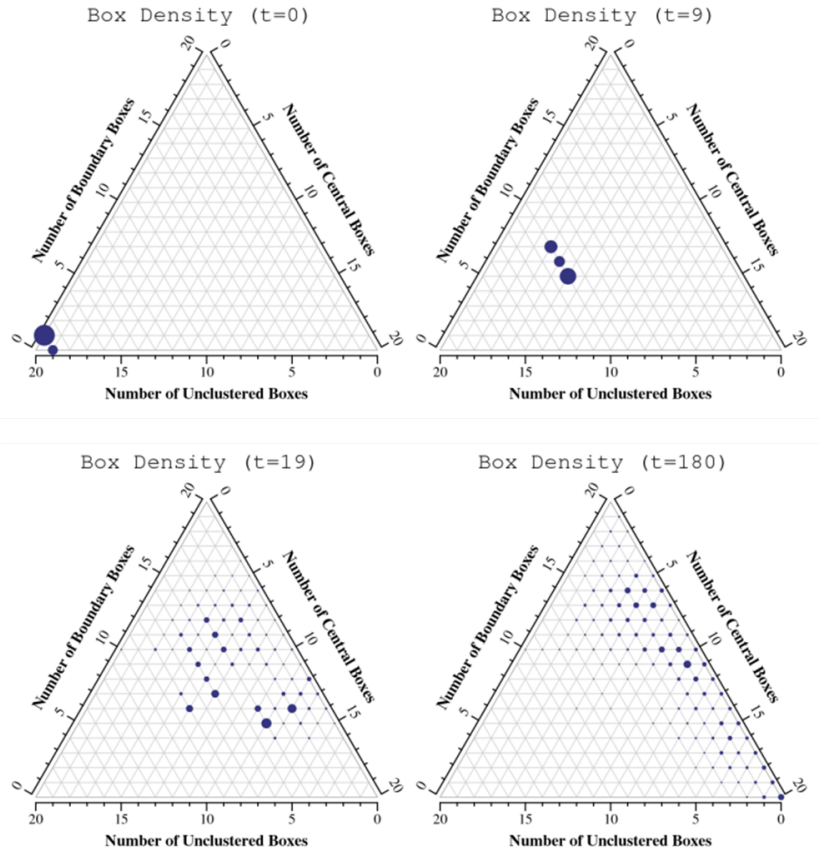

Figure 6.11: Variation of the probability distribution of states in n time-steps (n=0, 9, 19 and 180). The probability of large point is relatively higher than the probability of small point.

provides the possible states at each time step. The distribution spreads out because the number of entries having non-zero probability grows gradually with each transition, as time increases.

6.1.3 Selecting Sequence of Strategies

Having constructed a Markov chain model that predicts the clustering task performance for each of the twister versus digger mixes, we now turn to selection of the sequence of labor mixtures which accomplishes the best performance of the clustering task; we seek a sequence that is both reliable and efficient. As a proof of this concept in this research, we consider the most basic sequence comprised of only two mixes but, as will be seen below, more complex varieties follow the same procedure directly.

From the Markov chain theorem, the state distribution of the sequence of two mixed strategies after n time-steps where they switch at time k is

$$M_{seq} = [M_A]^k [M_B]^{n-k}, \tag{6.4}$$

where M_A and M_B are the transition matrices of labor mix A and labor mix B, respectively, and k is the time at when the strategy is switched where $0 \leq k \leq n$.

With Equations. (6.3) and (6.4), the probability of a configuration during the clustering task, given the switching time, can be predicted. For example, if the initial configuration is $(0, 0)$ in which is no objects in the central clusters or the boundary clusters, the initial vector, $X_0 = [1, 0, \cdots, 0]$, here X_0 has size $1 \times d$. That is, the probability distribution of the final state after n time-steps can be computed by $X_0 M_{seq}$. We can use the probability distribution of the final states to determine the best strategy for the clustering task.

To quantify the clustering performance, we introduce a performance metric.

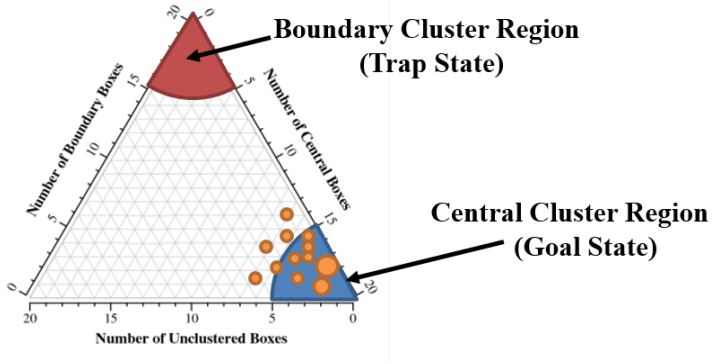

Figure 6.12: An example of the clustering result of a sequence having high performance.

Given an initial configuration, a perfect central cluster has state $(N_0, 0)$, and ought to be assigned a high weighting factor for quantifying the clustering performance. Smoothing this function, weights are assigned up to clusters composed of more than 90% objects in a central cluster. For example, since we use 20 objects in our experiment, we consider up to the states, (18,0), (18,1), and (18,2) for measuring the clustering performance. Let $P\{S_{t_{180}} = (i,j) | S_{t_0} = (0,0)\}$ be $M_{seq}(i,j)$. Then, the performance metric is defined as follows.

$$\begin{aligned} Performance\ Metric &= M_{seq}(20,0) + 0.9\,(M_{seq}(19,0) + M_{seq}(19,1)) + \\ &\quad 0.8\,(M_{seq}(18,0) + M_{seq}(18,1) + M_{seq}(18,2)) \\ &= \sum_{u=\lfloor 0.9 \times N_0 \rfloor}^{N_0} \frac{u}{N_0} \sum_{v=0}^{N_0-u} M_{seq}(u,v). \end{aligned} \tag{6.5}$$

Figure 6.12 provides an example of a result from a sequence having high performance. For example, as shown in Figure 6.12, if the objects are located in the central region of the arena at the final time step, we can assume that the sequence of mixed strategies produce a good result with high probably.

6.2 Physical Robot Experiments

We first describe how the Markov chain model is built based on data obtained from calibration runs. Next, we validated our Markov chain model by comparing the model prediction with physical robot experiments.

6.2.1 The Markov Chain Model

In order to build the Markov chain model, we first conducted a calibrated run for all possible combinations of Twister(T) and Digger(D) with five robots: 0T5D, 1T4D, 2T3D, 3T2D, 4T1D, and 5T0D. Each trial lasted 90 minutes, with 20 objects. All experiments were videotaped and annotated with $n = 180$ moments by observing frames every 30 seconds. For each division of labor, a total number of 540 transitions between states was observed. From this statistical data, we obtained the state transition matrix.

In order to find the best sequence of strategies having the maximum clustering performance, we compared the performance by varying the switching time from $k = 0$ to $k = 180$. Figure 6.13 shows the performance metric for all sequences of motion strategies. The Markov chain model predicts that the best sequence of strategies was switching from 2T3D to 0T5D, and it outperformed the clustering performance of a single strategy between 22 to 89 minute. The switching sequences of 2T3D→1T4D and 1T4D→0T5D also outperformed the clustering performance of a single strategy between 55 to 89 minute, and between 17 to 89 minute, respectively. Note that the end points of each line, $k = 180$, shows the performance of a pure strategy where no switching occurs.

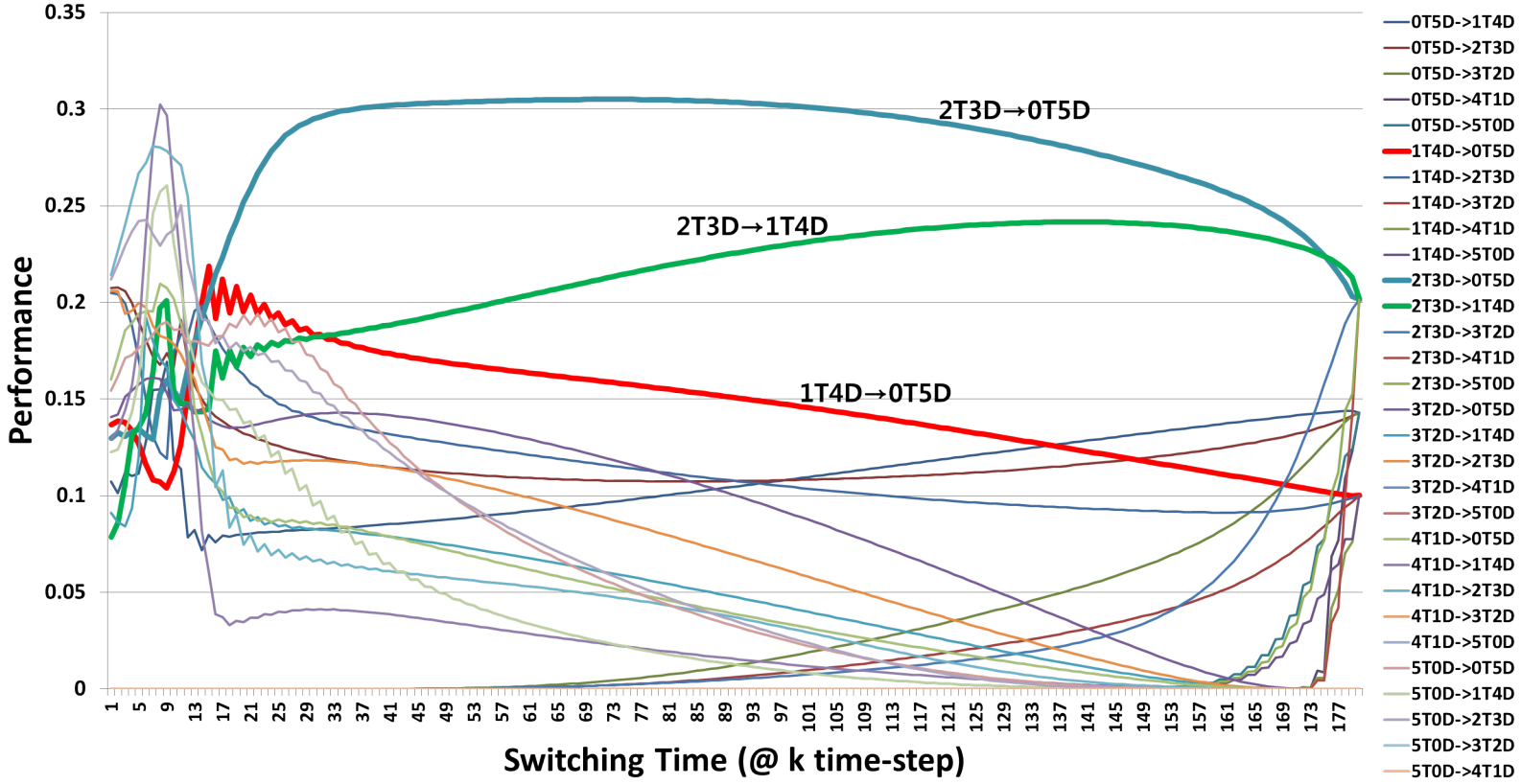

Figure 6.13: A comparison of predicted performance via the Markov chain model with varying switching time.

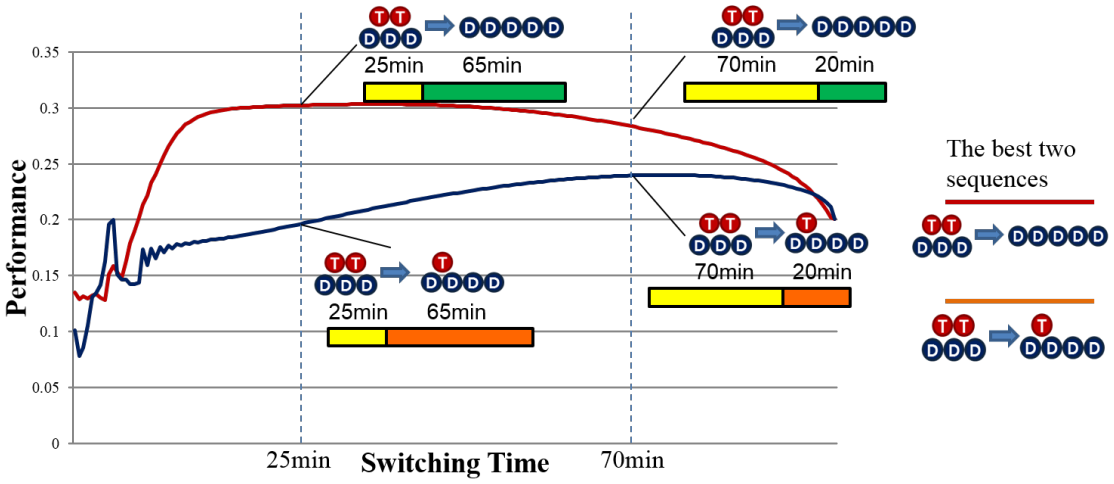

Figure 6.14: A comparison the predicted performance between the best two sequences.

6.2.2 Model Validation

The model suggests that the best strategy is a sequence where 2T3D is switched to 0T5D after 25 minutes (shown in Figure 6.14). We examined the ordering by comparing the clustering performance predicted by the Markov chain with an actual experiment. We selected the two best sequences: the sequence from 2T3D to 0T5D and the sequence from 2T3D to 1T4D, and carried out physical experiments for both cases, switching at 25 minutes. Each set of sequences was conducted five times under the same initial configuration with 5 robots and 20 objects. We assumed that the average size of a single central cluster at the final step, 180 time-step, is a good measurement of the task performance.

Table 6.3 shows the average size of a single central cluster at the final step in each sequence, and represents the clustering results of each experiments after 90 minutes. Since the average size of a single central cluster in the sequence from 2T3D to 0T5D is larger than the average size of the sequence from 2T3D to 1T4D, the

result supports that idea that the ordering predicted from the model at 25 minutes, is also reflected in physical experiments.

This observation is further confirmed with a statistical test. We assumed that the gap in performance between two sequences in physical experiment is identical to the difference of the statistical mean. In order to test a statistical hypothesis, we conducted the two-sample t-test with unequal variance based on experimental data. The two-sample t-test is used to determine if two population means are equal or not. The two-sample t-test is defined as

$$H_0 : \mu_a = \mu_b,$$
$$H_a : \mu \textit{ are not equal}.$$

We then select the level of significance to be used in the test as 0.05. After performing the hypothesis test, we could get the P-value. Since the P-value, 0.0425, is below 0.05 in one-tailed test, we can reject the null hypothesis of no difference between the means from the two samples in favor of the alternative. In other words, we accept that the mean of the size of a single central cluster between the sequence from 2T3D to 0T5D and the sequence from 2T3D to 1T4D are unequal with 95% confidence. That is, the difference of the performance between two sequences in physical experiments has significant difference. Consequently, the ordering of the clustering performance predicted by the Markov chain model corresponds to the ordering of the clustering performance by physical robots.

6.3 Summary and Contributions

In this section, we verified that the Markov chain model is effective in predicting the clustering progress and performance of self-organized multi-robot clustering sys-

Table 6.3: Experimental results and Two-sample t test.

		2T3D → 0T5D (Switching @25min)	2T3D→ 1T4D (Switching @25min)
Trials	1	18 objects	11 objects
	2	19 objects	20 objects
	3	19 objects	9 objects
	4	18 objects	17 objects
	5	20 objects	14 objects
Average size of a single central cluster at the final step		18.8 objects (95% collecting rate)	14.2 objects (70% collecting rate)
P(T ≤ t) one-tail		0.0425	

tems. Through the stochastic model, we obtained an optimal sequence of changes to the division of labor and validated it with a statistical test. The experiments provide practical suggestion that the model's predictions permits to infer the clustering performance of physical robots.

This work showed that a sequence of one division of labor followed by another improves clustering performance over a single strategy. It might be a good example that group level behaviors can be control parameters for improving the system performance.

7. CONCLUSION

7.1 Summary of Contributions

In this dissertation, we developed models to understand accurately the self-organized multi-robot clustering developing, with a view toward improving the clustering performance.

Our clustering system is differentiated from previous work by two key aspects: first, we cluster square objects. These are both more challenging and potentially more useful than previous cases. Secondly, we employ less capable robots than earlier clustering work. We attempted to implement the more challenging clustering system since the object geometry causes radically different packings and sensitivity to environmental boundaries which cause existing approaches to interfere to form spatially centralized clusters. We proposed an effective solution that simple robots can pry loose the boundary objects from the wall by exploiting the mechanics of the object geometry. Repetitive prying motions resolve partial sensor blindness problem via open-loop control strategies because a single object is imperceptible to the robots. The approach we have taken uses mechanical interactions with boxes on the perimeter, and emphasizes action rather than sensing. In this regard, it is closer to the spirit underlying the self-organized clustering process itself.

We also proposed two complementary behaviors for object clustering, twisting and digging, and demonstrated that the robots executing proposed behaviors overcome the effect of the boundary and successfully form only one central cluster. Additionally, we examined the effect of different ratios of diggers and twisters, illustrating that managing the local densities of robots is important. This represents a new task domain for the division of labor problems. It implies that one way to control such

self-organized systems might be to manage where they spend their time in the environment. This simple idea, it seems, has not been the focus of existing implicitly coordinated self-organized multi-robot systems.

We contribute a model which considers heterogeneous behaviors differing with the location. To prevent boundary cluster growth, we focused on managing the spatial distribution of robots, executing simple motion behavior, rather than specialized manipulation of the objects. Through this we can acquire a notion of local spatial density, and also enrich prior clustering models by treating state transitions of the objects being clustered (in this study, a transition of the object into a pried object), and context dependency (boundary objects are modeled as behaving differently from one in the central region). Using this model, we derived a condition not only for evolution of the largest central cluster but for also degeneration of boundary clusters. Through physical robot experiments, we verified that the robot team, satisfying the condition to avoid the boundary interference, achieve the clustering goal.

This study is also the first to attempt to investigate the impacts of the geometric characteristics of clusters and objects on the clustering dynamics. We explored a measure of compactness to quantify the shape of clusters, showing that it captures useful information and can result in improved models. Using the measure of the compactness, we proposed probabilistic models to predict the geometry of clusters that arise during the clustering process and examined how the clustering dynamics are affected by changes in object geometries. Interestingly, we observed that the shape of the cluster reflects the geometry of the object. This observation was used to allow the better development cluster occurrence models.

Also, we proposed a sequencing strategy to improve the system performance by managing global level behavior. We showed that a stochastic model is useful at predicting the performance of self-organized robots performing an object clustering

task, and the model permits planning of a sequence of changes to the division of labor for the maximum performance. The experiments suggest that the model's predictions of the relative performance of different switched strategies of the labor mix are useful for reasoning about the performance of physical robots. This study showed that a particular sequence of one division of labor followed by another improves clustering performance over a single strategy.

7.2 Future Work

Future work could include the analysis of clustering of mixes of different objects. It can provide a solution for the problem of object separation. For example, if robots executing our proposed behaviors cluster mixes of squares and rectangles, one might expect that square objects are collected into a single central cluster by prying motions whereas the rectangles are located on the boundary because the robots cannot separate the boundary rectangles from the wall. Unlike collective sorting with multiple robots, depending on sensing (Wang and Zhang, 2004), this may form a solution to the problem of spatially sorting the different objects only with simple behaviors without any sensor to distinguish an object's type. We also expect that those behaviors may be applicable to other cases, such as triangular objects or hexagonal objects. Generalization to other shapes is important for the application to construction tasks and, also will allow a better understanding of the role played by the packing configurations of the objects.

For improving the clustering performance, future work include sequences of more than two strategies. In addition, since the results verify the utility of the stochastic model with the object clustering, our method will be able to adapt to different self-organized multi-robot systems for collective manipulation tasks such as object transportation.

REFERENCES

W. Agassounon, A. Martinoli, and K. Easton. Macroscopic modeling of aggregation experiments using embodied agents in teams of constant and time-varying sizes. *Autonomous Robots*, 17(2-3):163–192, 2004.

J. Amat, R. L. de Mántaras, and C. Sierra. Cooperative autonomous low-cost robots for exploring unknown environments. In *Experimental Robotics IV*, pages 40–49. Springer, 1997.

H. Anil, K. S. Nikhil, V. Chaitra, and B. S. Sharan. Revolutionizing farming using swarm robotics. In *Proceedings of the 2015 6th International Conference on Intelligent Systems, Modelling and Simulation*, pages 141–147. IEEE Computer Society, 2015.

B. Ayoub. The eccentricity of a conic section. *The College Mathematics Journal*, 34(2):116, 2003.

E. Bahgeçi. Evolving aggregation behaviors for swarm robotic systems: A systematic case study. In *Swarm Intelligence Symposium, 2005. SIS 2005. Proceedings 2005 IEEE*, pages 333–340. IEEE, 2005.

T. Balch and R. C. Arkin. Behavior-based formation control for multirobot teams. *Robotics and Automation, IEEE Transactions on*, 14(6):926–939, 1998.

R. Beckers, O. E. Holland, and J.-L. Deneubourg. From local actions to global tasks: stigmergy and collective robotics. In *Proceedings of Artificial Life IV*, pages 181–189, 1994.

G. Beni. From swarm intelligence to swarm robotics. In *Swarm robotics*, pages 1–9. Springer, 2005.

S. Berman, Q. Lindsey, M. S Sakar, V. Kumar, and S.C. Pratt. Experimental study

and modeling of group retrieval in ants as an approach to collective transport in swarm robotic systems. *Proceedings of the IEEE*, 99(9):1470–1481, Sept 2011.

E. Bonabeau, M. Dorigo, and G. Theraulaz. *Swarm Intelligence: from Natural to Artificial Systems*. Oxford University Press, Inc., New York, NY, USA, 1999.

E. Bonabeau, M. Dorigo, and G. Theraulaz. Inspiration for optimization from social insect behaviour. *Nature*, 406(6791):39–42, 2000.

S. Camazine. *Self-organization in biological systems*. Princeton University Press, 2003.

A. Campo, S. Nouyan, M. Birattari, R. Groß, and M. Dorigo. Enhancing cooperative transport using negotiation of goal direction. In *BNAIC 2006*, number LSRO-CONF-2008-044. University of Namur, 2006.

E. Catto. Box2d, a 2 dimensional physics engine for games. http://box2d.org, 2009.

H. Çelikkanat and E. Şahin. Steering self-organized robot flocks through externally guided individuals. *Neural Computing and Applications*, 19(6):849–865, 2010.

W. W. Cohen. Adaptive mapping and navigation by teams of simple robots. *Robotics and autonomous systems*, 18(4):411–434, 1996.

M. F. Copeland and D. B. Weibel. Bacterial swarming: a model system for studying dynamic self-assembly. *Soft Matter*, 5(6):1174–1187, 2009.

S. Damer, L. Ludwig, M. A. LaPoint, M. Gini, N. Papanikolopoulos, and J. Budenske. Dispersion and exploration algorithms for robots in unknown environments. In *Defense and Security Symposium*, pages 62300Q–62300Q. International Society for Optics and Photonics, 2006.

A. Decugniére, B. Poulain, A. Campo, C. Pinciroli, B. Tartini, M. Osèe, M. Dorigo, and M. Birattari. Enhancing the cooperative transport of multiple objects. In *Proceedings of the 6th International Conference on Ant Colony Optimization and Swarm Intelligence*, pages 307–314, 2008.

A. Decugniere, B. Poulain, A. Campo, C. Pinciroli, B. Tartini, M. Osée, M. Dorigo, and M. Birattari. Enhancing the cooperative transport of multiple objects. In *Ant Colony Optimization and Swarm Intelligence*, pages 307–314. Springer, 2008.

J.-L. Deneubourg and S. Goss. Collective patterns and decision-making. *Ethology Ecology & Evolution*, 1(4):295–311, 1989.

J.-L. Deneubourg, S. Goss, N. Franks, A. Sendova-Franks, C. Detrain, and L. Chrétien. The dynamics of collective sorting robot-like ants and ant-like robots. In *Proceedings of Simulation of Adaptive Behavior*, pages 356–363, 1991.

J. P. Desai, V. Kumar, and J. P. Ostrowski. Control of changes in formation for a team of mobile robots. In *Robotics and Automation, 1999. Proceedings. 1999 IEEE International Conference on*, volume 2, pages 1556–1561 vol.2, 1999.

D. V. Dimarogonas and K. J. Kyriakopoulos. Connectedness preserving distributed swarm aggregation for multiple kinematic robots. *Robotics, IEEE Transactions on*, 24(5):1213–1223, 2008.

M. Dorigo and A. F. Roosevelt. Swarm robotics. In *Special Issue, Autonomous Robots*. Citeseer, 2004.

F. Ducatelle, A. Förster, Gianni A. Di C., and L. M. Gambardella. New task allocation methods for robotic swarms. In *9th IEEE/RAS Conference on Autonomous Robot Systems and Competitions*, 2009.

H. R. Everett, G. A. Gilbreath, T. A. Heath-Pastore, and R. T. Laird. Coordinated control of multiple security robots. In *Optical Tools for Manufacturing and Advanced Automation*, pages 292–305. International Society for Optics and Photonics, 1994.

E. Ferrante, A. E. Turgut, C. Huepe, A. Stranieri, C. Pinciroli, and M. Dorigo. Self-organized flocking with a mobile robot swarm: a novel motion control method. *Adaptive Behavior*, 2012.

E. Ferrante, M. Brambilla, M. Birattari, and M. Dorigo. Socially-mediated negotiation for obstacle avoidance in collective transport. In *Distributed Autonomous Robotic Systems*, pages 571–583. Springer, 2013.

M. Fialkowski, K. JM Bishop, R. Klajn, S. K Smoukov, C. J. Campbell, and B. A. Grzybowski. Principles and implementations of dissipative (dynamic) self-assembly. *The Journal of Physical Chemistry B*, 110(6):2482–2496, 2006.

P. Flocchini, G. Prencipe, N. Santoro, and P. Widmayer. Arbitrary pattern formation by asynchronous, anonymous, oblivious robots. *Theoretical Computer Science*, 407(1):412–447, 2008.

S. Franklin. Coordination without communication. *University of Memphis*, 1996.

N. R. Franks and A. B. Sendova-Franks. Brood sorting by ants: distributing the workload over the work-surface. *Behavioral Ecology and Sociobiology*, 30(2), March 1992.

D. W. Gage. Many-robot mcm search systems. In *Proceedings of Autonomous Vehicles in Mine Countermeasures Symposium*, pages 9–55, 1995.

S. Garnier, C. Jost, R. Jeanson, J. Gautrais, M. Asadpour, G. Caprari, and G. Theraulaz. Aggregation behaviour as a source of collective decision in a group of cockroach-like-robots. In *Advances in artificial life*, pages 169–178. Springer, 2005.

S. Garnier, J. Gautrais, and G. Theraulaz. The biological principles of swarm intelligence. *Swarm Intelligence*, 1(1):3–31, 2007.

M. Gauci, J. Chen, W. Li, T. J. Dodd, and R. Groß. Clustering objects with robots that do not compute. In *Proceedings of the 2014 International Conference on Autonomous Agents and Multi-agent Systems*, AAMAS '14, pages 421–428, Richland, SC, 2014.

P. P. Grassé. La reconstruction du nid et les coordinations interindividuelles chez-bellicositermes natalensis etcubitermes sp. la théorie de la stigmergie. *Insectes*

sociaux, 6(1):41–80, 1959.

R. Groß and M. Dorigo. Towards group transport by swarms of robots. *International Journal of Bio-Inspired Computation*, 1(1/2):1–13, January 2009.

R. Groß, S. Nouyan, M. Bonani, F. Mondada, and M. Dorigo. Division of labour in self-organised groups. In *From Animals to Animats 10*, pages 426–436. Springer, 2008.

A. T. Hayes. How many robots? group size and efficiency in collective search tasks. In Hajime Asama, Tamio Arai, Toshio Fukuda, and Tsutomu Hasegawa, editors, *Distributed Autonomous Robotic Systems 5*, pages 289–298. Springer Japan, 2002.

O. Holland and C. Melhuish. Stigmergy, self-organization, and sorting in collective robotics. *Artificial Life*, 5(2):173–202, 1999.

A. Howard, L. Parker, and G. Sukhatme. The sdr experience: Experiments with a large-scale heterogeneous mobile robot team. In Jr. Ang, MarceloH. and Oussama Khatib, editors, *Experimental Robotics IX*, volume 21 of *Springer Tracts in Advanced Robotics*, pages 121–130. Springer Berlin Heidelberg, 2006.

S. Ichikawa and F. Hara. Experimental characteristics of multiple-robots behaviors in communication network expansion and object-fetching. In *Distributed Autonomous Robotic Systems 2*, pages 183–194. Springer, 1996.

C. Jones and M. J. Matarić. Adaptive division of labor in large-scale minimalist multi-robot systems. In *Intelligent Robots and Systems, 2003. (IROS 2003). Proceedings. 2003 IEEE/RSJ International Conference on*, volume 2, pages 1969–1974 vol.2, Oct 2003.

C. Jones and M. J. Matarić. Automatic synthesis of communication-based coordinated multi-robot systems. In *Proceedings of the IEEE/RSJ International Conference on Intelligent Robots and Systems*, pages 381–387, 2004.

G. Kaminka, R. Schechter-Glick, and V. Sadov. Using sensor morphology for multi-

robot formations. *Robotics, IEEE Transactions on*, 24(2):271–282, 2008.

S. Kazadi, A. Abdul-Khaliq, and R. Goodman. On the convergence of puck clustering systems. *Robotics and Autonomous Systems*, 38(2):93–117, 2002.

S. Kazadi, M. Chung, B. Lee, and R. Cho. On the dynamics of clustering systems. *Robotics and Autonomous Systems*, 46(1):1–27, 2004.

S. Kazadi, J. Wigglesworth, A. Grosz, A. Lim, and D. Vitullo. Swarm-mediated cluster-based construction. *Complex Systems*, 15(2):157, 2004.

J.-H. Kim and D. A. Shell. Improving the performance of self-organized robotic clustering: Modeling and planning sequential changes to the division of labor. In *2013 IEEE/RSJ International Conference on Intelligent Robots and Systems (IROS)*, pages 4314–4319, Nov 2013.

J.-H. Kim and D. A. Shell. A new model for self-organized robotic clustering: Understanding boundary induced densities and cluster compactness. In *2015 IEEE International Conference on Robotics and Automation (ICRA)*, pages 5858–5863, May 2015.

J.-H. Kim, Y. Song, and D. A. Shell. Robot spatial distribution and boundary effects matter in puck clustering, March 2011. AAAI Spring Symposium Series: Multirobot Systems and Physical Data Structure.

C. R. Kube and E. Bonabeau. Cooperative transport by ants and robots. *Robotics and autonomous systems*, 30(1):85–101, 2000.

A. Lein and R. T. Vaughan. Adaptive multirobot bucket brigade foraging. In *Proceedings of the Eleventh International Conference on Artificial Life*, pages 337–342. MIT Press, 2008.

K. Lerman and A. Galstyan. Mathematical model of foraging in a group of robots: Effect of interference. *Autonomous Robots*, 13(2):127–141, September 2002.

K. Lerman and A. Galstyan. Two paradigms for the design of artificial collectives.

In *Collectives and the Design of Complex Systems*, pages 231–256. Springer New York, 2004.

K. Lerman, A. Galstyan, A. Martinoli, and A. J. Ijspeert. A macroscopic analytical model of collaboration in distributed robotic systems. *Artificial Life*, 7:375–393, 2001.

M. Maris and R. Boeckhorst. Exploiting physical constraints: heap formation through behavioral error in a group of robots. In *Proceedings of the IEEE/RSJ International Conference on Intelligent Robots and Systems*, pages 1655–1660, 1996.

A. Martinoli, A. J. Ijspeert, and L. M. Gambardella. A probabilistic model for understanding and comparing collective aggregation mechanisms. In *Proceedings of the 5th European Conference on Advances in Artificial Life (ECAL-99)*, pages 575–584. Springer, 1999.

A. Martinoli, A. J. Ijspeert, and F. Mondada. Understanding collective aggregation mechanisms: From probabilistic modelling to experiments with real robots. *Robotics and Autonomous Systems*, 29(1):51–63, 1999.

A. Martinoli, K. Easton, and W. Agassounon. Modeling swarm robotic systems: A case study in collaborative distributed manipulation. *The International Journal of Robotics Research*, 23(4-5):415–436, 2004.

A. Martinoli. *Swarm intelligence in autonomous collective robotics from tools to the analysis and synthesis of distributed control strategies*. PhD thesis, École Polytechnique Fédérale de Lausanne, 1999.

J. McLurkin and D. Yamins. Dynamic task assignment in robot swarms. In *Robotics: Science and Systems*, volume 8, 2005.

F. Mondada, G. C. Pettinaro, A. Guignard, I. W. Kwee, D. Floreano, J.-L. Deneubourg, S. Nolfi, L. M. Gambardella, and M. Dorigo. Swarm-bot: A new distributed robotic concept. *Autonomous Robots*, 17(2-3):193–221, 2004.

A. Okubo. Dynamical aspects of animal grouping: swarms, schools, flocks, and herds. *Advances in biophysics*, 22:1–94, 1986.

C. A. Parker and H. Zhang. Collective robotic site preparation. *Adaptive Behavior - Animals, Animats, Software Agents, Robots, Adaptive Systems*, 14(1):5–19, March 2006.

C.A.C Parker, H. Zhang, and C.R Kube. Blind bulldozing: Multiple robot nest construction. In *Proceedings of the 2003 IEEE/RSJ International Conference on Intelligent Robots and Systems*, volume 2, pages 2010–2015, 2003.

L. E. Parker. Multiple mobile robot systems. In *Handbook of Robotics*, chapter 40. Springer, 2008.

I. M. Rekleitis, G. Dudek, and E. E. Milios. Multi-robot exploration of an unknown environment, efficiently reducing the odometry error. In *International Joint Conference on Artificial Intelligence*, volume 15, pages 1340–1345, 1997.

S. M. Ross. *Introduction to Probability Models, Eighth Edition.* Academic Press, 8 edition, January 2003.

J. A. Rothermich, M. Ecemiş, and P. Gaudiano. Distributed localization and mapping with a robotic swarm. In *Swarm Robotics*, pages 58–69. Springer, 2005.

L. Schmetterer. *Introduction to mathematical statistics*, volume 202. Springer Science and Business Media, 2012.

S. R. Scholes, A. B. Sendova-Franks, S. T. Swift, and C. Melhuish. Ants can sort their brood without a gaseous template. *Behavioral Ecology and Sociobiology*, 59:531, 2005.

A. J. C. Sharkey. Swarm robotics and minimalism. *Connection Science*, 19(3):245–260, 2007.

S. Soh, M. Branicki, and B. A. Grzybowski. Swarming in shallow waters. *The Journal of Physical Chemistry Letters*, 2(7):770–774, 2011.

Y. Song, J.-H. Kim, and D. A. Shell. Self-organized clustering of square objects by multiple robots. In *Proceedings of the 8th International Conference on Swarm Intelligence*, ANTS'12, pages 308–315, 2012.

O. Soysal and E. Şahin. A macroscopic model for self-organized aggregation in swarm robotic systems. In *Swarm robotics*, pages 27–42. Springer, 2007.

R. L. Stewart and R. A. Russell. A distributed feedback mechanism to regulate wall construction by a robotic swarm. *Adaptive Behavior*, 14(1):21–51, 2006.

V. Trianni, R. Groß, T. Labella, E. ahin, and M. Dorigo. Evolving aggregation behaviors in a swarm of robots. In *Advances in Artificial Life*, volume 2801 of *Lecture Notes in Computer Science*, pages 865–874. Springer Berlin Heidelberg, 2003.

A. E. Turgut, H. Çelikkanat, F. Gökçe, and E. Şahin. Self-organized flocking in mobile robot swarms. *Swarm Intelligence*, 2(2-4):97–120, 2008.

R. Vaughan. 36 irobot create robots clustering boxes. . http://www.youtube.com/watch?v=b_kZmatqAaQ, 2007.

T. Wang and H. Zhang. Collective sorting with multiple robots. In *Robotics and Biomimetics, 2004. ROBIO 2004. IEEE International Conference on*, pages 716–720, Aug 2004.

J. Wawerla, G. S. Sukhatme, and M. J. Matarić. Collective construction with multiple robots. In *IEEE/RSJ International Conference on Intelligent Robots and Systems*, volume 3, pages 2696–2701. IEEE, 2002.

J. Werfel and R. Nagpal. Extended stigmergy in collective construction. *IEEE Intelligent Systems*, 21(2):20–28, 2006.

G. M. Whitesides and B. Grzybowski. Self-assembly at all scales. *Science*, 295(5564):2418–2421, 2002.

H. Yamaguchi and G. Beni. Distributed autonomous formation control of mobile

robot groups by swarm-based pattern generation. In *Distributed Autonomous Robotic Systems 2*, pages 141–155. Springer, 1996.

S.-K. Yun, M. Schwager, and D. Rus. Coordinating construction of truss structures using distributed equal-mass partitioning. In *Robotics Research*, pages 607–623. Springer, 2011.